Christina Laura Kainz, BSc

Synthesis and Characterisation of Natural Steryl Glucosides

MASTER THESIS

to achieve the university degree of

Diplom-Ingenieurin

Master's degree programme: Technical Chemistry

submitted to

Graz University of Technology

Supervisor

Ao.Univ.-Prof. Dr.phil. Martin Mittelbach

Institute of Chemistry,

University of Graz

Graz, March 2017

Optimism is the faith that leads to achievement. Nothing can be done without hope and confidence.

Helen Keller

Affidativ

I declare that I have authored this thesis independently, that I have not used other than the declared sources / resources, and that I have explicitly marked all material which has been quoted either literally or by content from the used sources.

…… ……

(date) (signature)

Eidesstaatliche Erklärung

Ich erkläre an Eides statt, dass ich die vorliegende Arbeit selbstständig verfasst, andere als die angegebenen Quellen/Hilfsmittel nicht benutzt und die den benutzten Quellen wörtlich und inhaltlich entnommene Stellen als solche kenntlich gemacht habe.

Graz, am…… ……

Unterschrift

Acknowledgement

At this point I want to thank everybody who helped, supported and motivated me throughout my studies and during my master thesis.

Initially I'd like to express my sincere gratitude to Ao.Univ.-Prof. Mag.rer.nat. Dr.phil. Martin Mittelbach for the provision of the topic for my master thesis and for his skilled and kind support throughout my work on it. I'm also very grateful that he supported me in doing part of my master thesis abroad, which was a great enrichment for me.

A special thanks goes also to Philipp Marco Neu, MSc., for helping me with all big and little problems concerning my thesis and for his never ending patience. In general, I want to thank all members of the working group NAWARO for the professional support and for the pleasant working atmosphere.

I am very happy and thankful to have been given the possibility to be invited as an academic guest to the Laboratory of Food Biochemistry at the ETH Zurich in Switzerland. I want to thank Prof. Dr. Laura Nyström for welcoming me in her working group as well as for her kind support and expert supervision. Additionally, I'd like to express my gratitude to the whole working group for always providing me with comprehensive assistance and for making my stay in Zurich so pleasant.

I am grateful to have met so many inspiring people during my studies, some of which are now good friends to me. I'd also like to express my gratefulness to Alexander Krainer, BSc who helped me get the most out me, professionally and personally. Thank you for believing in me and especially for making me believe in myself.

To conclude, I would like to thank my family for giving me the opportunity to follow my academic interests and for supporting me mentally and financially.

Abstract

Steryl glucosides are sterol derivatives occuring in minor concentrations in oleaginous plants, where they either exist as free steryl glucosides (SG) or acylated with a fatty acid chain at position 6, called acylated steryl glucosides (ASG). The base catalysed transesterification of plant oil with methanol to obtain the desired fatty acid methyl esters (FAME) has been established for the industrial production of biodiesel. High basicity during this process results in the conversion of ASG to the more polar SG, which are insoluble in the obtained biofuel. Upon standing, they precipitate and form particles, which increases the likelihood for clugging of filters and valves. The given problem can already be observed at SG concentrations of a few ppm, thus methods for the qualititave and quantitative analysis of these compounds are needed to improve the competitiveness of biodiesel compared to fossil based or other bio fuels.

In the present thesis, a five step synthesis pathway for steryl glucosides is described, starting from cheap and environmental friendly sucrose. Stigma- and β-sitosteryl-D-glucopyranoside are the most common steryl glucosides found in plant oils. The current strategy gives therefore not only the possibility for the preparation of analytical standard materials, but also for the synthesis of natural products. The achieved results are compared with the outcome of the Koenigs Knorr mechanism with regard to yield and purity to get information on the relevance of the new method. Acylated steryl glucosides are further obtained in a biocatalytic reaction upon the application of different lipases, enabling mild conditions without cleavage of the glycosidic bond. Considering acyl donor, solvent, temperature, steryl moiety and purification method, the ideal conditions for the acylation are investigated. Characterisation of these compounds is performed using various instrumental methods, as LC/MS-ToF, Q-ToF-MS, GC-MS and NMR spectroscopy. Steryl polyglucosides were analysed by UPLC/MS-ToF, ion mobility MS and tandem MS and were found in azuki beans and rice.

Kurzfassung

Sterylglucoside sind Sterolderivate, die in geringen Konzentrationen in ölhaltigen Pflanzen vorkommen und entweder als freie Sterylglucoside (SG) oder acyliert mit einer Fettsäurekette (ASG) an C-6 vorliegen. Während der Umesterung des pflanzlichen Öls zu den Fettsäuremethylestern im Zuge des Biodieselprozesses werden die ASG in SG gespalten, welche aufgrund ihrer Polarität unlöslich in Biodiesel sind. Sie fallen in weiterer Folge aus und bilden Partikel. Dies führt zu einer Verminderung der Qualität des Biodiesels, da die Wahrscheinlichkeit des Verstopfens von Filtern und Ventilen erhöht wird. Nachdem dies bereits bei geringem Vorkommen der Sterylglucoside auftritt, sind qualitative und quantitative Analysenmethoden unerlässlich für die Markttauglichkeit von Biodiesel im Vergleich zu anderen erneuerbaren Energien.

In der vorliegenden Arbeit wird ein fünfstufiger Syntheseweg für die Herstellung von Sterylglucosiden, ausgehend von kostengünstigem und umweltfreundlichem Haushaltszucker (Saccharose), beschrieben. β-Sito- und Stigmasterylglucosid sind die in Pflanzenölen wichtigsten SG, Cholesteryl-β-D-glucopyranosid wird als interner Standard für deren Analyse verwendet. Die Reaktionskaskade wird in Hinblick auf Ausbeute und Reinheit mit den Ergebnissen der Koenigs-Knorr-Methode verglichen, welche bisher nur für die Reaktion mit Cholesterol beschrieben wurde.

In weiterer Folge wird die biokatalytische Synthese von acylierten Sterylglucosiden untersucht, da diese in größeren Maßstäben bisher nur unter Acylchloriden beschrieben wurde. Der Einsatz von Lipasen bietet den Vorteil von umweltfreundlichen Edukten sowie milden Reaktionsbedingungen. Unter Variation des Acyldonors, des Lösungsmittels, der Temperatur, des Ausgangsmaterials und der Aufreinigung werden die idealen Bedingungen für die Acylierung untersucht. Die Charakterisierung der synthetisierten Zwischen- und Endprodukte erfolgt unter Verwendung verschiedener instrumenteller Methoden, wie LC/MS-ToF, Q-ToF-MS, GC-MS und NMR Spektroskopie. Sterylpolyglucoside wurden unter Verwendung von UPLC/MS-ToF, Ionenmobilitäts-MS und Tandem MS untersucht und auf ihren Gehalt in Reis und Azukibohnen getestet.

1 INTRODUCTION 1

2 REVIEW OF LITERATURE 3

2.1 Steroids 3

2.2 Carbohydrates 6

2.3 Steryl glucosides 10

3 ANALYTICAL METHODS 18

4 EXPERIMENTAL AND METHODS 25

4.1 Instruments 25

4.2 Chemicals 26

4.3 Synthesis of steryl glucosides starting from sucrose 28

4.4 Synthesis of steryl glucosides using the Koenigs Knorr mechanism 31

4.5 Enzymatic acylation of SG to ASG 32

4.6 Analysis of steryl polyglucosides in food samples 34

4.7 Sample preparation for analytical methods 35

5 RESULTS AND DISCUSSION 39

5.1 Synthesis of steryl glucosides starting from sucrose 40

5.2 Synthesis of steryl-D-glucopyranoside using the Koenigs Knorr mechanism 57

5.3 Enzymatic acylation of SG to ASG 59

5.4 Analysis of steryl polyglucosides 64

6 CONCLUSION AND OUTLOOK 70

7 LIST OF FIGURES AND TABLES 72

8 REFERENCES 76

LIST OF ABREVIATIONS

Ac	Acetyl
ASE	Accelerated solvent extraction
ASG	Acylated steryl glucosides
ATR	Attenuated total reflection
APCI	Atmospheric pressure chemical ionisation
BSA	N,O-bis(trimethylsilyl) acetamide
Bz	Benzyl
DCM	Dichloromethane
Dm	Dry matter
DMF	Dimethylformamide
EIC	Extracted ion current
Et_2O	Diethyl ether
EtOAc	Ethyl acetate
ESI	Electro-spray ionisation
EtOH	Ethanol
Et_3N	Triethylamine
FABE	Fatty acid butyl ester
FAEE	Fatty acid ethyl ester
FID	Flame ionisation detector
FTMS	Fourier transform mass spectrometry
GC	Gas chromatography
HPLC	High performance liquid chromatography
IMS	Ion mobility spectrometry
IR	Infrared
LC	Liquid chromatography
LOQ	Limit of quantification
MALDI	Matrix assisted laser desorption ionisation
MeOH	Methanol
MHz	Megahertz
MS	Mass spectrometry
MSTFA	N-Methyl-N-(trimethylsilyl)trifluoroacetamide
Nd	Not detectable
NDP	Nucleoside diphosphate
NMR	Nuclear magnetic resonance
OAME	Oleic acid methyl ester

PAME	Palmitic acid methyl ester
PE	Petrol ether
ppm	Parts per million
Q-ToF	Quadrupol time of flight
R_f	Retention factor
rpm	Revolutions per minute
RT	Room temperature
SG	Free steryl glucosides
S_N	Nucleophilic substitution
SPE	Solid phase extraction
TG	Triglycerides
TLC	Thin layer chromatography/chromatogram
TMCS	Trimethylchlorosilane
TMSOTf	Trimethylsilyl trifluoromethansulfonate
ToF	Time of Flight
UPLC	Ultra performance liquid chromatography

1 Introduction

Sterols and their derivatives occur in plant and animal based organisms and fulfil various important functions in the cell, especially concerning hormone synthesis and flexibility of the cell membrane [1,2]. In addition to free sterols, also sterol esters, steryl glucosides (SG) and acylated steryl glucosides (ASG) have been reported in plants [3,4]. SG and ASG are found in varying concentrations in vascular plants, in some species contributing up to 56.3 % to the total sterol content [5]. Beneficial dietary effects have been reported, as these compounds lower, as well as the free phytosterols, the uptake of cholesterol from the diet [6]. However, for the biodiesel industry, these compounds are of major concern, especially when using plant oils from species with a high steryl glucoside content. During the transesterification of the oil to the methyl esters, the base labile ester bond between the sugar moiety and the fatty acid chain is cleaved, resulting in the conversion of ASG to SG. By cause of their higher polarity, SG are insoluble in the unpolar biodiesel and form microscopic hazy precipitates; clogging of filters, pumps and valves is the result [7]. Therefore, information on the type and amount of these compounds as well as methods for mechanical and chemical removal are of major interest for improving the performance of biodiesel.

In the present thesis, a five step synthesis of steryl glucosides starting from commercially available and environmental credible sucrose is described. The reaction pathway developed for cholesteryl -D-glucoside is tested on its applicability for phytosteryl moieties in order to produce standard materials also for plant derived steryl glucosides. In addition, the performed pathway is compared to yield and purity achieved when applying the Koenigs Knorr method, which has been reported so far only for cholesteryl-β-D-glucoside [8,9]. The success of the reaction is studied considering varying molar ratios and reaction times, the choice of the purification methods and different promotors applied during the glycosylation.

Due to the fact that the synthesis of ASG in higher scale has only been described using acyl chlorides and vinyl esters so far [10,11], an enzymatic approach using fatty acid methyl esters and lipases is envisioned, presenting the advantages of eco-friendly materials and mild conditions. Varying the molar ratios of the educts, temperature, reaction time, acyl donor, solvent, heating method and enzymes, the optimal conditions for the acylation were evaluated. Although column chromatography could not be circumvented, this method offers a suitable alternative to the harsh conditions applied when using acyl chlorides.

A variety of instrumental methods was used both to control the progress of the reaction and to characterise the synthesised pure standards. Due to the low detection limits and the small amount of time consumption, LC/MS-ToF was the method of choice for the majority of the central issues. Additionally the results obtained by ^{1}H and ^{13}C-NMR-spectroscopy and GC/MS were consulted for the characterisation of the compounds.

To the best of our knowledge, there are only few reports on the occurrence of steryl polyglucosides [12,13], so a suitable UPLC-MS method for the characterisation of these compounds in food samples was envisioned. After investigating the ideal conditions for the UPLC-MS measurement, the content of these compounds in azuki beans and rice was analysed.

2 Review of literature

2.1 Steroids

2.1.1 Structure and biosynthesis of steroids

Steroids are natural prevalent compounds and are the basic structure of various biological active substances, as for example hormons and steroid alkaloids, and therefore are of big interest not only in research, but also for pharmacological purposes. The basic structure of steroids is steran, which is a tetracyclic system with 17 carbon atoms; adding two methyl groups at C-10 and C-13 gives androstan, shown in Figure 1. The three six membered rings are in trans position towards each other, enabling a complete chain conformation [1].

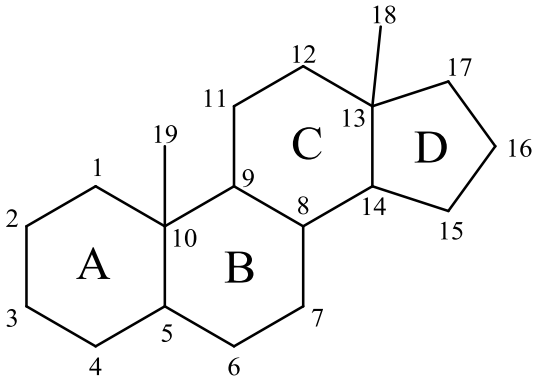

Figure 1: Structure of androstan

Squalene is the starting material for the biosynthesis of steroids, where in the first step folding of the molecule is achieved by the enzyme cyclase. Subsequent, a protosterol cation is formed upon oxidation, leading further to the formation of lanosterin, the precursor of cholesterol, or cycloartenol, the precursor of plant sterols. The mechanism is given in Figure 2. Adding an OH group in β-position at C-3 and a side chain at C-17 gives the basic structure of natural occurring sterols. Point of reference for the determination of the stereochemistry is the methyl group at C-13, which lies above the plane and is therefore in β-position; substituents that are situated under the plane are in α-position [1,14]. Partial unsatured steroids feature “en” or “in” in the systematic name; a lack of the methylene group in one of the six membered rings is indicated by the prefix “nor” [15].

Depending on their natural occurrence, sterols are divided into three groups: zoosterols, phytosterols and mycosterols. Due to the fact that only phyto- and zoosterols were studied in the experimental part of the thesis, mycosterols are not discussed in detail. Another classification can be done according to structural differences to give 4,4-dimethylsterols, 4α-methylsterols and 4,4-desmethylsterols; the latter one being that subclass studied in the experimental part of the thesis [16].

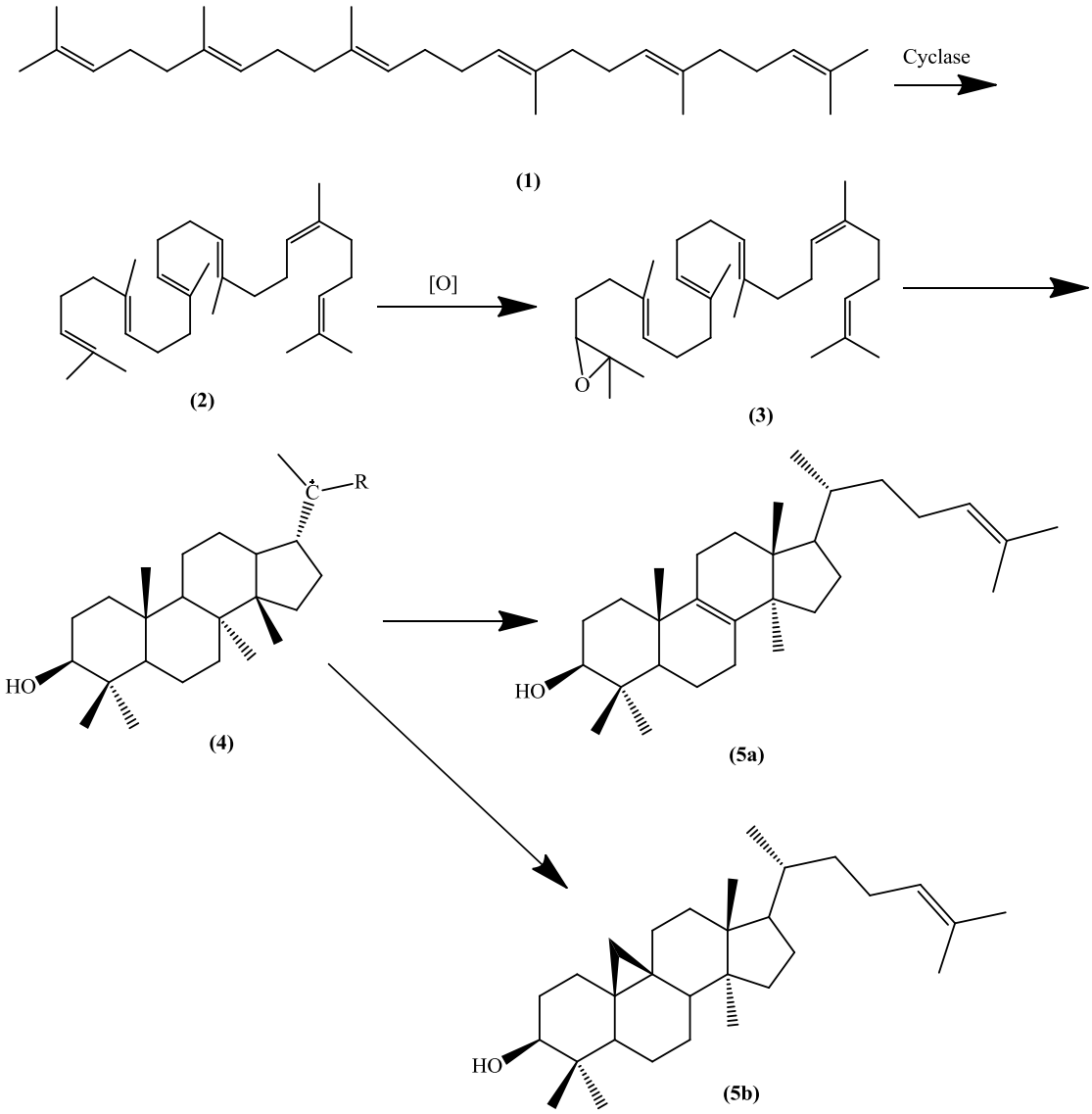

Figure 2: Biosynthesis of sterols; 1: squalene, 2: cyclic squalene, 3: squalene epoxide, 4: protosterol cation, 5a: lanosterin, 5b: cycloartenol based on [1]

Zoosterols

Derived from the Greek word for gall (*chole),* cholesterol is the most common sterol in animal tissue and the precursor in the biosynthesis of all other kinds of steroids needed for metabolism. It is crucial for the constitution of the cell membrane and the resorption of fatty acids through the gut wall. Per day the human body synthesizes some 800-1200 mg of cholesterol itself in the liver, intestines, reproductive organs and kidneys; upon the intake of animal based foods additional 300-500 mg are daily consumed [1,17]. Aliments featuring a high amount of cholesterol are for instance egg yolk (1085 mg/100 g), milk (10 mg/100 g) or red meat (60-100 mg/ 100 g) [1,18].

Phytosterols

So far, more than 250 different plant sterols have been identified with the most prevalent ones being β-sitosterol, stigmasterol and campesterol, which belong to the class of 4-desmethyl sterols [19]. Compared to cholesterol, they feature an additional methyl or ethyl residue in the side chain at C-17; their structures are given in Figure 3. The structure of the side chain heavily influences the chemical nature of the compound: the longer it is, the less polar the respective sterol; a double bond on the other hand, as in stigmasterol, increases the polarity.

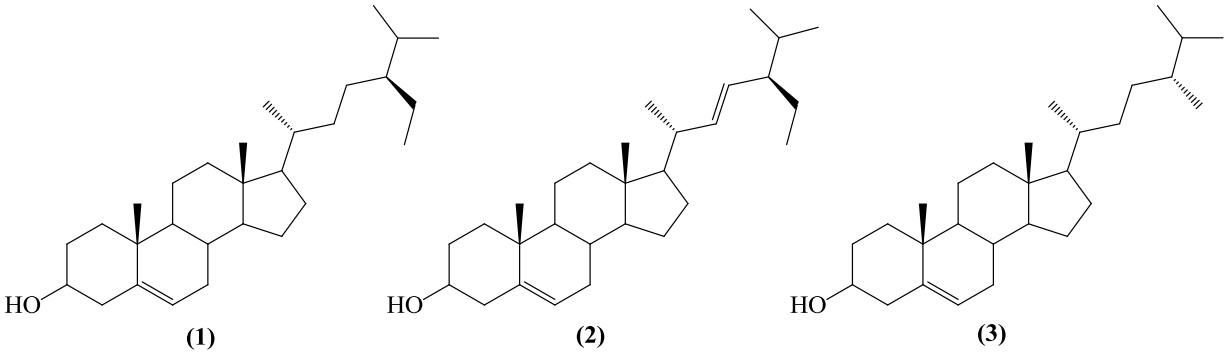

Figure 3: Structure of β-sitosterol (1), stigmasterol (2) and campesterol (3)

On the fact that the intake of phytosterols lowers both the total serum cholesterol and the low density lipoprotein cholesterol level [20], they are used in the treatment of hypercholesterolaemias and therefore have a positive effect on the cardiovascular system. In addition, β-sitosterol was proven to have anti-atherogenic effects due to inhibition of the blood platelet aggregation as well as anti-inflammatory, antibacterial and antifungial activity. Furthermore, an increased intake of phytosterols seems to reduce the risk of different types of cancer, as for example colon cancer [21]. Phytosterols are comprised in various oleaginous plants and therefore also occur in plant oils used in the food or biodiesel industry. They are part of the unsaponifiable fraction of the oil, which is a critical parameter for the performance of a plant oil used for biodiesel production [22]. Table 1 gives the total amount of phytosterols and the content in the unsaponifiable fraction of selected oils.

Table 1: Phytosterol content of selected plant oils [from 22]

	Total sterol content [mg/100 g]	Sterols in the unsaponifiable fraction [%]
Maize	900	69.2
Rapeseed	840	93.3
Sunflower	450	64.3
Soybean	370	61.6
Coprah	200	50.0
Palm kernel	90	22.5

2.2 Carbohydrates

2.2.1 Structure and classification of carbohydrates

Carbohydrates are the most abundant compounds in nature and are indispensable for life on earth, as they build up the cell wall of all plant based material and serve as chemical energy storage. Per year, plants synthesise 10^{11} t of cellulose only, which accounts for the bulk of biomass produced on earth [1]. Saccharides, or sugars, exist in their mono-, di-, oligo- and polymeric form and are polyhydroxycarbonyl compounds, which enables the formation of cyclic hemiacetals or hemiketals [14]. Therefore, the amount of different stereoisomers even increases, making carbohydrates a highly versatile compound class. Carbohydrates are classified according to the number of the sugar monomers:

a) Monosaccharides: the simplest group of saccharides features only one monomer of sugar and belongs to one of the sub groups aldoses or ketoses. In addition to the functional end groups, a classification can be done as well according to the number of carbon atoms; e.g. a sugar featuring three carbon atoms is called triose, with glyceraldehyde being the most important one. The insertion of HCOH between C-1 and the α-C of glyceraldehyde yields aldotetroses, successive addition of more HCOH groups eventually gives aldopentoses and -hexoses. Figure 4 shows the structure of β-D-glucose, an aldohexose and its isomer β-D-fructose, which belongs to the class of ketohexoses.

   Pentoses and hexoses exist in equilibrium between cyclic hemi acetals and the open conformation. The notation of the structure can be done either in Fischer, Hayworth or Mills depiction [14,23] .

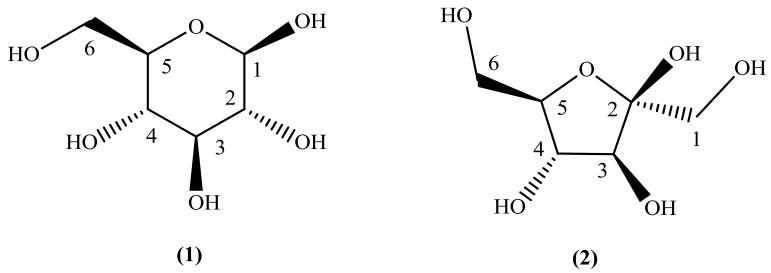

Figure 4: Structure of β-D-glucose (1) and β-D-fructose (2) in Mills depiction

b) Disaccharides: the dimers of sugars are derived, when a reducing sugar reacts with a second monosaccharide to form a glycosidic bond. The most important disaccharide in nature is sucrose, being also the starting material in the synthetic pathway described in the experimental part of the thesis. α-D-glucopyranose and β-D-fructofuranose are linked by a glycosidic bond, which connects the C-1 carbon of glucose to the oxygen atom at the C-2 carbon fructose; H_2O is formed as a side product of the condensation reaction. In acidic conditions, the glycoside bond is cleaved and invert sugar, which features an equimolar ratio of glucose and fructose, is obtained [14,23].

c) Oligo – and polysaccharides: oligosaccharides feature a defined low number of glycosidic linked monomers. The exact boundary to polysaccharides, which account for the highest amount on earth's biomass, varies with the used literature.

2.2.2 Carbohydrate chemistry and glycosylation

In behalf of the high versatility of carbohydrate based compounds, they are heavily studied for purposes in industry and pharmacy. To name only a few examples, acarbose is an antidiabetic drug, which inhibits the α-amylase activity [24]; Streptomycin is a carbohydrate derivative used to treat diseases caused by penicillin resistant bacteria [25].

Glycosylation reactions are of high importance in research and therefore have been studied extensively; three different strategies are described in literature:

a) Fischer-Helferich method: following an S_N1 mechanism, the formation of the O-glycoside is enabled, as the OH group is removed due to its spatial vicinity to the heteroatom. In the first step, water is removed from the cyclic hemiacetal as the result of an acidic attack at the anomeric OH group yielding a stable oxocarbenium ion. The subsequent reaction with an alcohol yields the desired glycoside [23]; the general reaction scheme is given in Figure 5. In a variation of this method, the Helferich synthesis, the peracylated compound is used, whereas an acetoxy group serves as leaving group. Harsh conditions are needed hereby due to the bad leaving group character of acetoxy residues [26].

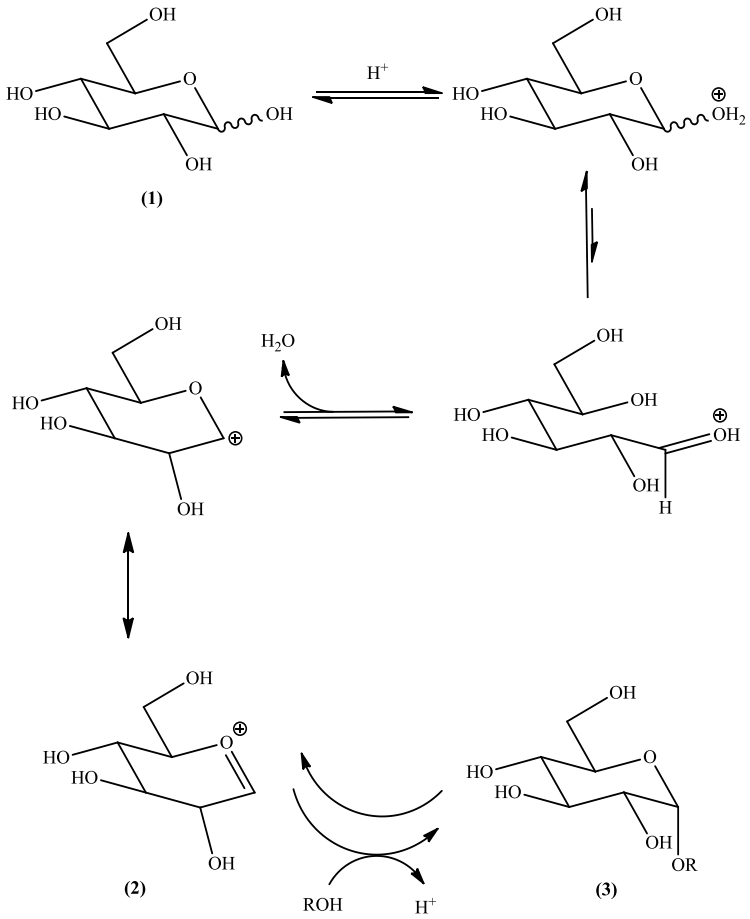

Figure 5: General reaction scheme of Fischer glycosylation; 1 = cyclic hemiacetal, 2 = oxocarbenium ion, 3 = glycoside based on 23

b) Koenigs Knorr method: α-acetobromoglucose is hereby used as glycosyl donor. Obtaining only the desired α-anomer can be explained by the anomeric effect: in the stable anomer, the partial dipole moment of the oxygen's free electron pair negates the one between the anomeric carbon and its strong electronegative residue. Therefore, the β-anomer, where the bromine group is in equatorial position, is unstable. A schematic representation of the anomeric effect is given in Figure 6.

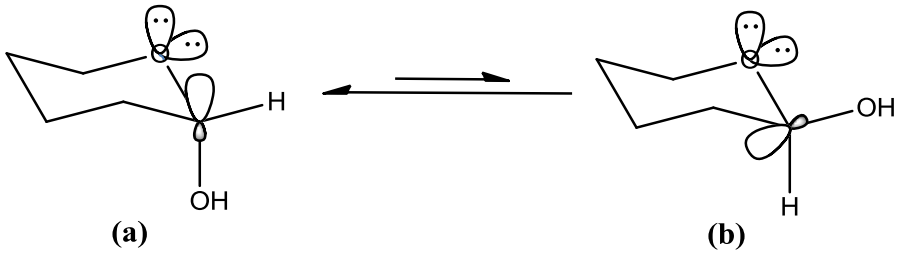

Figure 6: Representation of the orbital induced favorisation of the compound in axial, respective α, (a) to the one in equatorial, respective β, (b) position

The actual insertion of the glycosidic bond is achieved using silver carbonate as promotor, at the surface of which the reaction to the trans glycoside takes place [27].
However, the formation of orthoesters and acetates cannot be circumvented, making column chromatography necessary to obtain the pure compound and expensive Ag_2CO_3 has to be used in high amounts [28].

c) Trichloracetimidate method: compared to the Koenigs Knorr method, this synthesis pathway offers both the advantages of cheaper starting materials, as no heavy metal salts are needed, and of stable products, which is not true for acetobromoglucose. In addition, trichloroacetimidates are good leaving groups and therefore facilate the further glycosylation. Under strong alkaline conditions (e.g. NaH) the reaction of a protected reducing sugar with trichloroacetonitrile enables the formation of the thermodynamically more stable α-anomer; the β-anomer isomerises preferentially when applying prolonged reaction times [23,29].

2.2.3 Protection groups

Considering the fact that carbohydrates feature various OH groups, each of other reactivity, due to absolute position and stereochemistry, synthesis of regioselective pure compounds is only possible using protecting groups. Glucose for instance features the highly reactive anomeric OH group, the primary hydroxyl group has a high reactivity as well, but the secondary OH groups are quite unreactive [23,30]. In addition to acyl and benzyl ether protection groups, which are described in detail, also silyl [23] and allyl [31] ethers, acetals [32] and orthoesters [33] can be installed.

Acyl protecting groups

An example for the use of acyl protecting groups has been given above: in order to derive α-acetobromoglucose, glucose is fully acetylated using acetic anhydride to give pentaacetyl glucose [23]. The transfer of free OH groups into acetyl groups decreases the polarity of the compound, making it better soluble in organic solvents. Deprotection of the acetylated sugar is achieved by the Zemplén method, where the desired carbohydrate is obtained in a saponification reaction after short reaction times when using alkaline conditions [34].

Benzyl ether protecting groups

Benzyl ethers can be installed under neutral, acidic or, as described in 4.3.1, basic conditions. Following the Williamson ether synthesis, in the first step, the reaction of a strong base (e.g. NaH) with the respective non reducing sugar results in the formation of the alkoxide.
Subsequently, the reaction with an alkyl or aryl halogenide to give the desired benzylated compound is possible. Benzyl ethers are inert in the following reaction steps and can easily be removed by hydrogenation, as in the described pathway using palladium on charcoal as mild catalyst and cyclohexene as hydrogen donor [23].

2.3 Steryl glucosides

2.3.1 Classification

Steryl glucosides are minor constituents of vascular plants, where the oxygen at C-3 of a steryl moiety is linked to the anomeric carbon of a sugar by a glycosidic bond. These compounds have also been reported in some kinds of fungi [4], bacteria, algae and animals [35,36,37]. A high degree of heterogeneity in steryl glucosides is given due to four possibilities of variation:

a) Sterol moiety: depending on the origin, phytosterols (e.g. β-sitosterol, stigmasterol, campesterol), animal based sterols (e.g. cholesterol) or mycosterols (e.g. ergosterol) represent the steryl moiety of the steryl glucosides.
b) Type and stereochemistry of the sugar moiety: the most common carbohydrate in natural found steryl glucosides is β-D-glucopyranose; β-D-xylopyranose, β-D-galactopyranose or β-D-glucopyranuronic acid are only found in minor concentrations [3].

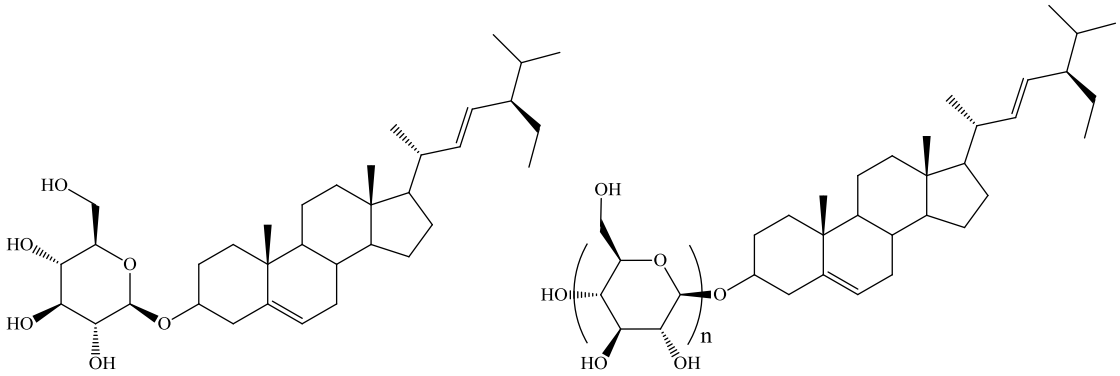

Figure 7: Structure of stigmasteryl-β-D-glucopyranoside (left) and stigmasteryl-(1→4)polysaccharide (right)

c) Number of sugar monomers: in addition to the previously mentioned steryl glucosides, where one carbohydrate molecule is linked to the steryl moiety, also compounds featuring up to five sugar subunits have been reported in azuki beans [12] and rice [13]. Figure 7 gives the structures of both a stigmasteryl mono- and disaccharide.
d) Acylated steryl glucosides (ASG): acylated with a fatty acid chain at C-6' oxygen atom, ASG are more prevalent in natural plant oils than SG (see Table 3).

2.3.2 Biosynthesis

As indicated in Figure 8, the biosynthesis of SG and ASG is a complex process, involving various enzymes and organic species to derive the glucosides. The first step, which is not mentioned in the chart, is the transformation of the membrane bound sterols into free sterols, which is achieved by the enzyme class of glycosyltranferases [3].

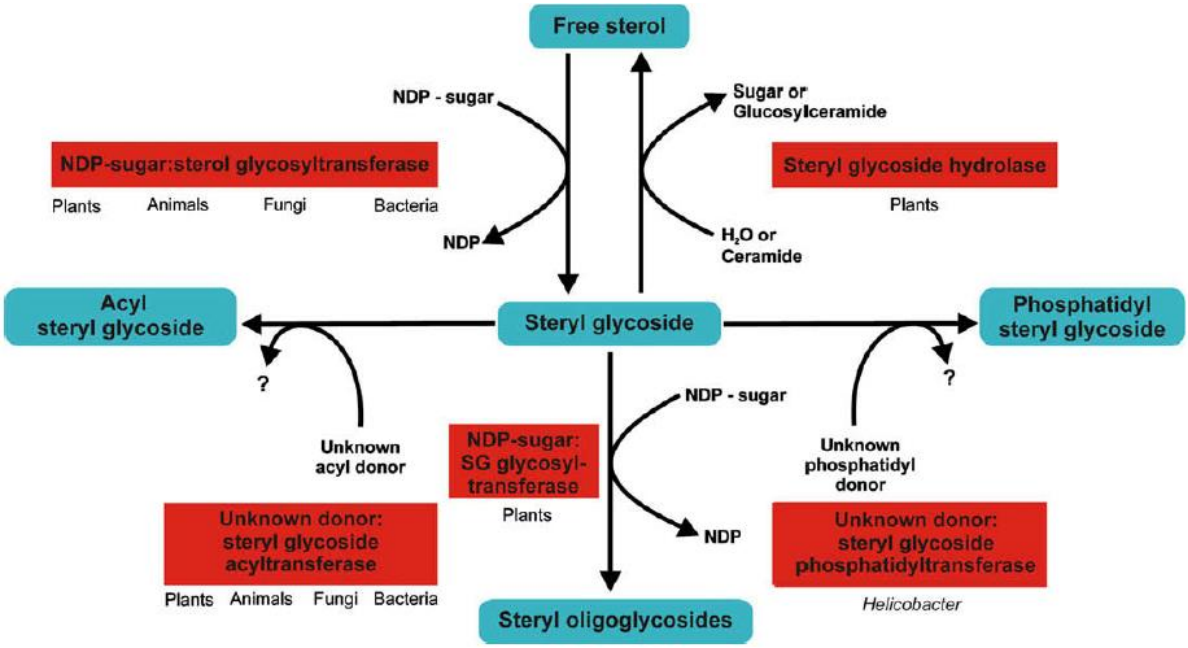

Figure 8: Biosynthetic pathway for the synthesis of SG and ASG; enzymes are highlighted in red, steryl derivatives in blue from 3

2.3.3 Biological function of sterols and their derivatives

Being essential constituents of the cell membrane in eukaryotic animal and plant cells, free sterols as well as steryl glucosides play an important role in the function and structure of the cell membrane, especially in means of fluidity, permeability and flexibility [38,39]. Free sterols are amphiphilic molecules which are being synthesised in the endoplasmatic reticulum and incorporate into different cellular membranes, as for example plasma and mitochondrial membranes [40]. As their size of approximately 2.1 nm resembles the one of a phospholipid layer, a good inclusion into biological membranes is possible [3].

Cholesterol is also involved in the formation of two dimensional liquid crystalline biomembranes. The lateral separation between a thicker ordered phase (L_O phase) and a thinner disorganised phase (L_d phase) can be explained by a better interaction of cholesterol with the organic residues of satured lipids compared to the ones of unsatured [41]. In addition to their importance in the function of cell membranes, sterols are also crucial for the cell's metabolism, as they serve as substrates for various metabolic important compounds, as for example saponins or glycosylated alkaloids [19].

In case of SG and ASG, the sugar residue is located towards the aqueous phase as well. A higher amount of ASG has been found in freezing sensitive plants, which indicates a negative effect of these compounds on low temperature behaviour. This may be explained by the low head group hydration of ASG, which is thought to promote the formation of a hexagonal inverted phase.
This H_{II} phase is known to provoke high freezing stress in the cell, leading to drastic injuries of the protoplast [3]. Considering high temperature behaviour, an increased synthesis of steryl glucosides in different organisms resistant to heat shock has been reported in literature [42,43].

2.3.4 Occurrence in foods and oil plants

The two main fields of research dealing with plant based steryl glucosides are food sciences, as they have various positive effects on health, and biodiesel industry; the latter one is discussed in further detail in 2.3.5. Table 2 gives the content of SG and ASG in selected aliments.

Table 2: SG and ASG content in selected foods from [5]

Sample	SG content [mg/kg dm]	ASG content [mg/kg dm]
Vegetables		
Cauliflower	179.6 ± 7.8	310.9 ± 23.3
Tomato	50.5 ± 4.2	99.5 ± 16.3
Potato	44.0 ± 11.6	49.4 ± 14.7
Seeds		
Sunflower seeds	72.8 ± 2.9	48.7 ± 1.3
Pumpkin seeds	47.3 ± 1.9	71.1 ± 4.3
Nuts		
Peanuts	44.1± 1.8	76.7 ± 5.3
Cashew nuts	71.9 ± 4.6	108.2 ± 10.4
Legumes		
Azuki beans	43.8 ± 3.2	120.5 ± 23.9
Soy beans	89.2 ± 13.2	104.5 ± 18.1
Lentils (orange)	48.4 ± 3.1	57.4 ± 4.3

Lacoste et al. analysed the content of both SG and ASG in various oils and FAME often used for the biodiesel production, the results are given in Table 3 [44].

Table 3: Content of SG and ASG in selected plant oils and FAME [from 44]

Sample	SG content [mg/kg]	ASG content [mg/kg]
Jatropha oil	24	95
Palm oil	11	219
Refined rapeseed oil	nd	nd
Soya oil	13	21
Jatropha ME	18	nd
Rapeseed ME	12	nd
Soya ME	10	nd

As Table 2 and Table 3 show, the content of ASG in plants generally exceeds the content of SG; sunflower seeds nevertheless are an exception where more SG than ASG have been reported. Moreover, the contribution of SG and ASG to the total sterol content varies drastically, from 6.2 % in walnuts to 56.3 % in potatoes [5].

2.3.5 Problems in biodiesel industry related to steryl glucosides

As indicated in Table 3, various oils used for the biodiesel production feature a high amount of SG and ASG, provoking a major problem for this industry. During the transesterification of the triglycerides to FAME, the high pH value triggers the cleavage of the ester bond at C-6 of the sugar (given in Figure 9), resulting in an increase of the SG over the ASG concentration.

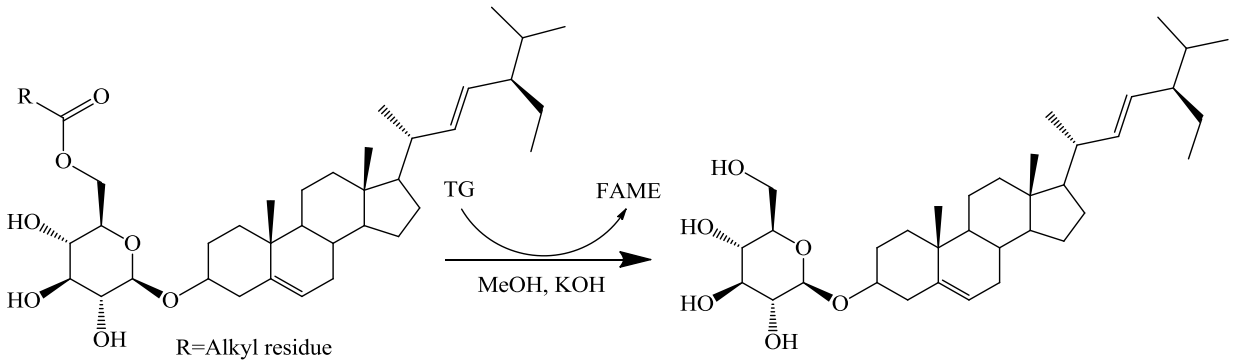

Figure 9: General reaction scheme of the base induced transformation of ASG to SG during the transesterification of triglycerides

The increase of polarity upon loss of the fatty acid chain results in poor solubility of SG in the highly nonpolar FAME, leading to precipitation of these compounds, which further exist in the biodiesel as fine suspended particles [7,45].

Due to the fact that SG precipitate yet at room temperature, the cloud point of the biodiesel is increased, which affects the performance adversely. The precipitation of the particles is facilated at low temperatures and only after long storage periods, the hazy particles deposit at the bottom [46].

Even small concentrations of 10-90 ppm can result in the formation of particles [47], which have been reported to cause clogging of filters, valves and pipes and therefore lowering the performance of the biodiesel upon application. Additionally, precipitation of other insoluble material, as for example saturated monoacyl glycerides, is facilated in biodiesel with a high amount of precipitated SG [48]. When blending biodiesel with fossil based diesel, the solubility of SG is even further decreased [49]. The European Committee for Standardization has therefore regulated the highest amount of insoluble material to a maximum of 24 ppm in biodiesel, which includes among other contaminents steryl glucosides [50].

The impact of SG on the performance of biodiesel with regard to clogging of filters is tested in lab scale by determination of the cold filter plugging point (CFPP): The CFPP is the lowest temperature, at which 20 mL of fuel can pass through a filter featuring a pore size of 45 µm in one minute, when a vacuum of 0.019 atm is applied [51,52].

A variety of mechanical, chemical or enzymatic procedures are available to decrease the amount of SG in biodiesel:

a) Filtration or centrifugation based methods:

One possibility for the removal of the haze forming SG is filtration, which can be performed at room and decreased temperature, the latter one being called cold soak filtration. Hereby, the biodiesel sample is stored at the desired temperature and allowed to reach room temperature without the application of heating or stirring. The sample is filtered under vacuum through a membrane or a filter and the time consumed for the filtration is noted [53]. Tang et al. reported a slightly better removal of SG at temperatures of 4°C compared to room temperature. The concentration of SG in a soybean based biodiesel sample could be reduced from 55 ppm to 49 ppm (11 % reduction) using a glass filter at RT. Applying decreased temperature a content of 40 ppm (27 % reduction) was achieved using the same type of filter. Both the material and the pore size of the membrane did not noteworthy influence the filtration efficiency [54].

Another possible treatment of SG is centrifugation, but as for filtration, the particles have to be allowed to form in order to remove them, which is both a time and a cost issue and does not reduce the amount of dissolved SG.

b) Vacuum distillation:

A strategy to get rid of dissolved SG as well is distillation, upon whose application a decrease of the unwanted compounds' concentration to non detectable levels is possible. However, elevated temperatures can't be circumvented also when performing vacuum distillation [54]. Not only is this an issue concerning cost and time investment, natural antioxidants in the biodiesel, e.g. α-tocopherol, remain in the distillation residue or are not stable at elevated temperatures [55].

c) Chemical adsorption:

Sohling et al. reported a process based on the chemical adsorption of SG to smectite-silica gel, enabling the removal of precipated SG with a concentration of up to 100 ppm in the feedstock to < 20 ppm in the purified biodiesel [56].

d) Enzymatic removal of SG:

As enzymes offer both the possibility of applying mild conditions and recycling, various methods have been described in literature dealing with an enzymatic treatment of biodiesel in order to remove SG. A big advantage of the use of enzymes over mechanical methods is the opportunity to remove SG before the formation of agglomerates and therefore removing dissolved SG as well. Menzella et al. reported the use of thermostable glycosidases or glucosidases, which are able to cleave the glycosidic bond both in SG and ASG to give the sugar residue and the steryl moiety. In addition to an achieved reduction of the SG of > 80 % respective a concentration of 20 ppm in the sample, also impeding monoacylglycerols could be reduced [57]. A similar strategy was applied by Peiru et al. who found that β-glucosidase from Thermococcus litoralis is able to catalyse the hydrolysis of the glycoside bond to give biodiesel with SG levels comparable with those achieved by vacuum distillation. Not only is the need for an emulisifier circumvented in the given method [58], the process has also shown to be applicable for industrial scales [48].

Another interesting approach was reported by Brask & Nielsen, who used fatty acid methyl esters in the biodiesel as acyl donors; different lipases and acyltransferases were used to catalyse the transformation of SG to the soluble ASG. Acyltransferases (EC 2.3.x.x.) are capable of transferring an acyl group from a suitable donor to an acceptor, in the present case from FAMEs to a hydroxyl group at the SG. This method enables a decrease of the SG concentration to lower 5 ppm or a diminution of > 80 % compared to the feedstock. Both Menzella and Brask reported the better performance of immobilised enzymes compared to free ones [59]. Figure 10 gives the chemical mechanisms of the mentioned strategies.

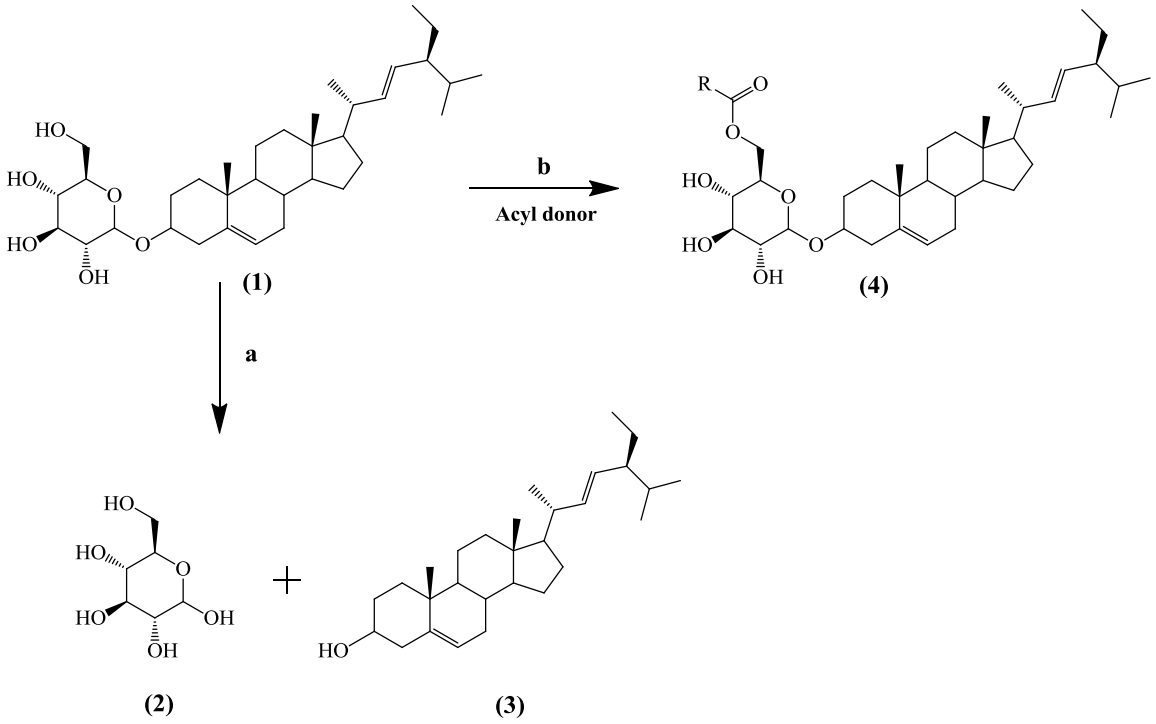

Figure 10: Reaction schemes of the possibilities for enzymatic biodiesel treatment; a = glucosidase, b = lipase or acyltransferase; 1 = SG, 2 = D-glucose, 3 = free sterol, 4 = ASG

2.3.6 Synthesis of steryl glucosides

Free steryl glucosides

For the synthesis of SG two different strategies have been described, being a conventional chemical synthesis upon the application of protection groups and a biocatalytic approach. Kunz & Harreus described the synthesis of cholesteryl-2,3,4,6-tetra-O-acetyl-β-O-glucopyranoside starting from acetobromo glucose and subsequent deprotection with methanolate. As a results of the anomeric effect, only the protected β-anomer is formed [28]; nevertheless, the need for column chromatography and expensive Ag_2CO_3 militate against this method.

A five step synthesis pathway starting from sucrose has been envisioned by Ludwig & Weiss [8,9]. Upon the use of benzyl ether protection groups, the glycosylation is achieved using TMSOTf, where in contrast to the Koenigs Knorr method no chromatographic purification is needed. The overall yield of 32 % exceeds the one of the previously mentioned method (27%), but does not give anomerically pure products.

A one-pot-glycosylation reported by Davis et al. starting from per-O-trimethylsilylated glucose gives the desired SG without the need for column chromatography with a yield of 78 % [60].

Münger et al. describe two different biocatalytic approaches for the synthesis of SG. Reverse hydrolysis with glycosylases and the addition of a surfactant gave β-sitosteryl glucoside with a yield of 16.7 % and cholestanyl glucoside with a yield of 36.9%. The long incubation time of 4 days and small scale applicability stand opposite the circumvention of time consuming protection group chemistry and expensive reagents. As mentioned in 2.3.2, the biosynthesis of SG involves sterol glycosyltransferases, which have also been studied for the obtention of SG in lab scale. Although the reaction has been described to be quantitative, the high price of the activated sugar needed for the reaction is a big drawback of this method [61].

Acylated steryl glucosides

Jäger et al. reported a method to obtain ASG upon the application of acyl chlorides; microwave heating could improve the yield to give 41 % of the desired compound. The reaction has been tested both on its applicability for plant and animal based SG. However, column chromatography is needed due to incomplete conversions and additionally to the monoacylated steryl glucosides, also polyacylated steryl glucosides have been observed [10].

Lipases (EC 3.1.1.3), an enzyme class catalysing the hydrolysis of lipids [62], has also been used for the insertion of ester bonds. In order to prevent hydrolysis, the application of a water free organic solvent is crucial [63]. Paczkowski et al. performed a regioselective acylation of SG upon the use of different lipases. Although high conversion rates were achieved, the small scale without purification, high time consumption and large excess of enzyme and acyl donor militate against this method [64].

Another interesting approach to yield the desired ASG upon the application of lipases has been presented by Davis et al. using vinyl esters as acyl donors and performing subsequent column chromatography, a quantitative acylation could be observed. The lower amount of both acyl donor and enzyme is a big advantage of this method compared to the one described by Paczkowski et al. [60].

3 Analytical methods

3.1.1 Mass spectrometry

The most commonly consulted analysis method in the experimental work was mass spectrometry due to the various advantages of the device. The possibility to obtain results within a few minutes is one major benefit of MS, enabling not only the control of the reaction outcome at the end of the work up, but also monitoring the reaction progress during the course of the synthesis is easy to perform.

In addition to the time saving, also the limit of detection of the used LC/MS-ToF cannot be outperformed by other methods like NMR, where a few milligrams are needed for the analysis. Using liquid chromatography with time of flight mass spectrometry, amounts in the range of femto- to attograms (10^{-15} – 10^{-18} g) can be detected [65].

The following devices are essential for the setup of every mass spectrometer:

1) Sample inlet: For the introduction of the compound of interest into the device different methods are available, being direct insertion, heated reservoir inlet and GC or LC with direct coupling .
2) Ionisation source: Due to the fact that the mass analyser detects sorely charged species, the compound has to be ionised. Therefore, the mass to charge ratio ($^{m}/_{z}$) rather than the molecular weight of the sample are given in the mass spectrum. For that reason, also the possibility of multiple charged ions has to be taken into account. There is a variety of different ionisation methods; the most crucial selection criteria being the nature of the sample and the degree of fragmentation [66].

Using hard ionisation methods like electron ionisation result in the formation of various fragments, whereas soft ionisation (e.g. MALDI) yields only the molecular ion. Table 4 gives an overview of the different methods with the respective outcome of the sample [66,67]:

Table 4: Overview of different ionisation methods

Ionisation method	Sample/species to analyse
APCI	Polar, ionic compounds; M_w up to 1500 Da
Electron Ionisation	Gas phase molecules
Electrospray	Ionics, inorganics, polymers
MALDI	Polymers, surfaces
Secondary Ion Mass Spectrometry	Chemical surface maps; ceramics, steal
Field Desorption	Non polar molecules with high molecular weight
Inductive Coupled Plasma	Elemental analysis

3) Mass analyser: Being the central part of the mass spectrometer, this device enables the separation of the different ions due to the varying mass to charge ratios. Table 5 lists the most important mass analysers with their respective advantages and disadvantages [67]:

Table 5: Overview of different mass analysers and their respective advantages and disadvantages

	Resolution	Mass accuracy	Scan speed	Mass range	Price
Quadrupole	+	-	++	++	+++
Time of Flight	+++	+++	++++	++++	++
Magnetic Sector	+++	+++	+	+++	-
FTMS	++++	++++	++	++	-
Orbitrap	++++	++++	++++	++	+

ToF:

All of the performed MS analyses have been done using a reflector time of flight analyser. The ions of different mass to charge ratios are separated following the principle, that species of a lower molecular mass to charge ratio reach the detector faster than those of a high molecular weight. This principle is clarified in equation 1 & 2.

$$\frac{m * v^2}{2} = E_k = q * V_s \qquad (1)$$

$$t = \frac{d}{v} \qquad (2)$$

The time t needed for an ion to reach the detector is dependent on its velocity v, which in turn is reliant on the kinetic energy E_k and the mass to charge ratio of the analyte [66].

When the resolution isn't sufficient for the analytical problem, a longer tunnel can be installed, as the flight time is proportional to the tunnel length.

4) Detector: As in various other analytical devices, the detector is used for the quantification of the species of interest. Discrete multipliers, channeltrons, post acceleration detectors and micro channel plates can be used [67].

A simplified setup of a ToF-MS is given in Figure 11.

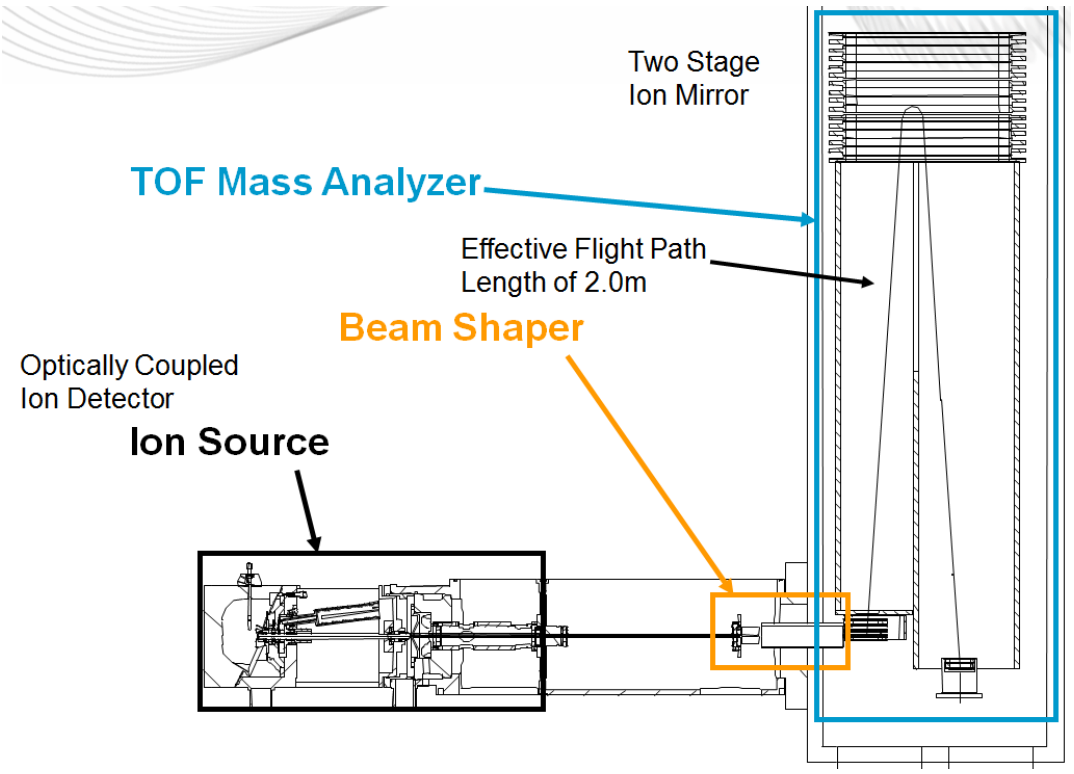

Figure 11: Schematic setup of a ToF MS; [from 68]

MS/MS

Tandem mass spectrometry (MS/MS) is an analytical method involving at least two subsequent steps of mass selection [69]. The first mass spectrometer (e.g. a quadrupole MS) separates the formed ions according to their mass to charge ratio. After the selection of ions of a given $^{m}/_{z}$ ratio, these ions undergo spontaneous or induced fragmentation. In the second mass analyser (e.g. a ToF-MS) the formed product ions are again separated and terminatory detected.

A distinction is made between MS/MS in space or in time: in the previously mentioned one the two mass selection steps take place spaced apart from each other in two different devices. Tandem mass spectrometry in time features a sequential mass analysis in a single analyser like in Iontrap or Orbitrap (FT-MS) analysers. Figure 12 gives a schematic diagram of the processes involved in a MS/MS measurement [66].

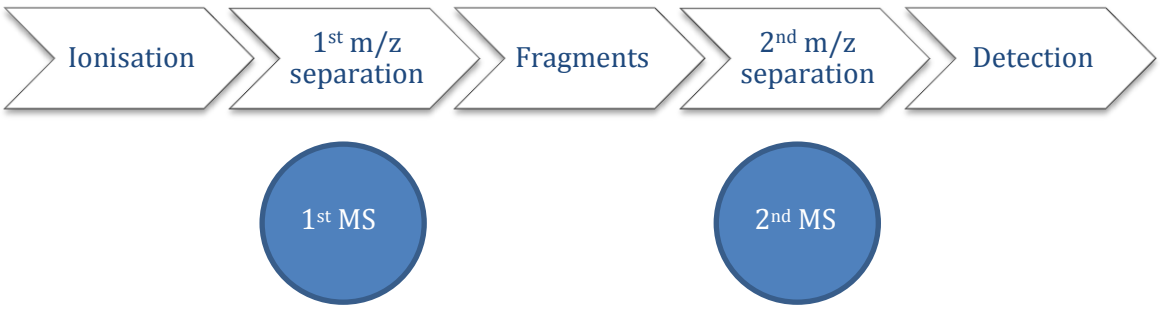

Figure 12: Schematic representation of the processes involved in MS/MS

As steryl glucosides provoke problems already at low concentrations in the feedstock [47], analysis methods with low detection limits are crucial for an accurate determination of this compound class. Mass spectrometry features the advantage of very low detection limits and is also a massive tool to identify the respective steryl moiety. This can be achieved when using soft ionisation methods like ESI or APCI, as the molecular ion peak corresponds hereby to the molecular weight of the compound with the respective ionisation species, as pseudo molecular ion. In addition to the fast measurement this method offers, no complex sample preparation is needed as for example in gas chromatography, where derivatisation is indispensable in the analysis of steryl glucosides.

A major drawback of MS is the fact, that the ionisation efficiency is not the same for all compounds, making exact statements on the actual purity and quantification impossible. Additionaly, the unability to get information on stereoselectivity, as only one signal for the different compounds is obtained, provokes a problem especially when working with carbohydrates. This issue nevertheless can be avoided when applying MS/MS, due to the fact, that different anomers result in diverging fragmentation and therefore can be distinguished from each other [70], offering an alternative to chromatographic methods.

Ion mobility MS

In ion mobility spectrometry, compounds are separated from each other depending on the mobility of the respective species in the gas phase in the presence of a weak electric field. The mobility of the ions is determined using the drift time. At a given electric field strength and a fixed length of the drift tube, it is the time consumed between the injection and the attainment of the drift region. The mobility is highly influenced by the molecular structure of the ion; the more branching the ion features, the higher is the mobility. Another crucial aspect for the mobility that has to be taken into account is the reduced mass μ, which is defined by the product of two masses divided by their sum [71].

$$\mu = \frac{m_1 * m_2}{m_1 + m_2} \qquad (3)$$

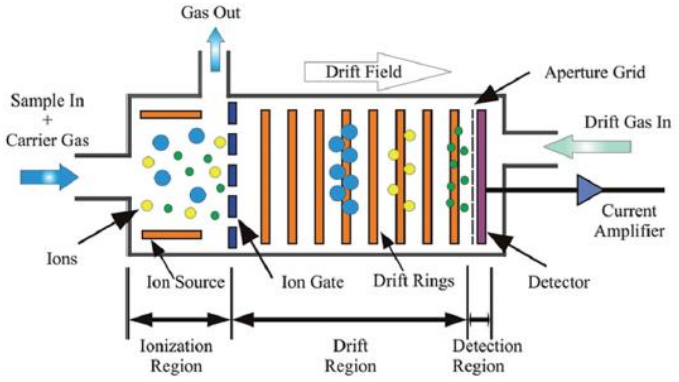

Figure 13: Schematic representation of an IMS system; the blue, green and yellow species correspond to molecules of different sizes from [72]

The separation of anomeric mixtures is a complex problem in liquid chromatography and due to the equal mass to charge ratio of the respective α- and β-anomer, the anomeric ratio cannot be determined with commonly used mass spectrometric methods. The variation in the geometry between the two compounds nevertheless can enable a separation using ion mobility mass spectrometry, as already small variations in the molecule's shape result in a change of the ion mobility.

3.1.2 NMR spectroscopy

In one of the most important methods for structure elucidation used in modern chemistry, the compound of interest is analysed based on its nuclear spin. The precondition for a NMR measurement is therefore a spin moment ≠ 0, which is true e.g. for ^{1}H or ^{13}C nuclei [73]. When applying an external magnetic field, the initial randomly arranged magnetic field produced by the nuclear spin aligns either towards this external source or in the opposite direction according to Boltzmann distribution. The variation of the spins provoked by an external magnetic field is called resonance and is the same for the same type of atom.

As it is influenced by the electrons in its chemical environment, atoms with different substituents feature slightly different resonance frequencies.

On that note it is possible to identify the structure of a substance depending on the electron density distribution of the atoms [74,75].

In the analysis of steryl glucosides, NMR spectroscopy is only of minor importance, as its application is not feasible when dealing with samples containing a variety of different substances. Time consumption, especially for ^{13}C-NMR, expensive deuterated solvents and high sample quantity needed are arguments against this method. However, in the synthesis of SG for analytical pure standards, NMR spectroscopy is crucial not only for confirmation of the desired compound, but also for the determination of the anomeric purity. Since there is a variation between the shifts corresponding to the anomeric carbon atom of the α respective the β-anomer, the anomeric purity can be estimated upon the application of NMR spectroscopy. The lower shift of the α-anomer (93.33 ppm) compared to the β-anomer (97.15 ppm) is the result of the shorter bond length between the anomeric carbon and the hydrogen atom attached to it [76,77].

3.1.3 Gas chromatography

As in all chromatographic methods, the separation of different compounds is enabled by the distribution between a stationary and a mobile phase. For the majority of organic analyses, gas liquid chromatography is applied, where a liquid serves as stationary phase, but also the use of a solid stationary phase is possible. Crucial for applicability of gas chromatography is the enabling of a transfer into the gas phase without simultaneous degradation of the compound of interest. In order for an ideal performance of the GC measurements, carrier gas, sample inlet, column and detector have to be adapted to the respective analytical problem [78,79].

Gas chromatography is a commonly used method for both the qualitative and quantitative analysis of SG in biodiesel. Pieber et al. describe a method for the quantification of SG in biodiesel with a LOQ of 50 µg/kg [80], in which cholesteryl-β-D-glucopyranoside serves as internal standard.

The poor volatility of SG and ASG requires derivatization of the compounds prior to measurement, which is achieved using a silylating agent, as for example MSTFA or BSA+TCMS. Hereby, the free OH groups of the sugar moiety are being silylated, resulting in a decrease of the boiling point which further enables the detection of the SG using a high temperature GC device. BSA+TCMS has been shown to be the more suitable silylating agent, as the resolution of the different steryl glucosides is not satisfying when using MSTFA [80]. This is an issue both for identification and quantification of steryl glycosides, as overlapping signals prevent an accurate analysis, as can bee seen in Figure 14. Another possibility for the analysis of SG is given by the official method for sterol analysis (ISO 12228). After an alkaline hydrolysis to give the sugar and the steryl moiety, the respective silylated sterol is analysed by GC [81].

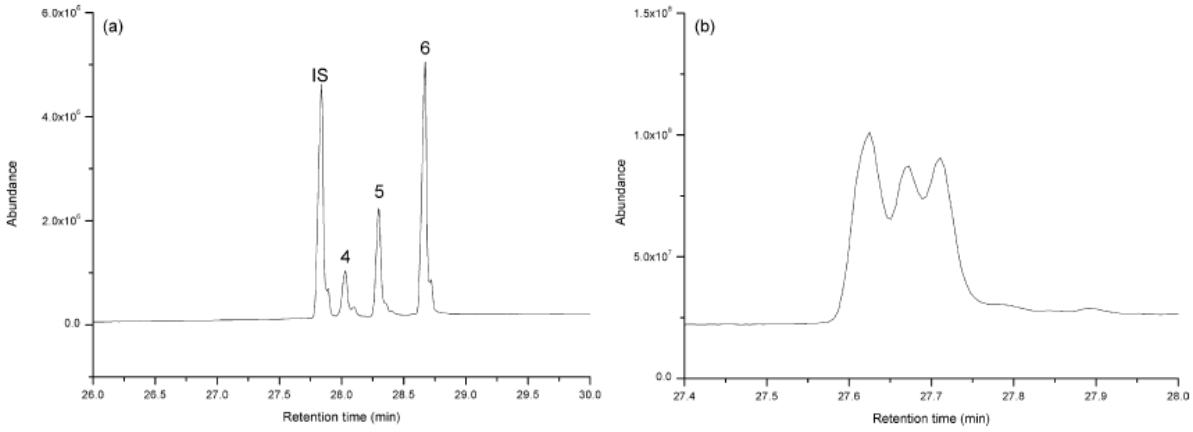

Figure 14: Gas chromatogram of silylated steryl glucosides when using BSA+TCMS (left) and MSTFA (right); 4 = campesteryl-, 5 = stigmasteryl, 6 = β-sitosteryl glucoside from 78

One big advantage of the gas chromatographic analysis of steryl glucosides is the possibility to distinguish between different anomers, as can be seen in Figure 15,which cannot be done using LC/MS-ToF. This feature is of particular importance in reactions which don't give anomerically pure substances, such as the glycosylation reaction with TMSOTf described in 4.3.4. The two obtained peaks with similar retention times correspond to the α-anomer and the β-anomer. Using a nonpolar column and applying the conditions of Pieber et al. [80], the β-anomer features the higher retention time, which was verified by cholesteryl-β-D-glucopyranoside as reference material obtained by Sigma-Aldrich [9].

The exact determination of the purity is a further point accounting for this method, which is possible upon the application of both FID and MS detector. Using ionisation based methods, where the ionisation efficiency is not the same for different compounds, lacks the possibility to get information on the actual purity of the compound.

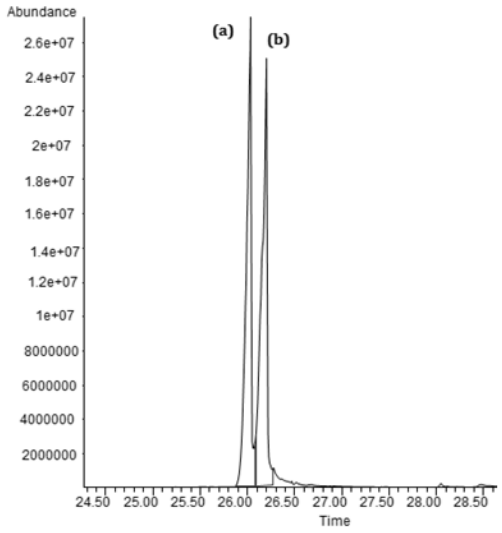

Figure 15: Gas chromatogram of sylilated cholesteryl glucoside, (a) = α-anomer, (b) = β-anomer

4 Experimental and methods

4.1 Instruments

4.1.1 Sample preparation

Balance: BP 3100 P, max. 3100 g, d = 0.01 g, Sartorius

Analytical balance: BP 300 S, max. 303 g, d = 0.0001 g, Sartorius

Rotavapor: HB10 digital, IKA

Auto vortex: SA6, Stuart Scientific

Ultrasonic bath: T460/H, Transsonic

Coulometer: 831 KF Coulometer, Metrohm

Accelerated solvent extractor: Dionex ASE 350, Thermo Fisher

4.1.2 High temperature GC-MS

GC system: 7890A, Agilent Technologies

Autosampler: 7693, Agilent Technologies

Detector: 5975C inert XL MSD with Triple-Axis Detector, Agilent Technologies

Software: MS ChemStation Data Analysis G1701EA E.02.02.1431

4.1.3 NMR

Bruker Avance III spectrometer, 300 MHz

Broadband observe probe head

4.1.4 HPLC MS/ToF

ToF-LC/MS: 6230 TOF LC/MS G6230B, Agilent Technologies

Autosampler: 1260 Infinity, Agilent Technologies

Degasser: G4225A, Agilent Technologies

DAD: Detector G4212B, Agilent Technologies

Software: MassHunter Workstation Rev.B.05.01SP2, Agilent Technologies

4.1.5 Shaker

Laboratory shaker: KS 130 basic, IKA

4.1.6 Microwave

Microwave synthesis reactor: Monowave 300, Anton Paar

Autosampler: MAS 24, Anton Paar

4.1.7 UPLC-Q-ToF-MS

UPLC: Acquity UPLC System, Waters

Column: Acquity UPLC BEH C18 column (50 mm × 2.1 mm, i.d., 1.7 μ m), Waters

MS system: Synapt G2, Waters

4.2 Chemicals

4.2.1 Solvents

2,4,6-Trimethylpyridine , Institute of Chemistry, University of Graz

2-Propanol, Merck

Acetone, Brenntag

Acetonitrile, for HPLC, VWR Chemicals

Chloroform, VWR chemicals

Deuterated Chloroform ($CDCl_3$), 99.8 atom % D, Sigma-Aldrich

Deuterated Dimethylsulfoxide (DMSO d_6), Euriso-top

Diethyl ether, Institute of Chemistry, University of Graz

Dimethylformamide, for synthesis, Merck

Dioxane, Institute of Chemistry, University of Graz

Dichloromethane, VWR chemicals

Ethyl acetate, VWR chemicals

Ethanol, 96 %, VWR Chemicals

Methanol, promochem

n-hexane, ≥ 99%, Roth

Petrol ether (40-60°C), Roth

Pyridine, ≥99%, Institute of Chemistry, University of Graz

Tert-butanol, Institute of Chemistry, University of Graz

4.2.2 Reagents

Acetic acid, Sigma-Aldrich

Ammonium acetate (NH_4Ac), Sigma-Aldrich

Ammonium formiate, Agilent

Azuki beans, grounded, Laboratory of Food Biochemistry, ETH Zürich

Benzyl bromide, 98%, Institute of Chemistry, University of Graz

BSA + TCMS, Sigma-Aldrich

Boron trifluoride diethyl etherate (BF_3*Et_2O), Sigma-Aldrich

Calcium Chloride ($CaCl_2$), Institute of Chemistry, University of Graz

Celite® 545, 89.6%, Roth
Charcoal, pro analysis, Merck
Cholesterol, ≥ 92.5%, Sigma-Aldrich
Cyclohexene, for synthesis, Institute of Chemistry, University of Graz
Formic acid, Sigma-Aldrich
Glucose pentaacetate, Sigma-Aldrich
Hydrochloric acid (HCl) conc., Institute of Chemistry, University of Graz
Hydrogen bromide (HBr), 33% solution in acetic acid (33% HBr/AcOH), for synthesis, Merck
Lipozyme, Novozymes A/S
Lipolase, Novozymes A/S
Molecular sieve 3 Å, Merck
Molecular sieve 4 Å, Merck
Oleic acid methyl ester, Institute of Chemistry, University of Graz
Oleic acid, 90 %, Sigma-Aldrich
Palladium hydroxide ($Pd(OH)_2$) on carbon, 20 wt%, Sigma-Aldrich
Palmitic acid, 98 %, Roth
Novozyme 435, Novozymes A/S
Phosphor pentoxide, Riedel de Haen
Rice grinding flour from basmati rice (India), Riseria Taverna Sa
Rice grinding flour from long grain rice (Italy), Riseria Taverna Sa
Silica gel 60, Fluka
Silver carbonate (Ag_2CO_3), Sigma-Aldrich
β-sitosterol, 60 %, Fluka
Steryl di-, tri- and tetrasaccharides, Werzlab, Technical University of Braunschweig
Stigmasterol, 95 %, Sigma-Aldrich
Sodium chloride (NaCl), (techn.), Institute of Chemistry, University of Graz
Sodium hydride (NaH), 95%, Sigma-Aldrich
Sodium bicarbonate ($NaHCO_3$), Riedel de Haen
Sodium sulfate (Na_2SO_4), ≥ 99%, Institute of Chemistry, University of Graz
Sucrose, Wiener Zucker
Sulfuric acid (H_2SO_4) 98 %, Institute of Chemistry, University of Graz
Trichloroacetonitrile, 98 %, Sigma-Aldrich
Triethylamine, 99%, Institute of Chemistry, University of Graz
Trimethylsilyl trifluoromethanesulfonate, 99%, Sigma-Aldrich

4.3 Synthesis of steryl glucosides starting from sucrose

4.3.1 1,3,4,6-Tetra-O-benzyl-β-D-fructofuranosyl-2,3,4,6-tetra-O-benzyl-α-D-glucopyranoside (2)

Sodium hydride (8.32 g, 347 mmol) was dissolved under vigorous stirring and under nitrogen atmosphere in 100 mL dry DMF, which had been tested on its water content by coulorimetrical Karl Fischer water content determination. 10.11 g (30 mmol) of sucrose **1**, commercially available as sugar, in 200 mL dry DMF were added to the stirred solution, followed by the addition of benzyl bromide (34 mL, 286 mmol) at 0°C. The reaction was allowed to stir for 4-½ h at RT before being quenched with 30 mL MeOH, which resulted in the formation of gas. During the course of the reaction, the colour of the solution changed to yellow and the precipitation of a colourless solid could be observed. The solvent and formed dibenzyl ether were removed under reduced pressure and the product was extracted with DCM, dried using Na_2SO_4 and the solvent was removed again. The product was dissolved in dry Et_2O, followed by filtration over charcoal/celite. After removing the solvent, 30.24 g (29 mmol, 98 %) of a brown oil were obtained.

R_f value: 0.64 (n-hexane/ethyl acetate 2/1)

4.3.2 2,3,4,6-Tetra-O-benzyl-α-D-glucopyranose (3)

The crude starting material **2** (30.24 g, 29 mmol) was dissolved in 300 mL acetone, followed by the slow addition of 17 mL HCl conc. The reaction was allowed to stir under reflux for 90 minutes, where the solution changed colour from yellow to dark brown. The solvent was removed under reduced pressure and the product was extracted with DCM, followed by drying over Na_2SO_4 and removing the solvent again. The obtained brown residue was dissolved in 100 mL hot EtOAc before adding n-hexane in order to precipitate the desired compound. The colourless solid was isolated using suction filtration and the filtrate was stored at -25°C in order for more product to precipitate. This step was carried out several times before recrystallising the compound from MeOH. 9.10 g (16.8 mmol, 58 %) of fine colourless crystals were obtained.

R_f value: 0.38 (n-hexane/ethyl acetate 2/1)

MP: 156°C

4.3.3 2,3,4,6-Tetra-O-benzyl-α-D-glucopyranosyl trichloroacetimidate (4)

Compound **3** (8.06 g, 14.9 mmol) was dissolved in 80 mL dry DCM, followed by the addition of 20 mg sodium hydride and 7 mL trichloroacetonitril (69.8 mmol). An additional 300 mg of NaH were added to enable complete conversion and anomerisation.

The reaction was monitored using TLC and was allowed to stir 4 h at room temperature. The product was filtered over silica gel and the solvent was removed under reduced pressure, before redissolving the compound in Et_2O and repeating the filtration and evaporation step. 10.03 g (14.7 mmol, 98 %) of an oily product were obtained.
R_f value: 0.61 (n-hexane/ethyl acetate 2/1)

4.3.4 Steryl 2,3,4,6- tetra-O-benzyl-D-glucopyranoside (5)

With TMSOTf

A sample of **4** was dissolved in dry DCM, which had been distilled over P_2O_5 and stored over molecular sieve 3 Å. After the addition of molecular sieve and the respective sterol moiety (see Table 6), the solution was allowed to stir for 15 minutes under nitrogen atmosphere. Freshly prepared 0.02 M TMSOTf solution was added slowly, which resulted in a colour change of light yellow to brown. The reaction was stirred until TLC indicated no more variation in the reaction progress. After quenching the reaction with Et_3N, the molecular sieve was filtered off and the solvent was removed under reduced pressure. Drying over night under reduced pressure over $CaCl_2$ yielded a brown solid. In order to purify the product, it was stirred in a solution of MeOH/dioxane (10/1). The colourless precipitate was isolated by repeatedly performed centrifugation to give a colourless solid.

Table 6 shows the quantities used, the applied conditions as well as the yield of the respective products. **5a** corresponds to stigmasteryl 2,3,4,6-tetra-O-benzyl-D-glucopyranoside, **5b** to cholesteryl 2,3,4,6-tetra-O-benzyl-D-glucopyranoside and **5c** to β-sitosteryl 2,3,4,6-tetra-O-benzyl-D-glucopyranoside. TLC was performed on silica with n-hexane/EtOAc 3/1. The two R_f values correspond to the two anomers, with the α-anomer featuring the lower and the β-anomer the higher number.

Table 6: Quantities, yields, conditions and characteristics of the respective steryl glucoside a = stigmasteryl, b = cholesteryl, c = β-sitosteryl moiety

	5a	**5b**	**5c**
Trichloroacetimidate	3.54 g, 5.2 mmol	2.12 g, 3.1 mmol	1.26 g, 1.8 mmol
Sterol	1.80 g, 4.4 mmol	1.00 g, 2.6 mmol	0.64 g, 1.6 mmol
Solvent [mL]	100	30	70
TMSOTf	83 µL in 23 mL DCM	50 µL in 14 mL DCM	29 µL in 8 mL DCM
Et_3N [mL]	3	1.80	1.10
Reaction time [h]	2-½	2-½	4
R_f value [ ]	0.60, 0.57	0.61, 0.58	0.63, 0.61
MP [°C]	118	114-119	119
Yield	2.02 g, 2.2 mmol, 50 %	1.71 g, 1.9 mmol, 59 %	0.89 g, 0.9 mmol, 60 %

*With BF_3*Et_2O*

A stirred solution of **4** (1.02 g, 1.46 mmol) and cholesterol (0.46 g, 1.13 mmol) in 50 mL dry DCM was cooled to –20°C and was allowed to stir 15 minutes under nitrogen protection in the presence of molecular sieve 3 Å. 1 mL BF_3*Et_2O was added and the reaction was allowed to stir 3 h at the given temperature. After quenching with Et_3N and removing the molecular sieve and the solvent, the crude product was dried over night over $CaCl_2$ under reduced pressure. Stirring in MeOH/dioxane (10/1) and subsequent centrifugation gave 505.3 mg of a colourless solid. Due to the presence of starting material in the product, a calculation of the yield in this step is not feasible.

R_f value: 0.61, 0.58, 0.22 (n-hexane/ethyl acetate 3/1)

4.3.5 Steryl-D-glucopyranoside (6)

The protected starting material **5** was dissolved in EtOH/cyclohexene 2/1 and was stirred under nitrogen atmosphere for 15 minutes. After the addition of approximately 100 mg of $Pd(OH)_2$, the reaction was heated to reflux conditions and stirred for 24 h, while the reaction was monitored using LC/MS-ToF and TLC. For a total conversion, two more spatula of catalyst were added and also additional solvent was supplied. The catalyst was removed upon suction filtration over celite and the solvent was evaporated under reduced pressure to yield a colourless powdery solid.

Table 7 shows the quantities used, the applied conditions as well as the yield of the respective products. **6a** corresponds to stigmasteryl-D-glucopyranoside, **6b** to cholesteryl-D-glucopyranoside and **6c** to β-sitosteryl-D-glucopyranoside.

Table 7: Quantities, conditions, yields and characteristics of the respective sterylglucosides; 6a = stigmasteryl, 6b = cholesteryl, 6c = β-sitosteryl moiety

	6a	6b	6c
Protected SG	2.02 g, 2.2 mmol	1.71 g, 1.9 mmol	0.87 g, 0.9 mmol
Solvent [mL]	150	150	80
R_f value [ ] $CHCl_3$/MeOH 10/1	0.17	0.18	0.21
MP [°C]	210	243	200
Yield	1.24 g, 2.2 mmol, > 99 %	1.02 g, 1.9 mmol, > 99 %	0.50 g, 0.9 mmol, 94 %

4.4 Synthesis of steryl glucosides using the Koenigs Knorr mechanism

4.4.1 2,3,4,6-Tetra-O-acetyl-α-D-glucopyranosylbromide

To glucose pentaacetate (8.00 g, 20.4 mmole) 18 mL of HBr (33 % in glacial acetic acid) were added at 0°C while vigorous stirring. In order to obtain a homogeneous mixture, the reaction flask was shaken in addition. After removing the ice bath, the reaction was allowed to stir for 4 h at RT, while being monitored using TLC. The solution was poured slowly onto ice water while stirring with a glass rod, which resulted in the formation of a colourless precipitate. This was finely grounded, before the water was removed by suction filtration. The product was dissolved and extracted in Et_2O. After drying over Na_2SO_4, the ether was removed under reduced pressure. The desired compound was obtained as a colourless viscous liquid; in order to obtain crystals, the compound was dissolved in Et_2O and petrol ether was added until the formed streaks didn't vanish anymore upon shaking. The compound was allowed to recrystallise overnight in the fridge, resulting in fine colourless needles, which were isolated by suction filtration. The compound was dried over $CaCl_2$ under reduced pressure in the fridge.

Yield: 7.52 g (18.3 mmol, 89 %)

R_f value: 0.70 (PE/acetone 5/4)

MP: 90°C

4.4.2 β-Sitosteryl-2,3,4,6-tetra-O-acetyl-β-D-glucopyranoside

Acetobromo glucose (1.45 g, 2.5 mmol) and Ag_2CO_3 (1.83 g, 3.0 mmol) were dissolved in Et_2O and stirred under nitrogen atmosphere before molecular sieve 3 Å (5.11 g) and β-sitosterol (1.12 g, 2.7 mmol) were added. The grey emulsion was allowed to stir overnight at RT under nitrogen atmosphere.

After filtration of the formed AgBr and the molecular sieve, the product was partioned between Et_2O and aq. sat. $NaHCO_3$ and the organic phase was dried over Na_2SO_4. The drying agent was removed by filtration before removing the ether under reduced pressure. 1.83 g of a colourless solid were obtained, which was purified by recrystallisation from MeOH/Acetone and flash chromatography (PE/Acetone 4/1 on silica gel).
Yield: 131 mg (0.05 mmol, 7 %)
Rf value: SG: 0.16, β-sitosterol: 0.34, orthoester: 0.23 (PE/Acetone 4/1)

4.5 Enzymatic acylation of SG to ASG

4.5.1 Enzyme reactions using the shaker

6b, alkyl ester of different fatty acids, the respective solvent and molecular sieve 3 Å were incubated on the shaker in a drying oven at a temperature of 50°C. Fatty acid butyl esters and fatty acid ethyl esters have been prepared in a previous thesis and were based on a tallow fat feedstock. The exact amounts of each compound are given in Table 8. Upon stirring at 240 rpm, approximately 100 mg of the respective enzyme were added. The course of the reaction was controlled using LC/MS-ToF in APCI negative mode.

Table 8: Test series for acylation of SG using the shaker

	SG [mg]	Acyl donor		Enzyme	Solvent	
		Type	Amount		Type	[mL]
1	30.2	OAME	347.3 mg	Novozyme 435	n-hexane	30
2	29.5	FAEE	352.1 mg	Novozyme 435	tert-butanol	30
3	31.3	FABE	350.6 mg	Novozyme 435	tert-butanol	30
4	9.8	FABE	10 mL	Novozyme 435	n-hexane	1
3	10.6	FAEE	10 mL	Novozyme 435	n-hexane	1
5	8.9	FAEE	10 mL	Lipozyme	tert-butanol	1
6	11.2	FAEE	10 mL	Lipozyme	n-hexane	1
7	10.7	FAEE	10 mL	Lipolase	tert-butanol	1
8	9.8	FAEE	30.2 mg	Novozyme 435	tert-butanol	1

4.5.2 Acylation using a thermomixer

6b and the respective acyl donor were dissolved in 1 mL n-hexane and molecular sieve 3 Å was added, before the test tubes were incubated on the epi shaker at a temperature of 55°C. The exact amounts used are given in Table 9. Approximately 100 mg of the respective enzyme were added and the reaction was allowed to stir 48 h at 400 rpm.

Table 9: Test series for acylation of SG using the epi shaker

	SG [mg]	Acyl donor		Enzyme
		Type	Amount	
1	19.6	OAME	430 µL	Novozyme 435
2	22.6	OAME	430 µL	Lipozyme
3	23.1	OAME	430 µL	Lipolase
4	18.9	Oleic acid	400 µL	Novozyme 435
5	20.7	Palmitic acid	327 mg	Novozyme 435

4.5.3 Acylation under conventional stirring

Cholesteryl-(6'-O-oleoyl)-D-glucopyranoside (7a)

A 0.50 g (0.9 mmol) sample of **6b** and oleic acid methyl ester (10 mL, 30.3 mmol) were dissolved in 200 mL n-hexane and 4.90 g molecular sieve 3 Å were added to the flask. The reaction was allowed to stir under nitrogen atmosphere and was heated to 60°C, before approximately 500 mg of Novozyme 435 were added in two portions. After stirring for 48 h, the molecular sieve and enzyme were removed by filtration over glass wool and smaller particles upon suction filtration. After rinsing with n-hexane and DCM, the solvent was removed under reduced pressure. The product was purified by flash column chromatography with $CHCl_3$/MeOH (95/5).

Yield: 0.35 g (0.43 mmol, 47 %)

R_f value: 0.14 ($CHCl_3$/MeOH 95/5)

Cholesteryl-(6'-O-palmitoyl)-D-glucopyranoside (7b)

Palmitic acid (12.53 g, 48.8 mmol), 30 mL MeOH and 0.125 mL H_2SO_4 conc. were heated to reflux conditions and stirred for 4 h. The mixture was washed with water, until the water phase featured a neutral pH value and the ester phase was dried under reduced pressure. The purity of the fatty acid methyl ester was controlled using GC/MS and the melting point.

6b (102 mg, 0.18 mmol) and 1.48 g (5.5 mmol) palmitic acid methyl ester were suspended in 150 mL dry hexane and heated to 60°C under nitrogen atmosphere. Molecular sieve 3 Å was added to the flask and the stirring was continued for 15 minutes, before 500 mg of Novozyme 435 was added. The reaction was allowed to stir for 24 h. When LC/MS-ToF did not indicate any more SG, the enzyme and molecular sieve were removed by suction filtration. After rinsing with n-hexane and DCM, the solvent was evaporated under reduced pressure. Purification by flash column chromatography with $CHCl_3$/MeOH (95/5) gave the desired ASG.

Yield: 87 mg (0.11 mmol, 61 %)

R_f value: 0.14 ($CHCl_3$/MeOH 95/5)

4.5.4 Microwave heating conditions

A 50 mg sample of the respective SG was suspended in 10 mL n-hexane and the respective amount of acyl donor and approximately 100 mg of Novozyme 435 were added. The reaction was carried out for 3 h at 60°C with an agitation speed of 400 rpm. Also solvent free systems were investigated. Table 10 gives the tested conditions.

Table 10: Test series for acylation of SG using the microwave

	SG moiety	Acyl donor	Molar ratio SG/ acyl donor	Solvent
1	Phytosteryl-SG	OAME	1:1	n-hexane
2	Phytosteryl-SG	OAME	1:10	n-hexane
3	Phytosteryl-SG	Oleic acid	1:10	n-hexane
4	Phytosteryl-SG	Palmitic acid	1:20	n-hexane
5	Phytosteryl-SG	Oleic acid	1:20	none
6	Stigmasteryl-SG	Oleic acid	1:20	none
7	Cholesteryl-SG	Oleic acid	1:60	none
8	Cholesteryl-SG	PAME	1:20	none

4.6 Analysis of steryl polyglucosides in food samples[1]

For the determination of steryl polyglucosides in aliments, three different food samples were investigated, being azuki beans, basmati rice and long grain rice. The extraction was done according to the method of Nyström et al. with small variations [5]. Approximately 2 g of the respective sample were extracted with acetone using an accelerated solvent extractor at a temperature of 120°C for 10 minutes. Each sample was extracted in three cycles. The obtained extract was evaporated under reduced pressure and redissolved in hexane/isopropanol 95/5. In order to obtain the steryl glucosides, solid phase extraction was performed with InertSep® 2 OH (Diol) SPE Tubes (500 mg, 3 ml). Table 11 gives the two tested strategies to obtain the steryl oligosaccharides from the matrix.

[1] Performed at the Laboratory of Food Biochemistry at the ETH Zurich

Table 11: Tested strategies for the obtention of steryl oligosaccharides when applying SPE

Method 1 based on 5	**Method 2** based on 82
Activation with 5 mL n-hexane	Activation with 5 mL n-hexane
Loading with sample dissolved in 2.5 mL n-hexane/isopropanol 95/5	Loading with sample dissolved in 2.5 mL n-hexane/isopropanol 95/5
Washing with 5 mL n-hexane	Washing with 5 mL n-hexane
Washing with 5 mL hexane/isopropanol 97/3	Washing with 5 mL n-hexane/Et_2O 9/1
Eluting with 7.5 mL hexane/isopropanol 92/8	Eluting with 7.5 mL n-hexane/Et_2O 1:1
Eluting with 7.5 mL n-hexane/isopropanol 70/30	Eluting with 7.5 mL acetone
Eluting with 7.5 mL isopropanol	

The presence of the desired compound was monitored by TLC with $CHCl_3$:MeOH:H_2O (65:25:4). After removing the respective solvent under mild nitrogen stream, the product was redissolved in MeOH and analysed using UPLC/MS-ToF according to the method by Oppliger et al. [83].

4.7 Sample preparation for analytical methods

4.7.1 Thin layer chromatography

TLC was performed on silica on aluminium plates, using different mobile phases for the respective compounds. Due to the lack of a conjugated π-system in the investigated samples, detection using UV was not possible. Therefore, the plates were sprayed with H_2SO_4 conc. and visualized upon subsequent heating or treated with bromocresol green.

4.7.2 LC/MS-ToF analyses

A small amount of the sample (ca 0.5 mg) was dissolved in acetonitrile and was measured applying the parameters given in Table 12. When the sample was not soluble in acetonitrile, a few drops of pyridine were added, the vial was shaken using a vortex and the sample was treated for a short period in the ultra-sonic bath. The sample was introduced into the device using a 1200 HPLC injector by Agilent.

Table 12: Parameters for LC/MS-ToF analyses

APCI	Positive/ Negative* mode	APCI	Positive/ Negative* mode
Gas Temp. (N_2)	325°C	**Injection**	0.5-2 µL
Corona	4 µA/22 µA*	**Isocratic flow**	0.3 mL/min
Capillary	0.078 µA	**Lock mass correction**	922,009798 Da/ 966,0007250 Da*
Chamber	5.33 µA	**Nebulizer**	40 psig
Column temp.	30°C	**OCT 1 RF Vpp**	750 V
Corona	176 V	**Skimmer**	65 V
Drying gas	8 L/min	**Solvent**	30% H_2O, 70% (90% ACN, 10% H_2O (0,1% Ammonium formate)) isocratic
Fragmentor	175 V	**Vaporizer**	350°C

4.7.3 UPLC/MS-ToF[1]

A solution of approximately 10 µM of the respective steryl mono-, di-, tri- or tetrasaccharide in MS grade MeOH was prepared and 1 to 10 µL were injected to the device. The steryl oligosaccharides were obtained from Professor Daniel B. Werz (Technical University of Braunschweig) [84]. The UPLC gradient for the measurements is given in Table 13, the MS conditions in Table 14. In order to obtain good ionisation, formic acid (0.1 v%) or a mixture of acetic acid (0.1 v%) and NH_4Ac (1 mM) were added to the mobile phase as additives. The flow rate was set to 0.3 mL/min at a column temperature of 40°C using a UPLC BEH C18 column.

Table 13: UPLC gradient for steryl polyglucoside measurements based on 83

Time [min]	H_2O [%] + additive	MeOH [%] + additive
0	50	50
1	50	50
3	12.5	87.5
5	10	90
7	0	100
10	0	100
13	50	50

[1] Performed at the Laboratory of Food Biochemistry at the ETH Zurich

Table 14: Parameters for MS-ToF analyses performed at the ETH Zurich based on 83

ESI	Positive/ Negative* mode	ESI	Positive/ Negative* mode
Capillary voltage	3 kV/2 kV*	**Desolvation gas flow rate**	850 L/h/ 800 L/h*
Sample voltage	60 V/30 V*	**Source temp.**	130°C
Cone voltage	4.5 V	**Cone gas flow**	20 L/h
Desolvation gas temp.	520°C/500°C*	**Column**	UPLC BEH C18 column

4.7.4 Ion mobility MS[1]

The sample preparation for the ion mobility measurements was done as described in 4.7.3, the respective parameters were the same as mentioned in Table 14, additional ones are given in Table 15.

Table 15: Additional parameters for IMS-MS

Source wave velocity	300 m/s	**IMS wave velocity**	500 or 600 m/s
Trap wave velocity	311 m/s	**IMS wave height**	40 V
Trap wave height	6 V	**Transfer wave velocity**	191 m/s
		Transfer wave height	4.0 V

4.7.5 Q-ToF-MS[1]

Tandem mass spectrometry was performed applying the parameters given in Table 16.

Table 16: Parameters for MSMS analyses

ESI	Positive mode	ESI	Positive mode
Capillary voltage	2.8 kV	**Desolvation gas flow rate**	800 L/h
Sample voltage	15 V	**Source temp.**	120°C
Cone voltage	4 V	**Cone gas flow**	20 L/h
Desolvation gas temp.	250°C		

[1] Performed at the Laboratory of Food Biochemistry at the ETH Zurich

The selected mass to charge ratios for the first ionisation in the MSMS measurements of the respective compounds are given in Table 17.

Table 17: Selected mass to charge ratios for the ionisation in the MSMS measurements

Compound	Selected $^{m}/_{z}$ ratio
Monosaccharide (α&β)	597.41
β-Disaccharide	759.47
α-Trisaccharide	921.53
α-Tetrasaccharide	1083.58

4.7.6 GC/MS

Owing to the high amount of free OH groups, evaporation of the derived steryl glucosides cannot be performed with the given parameters, making GC analysis unsuitable. Silylating the compound prior to GC/MS analysis lowers the boiling point and the compound can be detected. Approximately 4.5 mg of the sample were dissolved in 100 µL pyridine, before adding 100 µL BSA+TCMS and heating the reaction for 1 h at 70°C. After cooling to RT, the sample was diluted with 1 mL pyridine and GC/MS analysis was carried out; the parameters are given in Table 18.

Table 18: Parameters for GC/MS analyses based on 80

Column	DB-5HT (max. 400°C; 30 m; 0.25 mm; 0.10 µm)
Carrier gas	Helium 5.0
Carrier gas flow rate	1 mL/min
EI	70 eV
Injection volume	1 µL
Injector	COC
MS temperature	350°C
Quadrupole temperature	180°C
Syringe volume	5 µL
Temperature program	
Start temperature	100°C
Hold time	2 min
Gradient	10°C/min
End temperature	370°C
Hold time	15 min

5 Results and discussion

In order to avoid the use of costly silver carbonate as well as column chromatography needed in the Koenigs Knorr mechanism, a five step reaction pathway for the synthesis of steryl glucosides was studied and modified. So far, the reaction had only been tested on its applicability on cholesterol, but not on stigma- or β-sitosterol. Figure 16 shows the reaction scheme of the synthesis starting from sucrose.

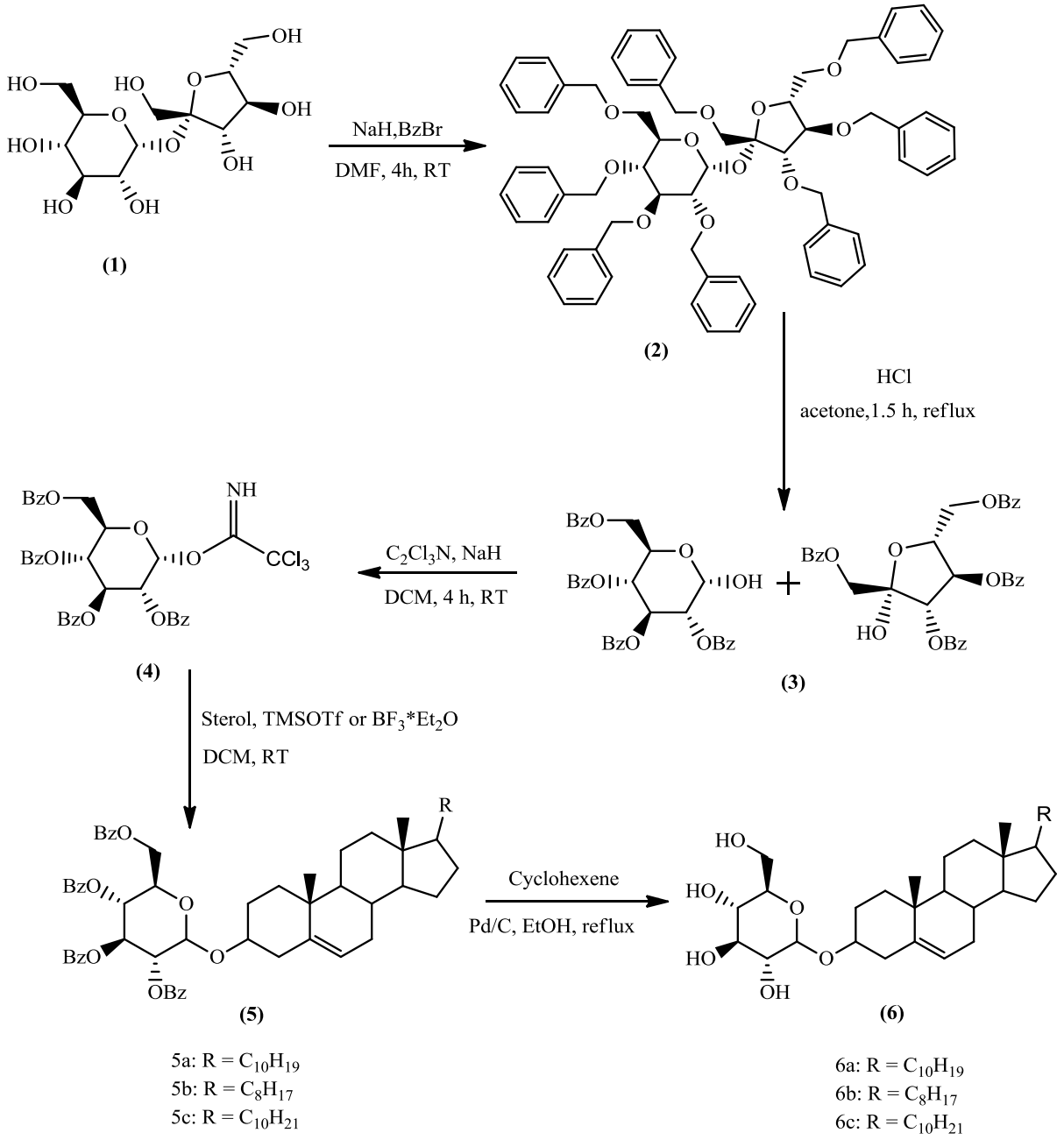

Figure 16: Reaction scheme of the synthesis pathway starting from sucrose

5.1 Synthesis of steryl glucosides starting from sucrose

5.1.1 1,3,4,6-Tetra-O-benzyl-β-D-fructofuranosyl-2,3,4,6-tetra-O-benzyl-α-D glucopyranoside (2) [85]

For the insertion of the benzyl ether protection groups the Williamson's ether synthesis was used, whereat the sucrose was activated in the first step using a strong base in order to convert the hydroxy groups into alkoxides. Alkoxides are excellent nucleophils, enabling the subsequent S_N2 reaction to derive the ethers. The bromine leaving groups react with sodium to give sodium bromide, leading to the formation of colourless precipitate during the course of the reaction.

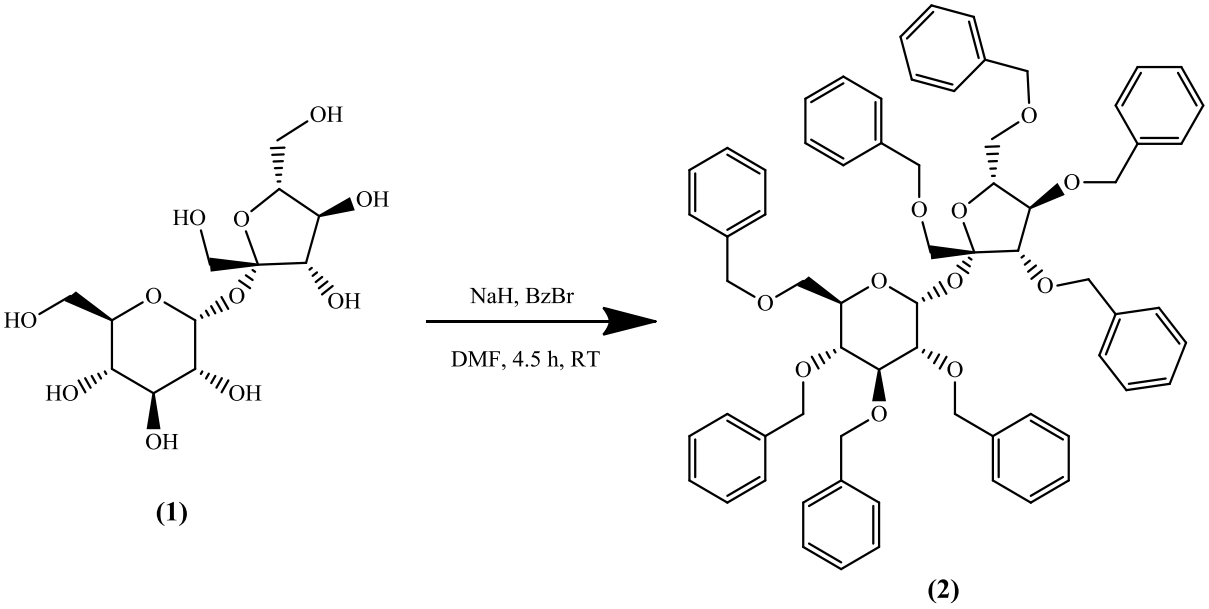

Figure 17: General reaction scheme step 1, insertion of the protection groups

The chosen reaction has various advantages compared to other methods as for instance the Koenigs Knorr method. On the one hand, sucrose is a cheap and nontoxic starting material, on the other hand, due to the fructanosyl residue, a protection of the anomeric OH group is not necessary. One drawback of the chosen method is the safety issue, as NaH reacts violently with water, so complete absence of water is crucial. Therefore, the water content of the used solvent was determined in advance using Karl Fischer titration and the solvent was stored over molecular sieve 4 Å. In order to prevent reactions with air moisture, the reaction was performed under nitrogen atmosphere.

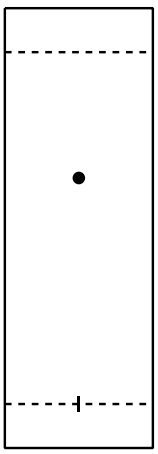

Figure 18: TLC, step 1, 4 h

In addition to safety issues, the presence of water also favours the formation of unwanted side products. Using fresh NaH is crucial for the success of the reaction as otherwise only an incomplete protection of the sugar will be achieved, which diminishes the yield in the subsequent step. Dibenzyl ether as the major side product can be removed at 75 mbar and 70°C, a distillation is not necessary.

The course of the reaction was followed using TLC and LC/MS-ToF. As only one spot was visible on the TLC, a high degree of purity of the product could be assumed; this was confirmed by LC/MS-ToF. The mass spectrum obtained using APCI in positive mode shows the main peak at 1081 $^{m}/_{z}$ which corresponds to the octabenzyl sucrose in combination with the ammonium ion.

Yield: 30.24 g (29 mmol, 98% theoretical, 99% literature)

R_f: 0.64 (n-hexane/ethyl acetate 2/1)

LC/MS-ToF

APCI positive mode: calculated for $[C_{68}H_{70}O_{11}+NH_4]^+$: 1080.52564 $^{m}/_{z}$, detected: 1080.52601 $^{m}/_{z}$, Δm: - 0.344 ppm

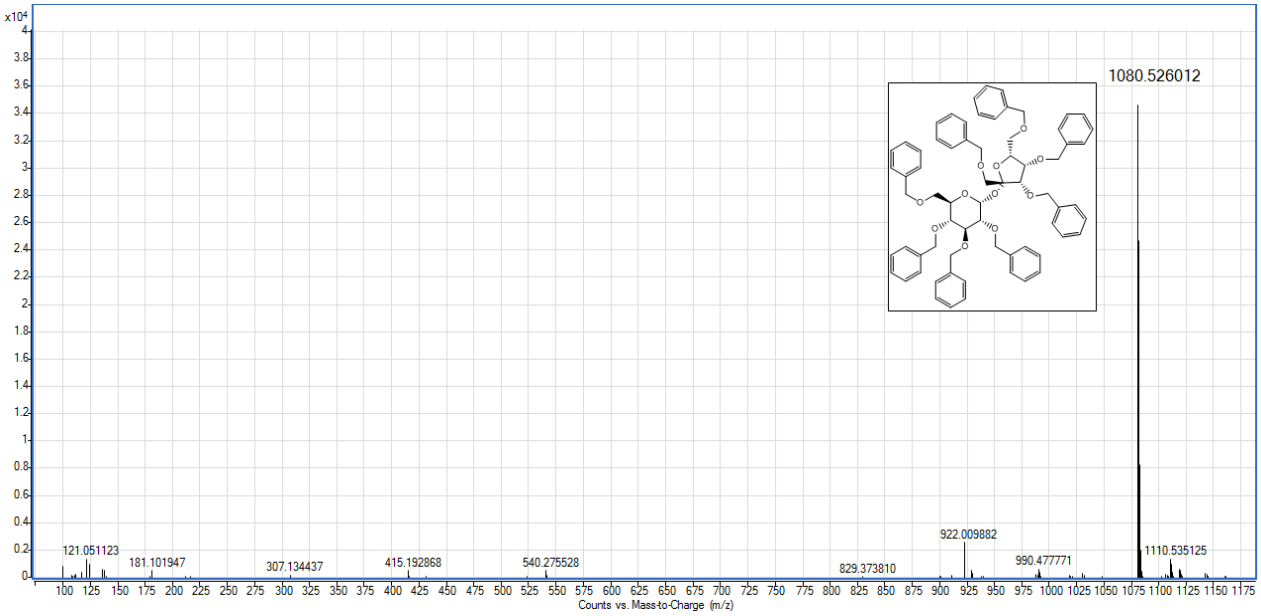

Figure 19: LC/MS-ToF, APCI positive mode, step 1

5.1.2 2,3,4,6-tetra-O-benzyl- α-D-glucopyranose (3) [85]

In the second step of the synthesis pathway, acid catalysed hydrolysis of the octabenzyl sucrose at the anomeric carbon was carried out. Using HCl conc. as H^+ donor poses the advantages of a cheap reactant and milder conditions compared to super acids or high temperatures. This is crucial, due to the fact that harsh conditions, like high temperatures, would result in a loss of protection groups. Additionally, the ether bond between the two saccharides is cleaved in the acid medium, making it possible to remove the fructose moiety without loss of the benzyl ether groups by simple precipitation of the fructanosyl residue.

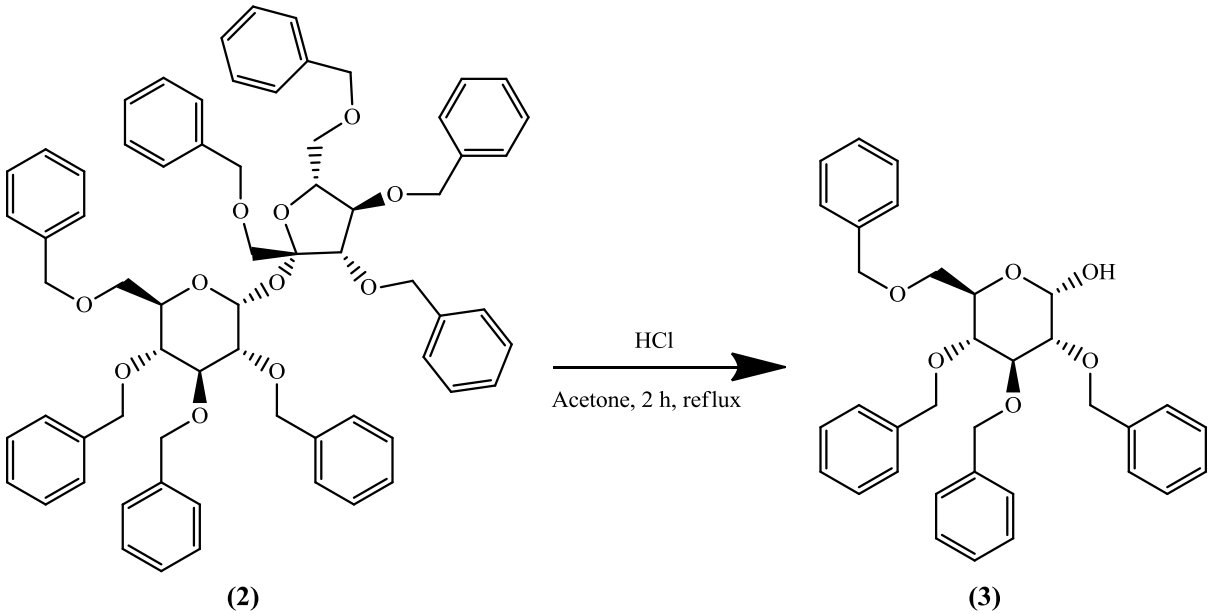

Figure 20: General reaction scheme step 2, hydrolysis of octabenzyl sucrose

For the reason that both TLC and LC/MS-TOF monitoring indicated an incomplete conversion after the given reaction time of 20 minutes [85], the reaction was allowed to stir for 2 h in order for all the educt to be transformed into product.

Although the crude yield obtained in the present step is very satisfying, the hydrolysis presents one of the yield diminishing steps in the synthesis pathway. On the one hand, the fructanosyl moiety cannot be used for further synthesis, as an isomerisation to the pyranoside is not possible. Former experiments with trehalose as starting material showed that due to the strong glycosidic bond, hydrolysis cannot be carried out or leads to a considerable loss of protection groups [9].

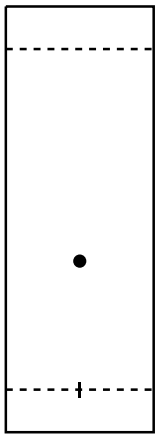

Figure 21: TLC, step 2, 2 h

On the other hand separating the desired tetra benzyl glucose from the tetra benzyl fructose is done by precipitating the pyranoside moiety from n-hexane, whereas the fructosyl residue stays in solution. As sorely the different polarities of the two formed compounds is made use of, a noticeable amount of the desired product stays in solution or precipitates only upon storing for several weeks at -25°C.

Although the mass spectrum indicated a high degree of purity, recrystallisation from MeOH was carried out in order to obtain the desired colourless crystals, which further provokes loss of the product. Nevertheless, time intensive and yield diminishing column chromatography is not needed which accounts for the used method.

Yield: 9.10 g (16.8 mmol, 58 % theoretical, 83 % literature)

R_f: 0.38 (n-hexane/ethyl acetate 2/1)

MP: 156°C (153-156°C)

LC/MS-ToF:

APCI positive mode: calculated for $[C_{34}H_{36}O_6+NH_4]^+$: 558.28501 $^m/_z$, detected: 558.28482 $^m/_z$, Δm: -0.34 ppm

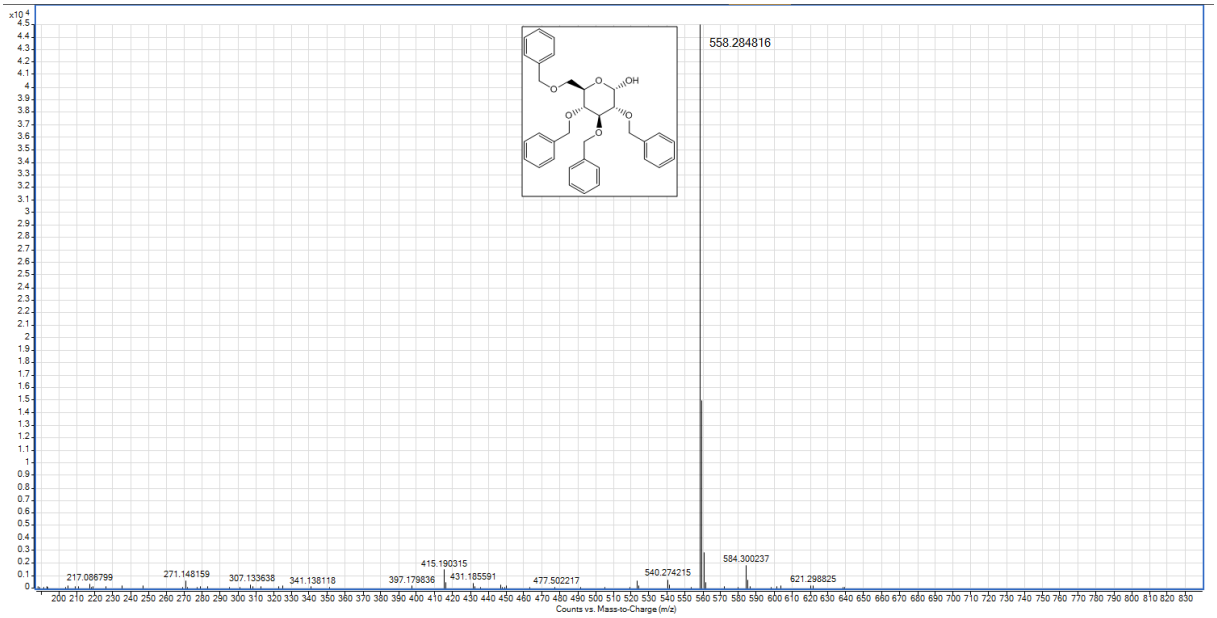

Figure 22: LC/MS-ToF APCI positive mode, step 2

5.1.3 2,3,4,6- Tetra-O-benzyl-α-D-glucopyranosyl trichloroacetimidate (4) [29]

To transfer the anomeric alcohol group the given nucleophilic addition reaction was used. When reacting with an electron poor nitrile, the desired trichloroacetimidates is obtained. NaH was again used to activate the anomeric OH group by transferring it into an alkoxide. Using a strong base and applying prolonged reaction times, it was possible to obtain the desired α-anomer over the β-anomer.

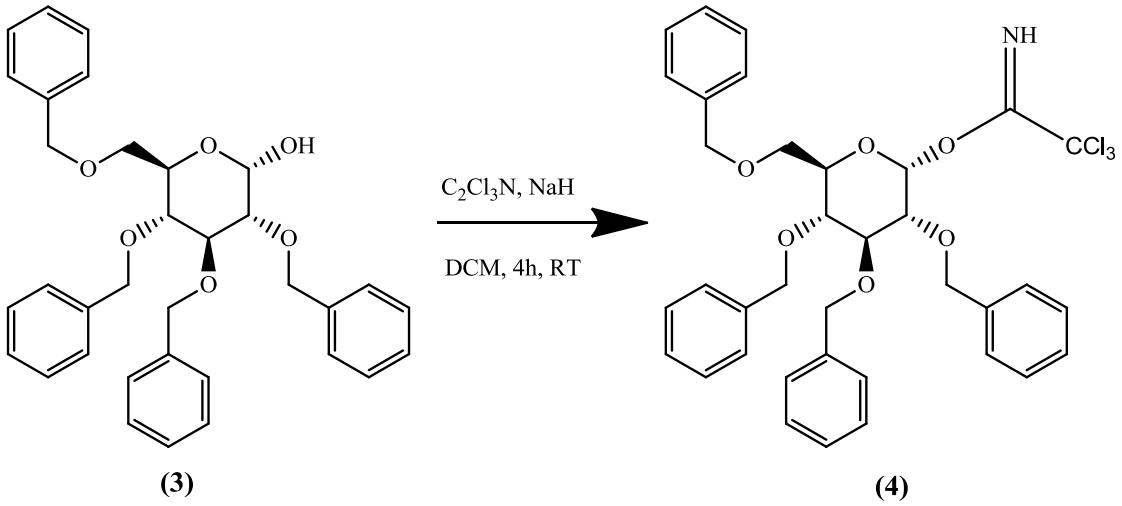

Figure 23: General reaction scheme step 3, synthesis of the trichloroacetimidate

Shortly after the addition of trichloroacetonitrile, two product spots could be detected using TLC, which correspond to the α and the β-anomer of the trichloroacetimidate. Adding additional NaH after 15 minutes enabled the complete anomerisation to the thermodynamically favoured compound. Due to safety issues and to prevent the formation of side products, the presence of water had to be avoided also in the third step of the reaction cascade. It had to be paid attention especially, when filtrating the compound over silica gel, as unreacted NaH can cause spontaneous inflammation when running dry.

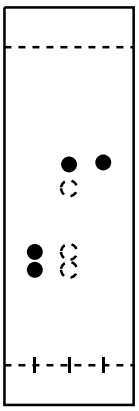

Figure 24: TLC of step 3; left: t=0 min, center: t= 15 min, right: t= 4 h

A prolonged reaction time was used in order for all the educt to convert and to enable the complete anomerisation. The obtained product was a brown oil, which only crystallised after storing it for several weeks at -25°C. The oily product was used in the subsequent insertion of the glycosidic bond in order to minimise dead time.

Due to the fact that it was not possible to detect the product using LC/MS-ToF neither in positive nor in negative ionisation mode, ^{1}H-NMR was carried out to control the success of the reaction.

Yield: 10.03 g (96 % theory, >99 % literature)

R_f value α-anomer: 0.61 (n-hexane/ethyl acetate 2/1)

NMR Spectroscopy

The obtained ^{1}H NMR is in good accordance with the literature [29].

^{1}H NMR: δ 8.60 (1 H,s), 7.32 – 7.13 (20 H, m), 6.50 (1 H, s), 5.00 – 4.50 (8 H, m), 4.20 – 3.50 (6 H, m)

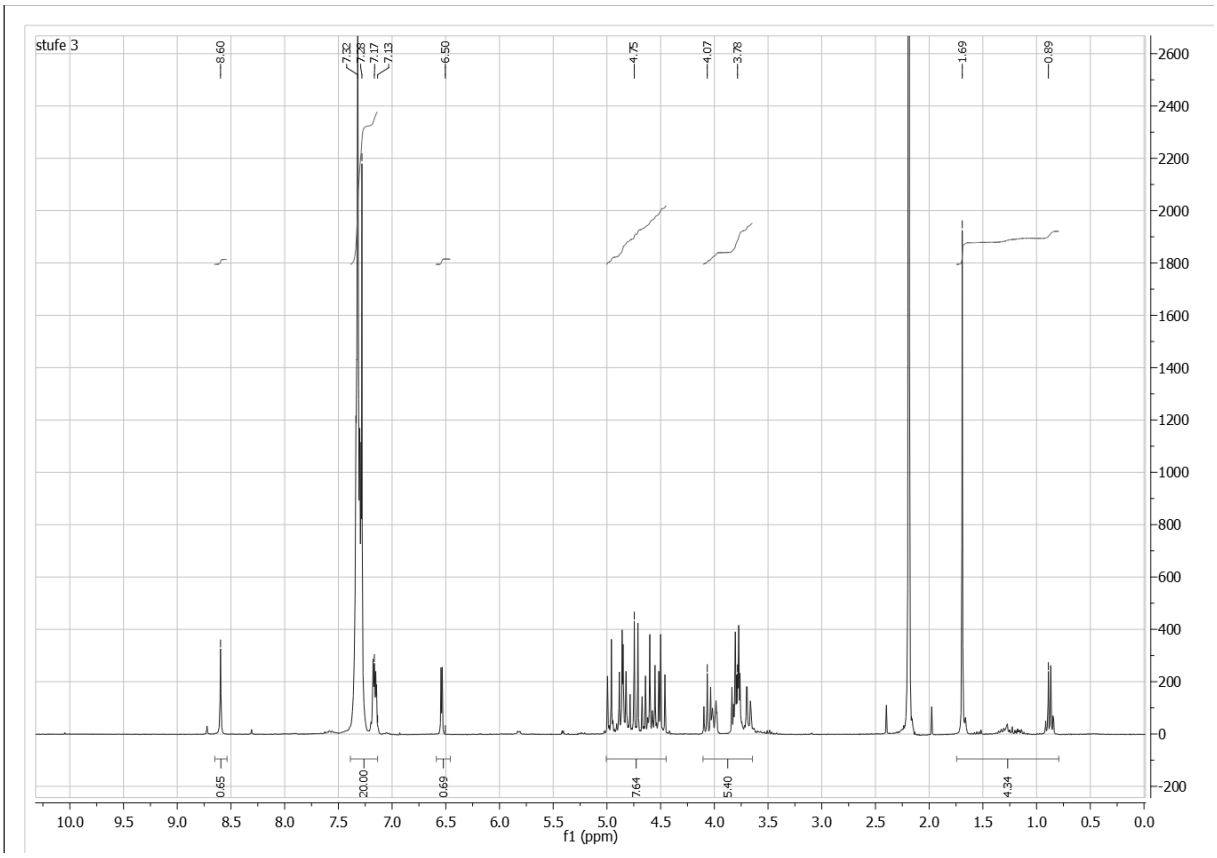

Figure 25: ^{1}H NMR step 3 in $CDCl_3$ at 300 MHz

5.1.4 Steryl 2,3,4,6- tetra-O-benzyl-D-glucopyranoside (5)

The forth step of the reaction pathway involved the acid catalysed formation of the glycosidic bond between the protected pyranoside and the respective sterol. In the present S_N2 reaction, the trichloroacetimidate is replaced by the steryl moiety.

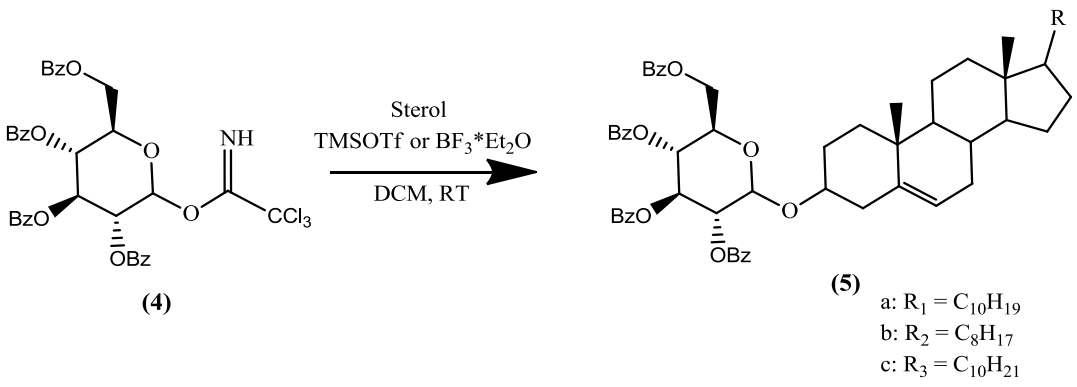

Figure 26: General reaction scheme step 4, glycosylation of steryl moiety

TMSOTf can be used as promotor for the glycosylation, but in order to prevent the formation of side residues, absence of water is crucial. Therefore, both the sterol and the trichloroacetimidate were dried prior to synthesis under reduced pressure. In addition, the used solvent was destilled over P_2O_5 and stored over molecular sieve 3 Å and molecular sieve was also added to the reaction flask. Furthermore, the reaction was performed under nitrogen atmosphere. The low yield in this step is mainly attributed to the precipitation of the compound from MeOH/dioxane. Although the desired compound features a low solubility in the given solvent, a remarkable amount of the protected steryl glucoside cannot be precipitated and stays in solution also after repeatedly performed precipitation. Using LC/MS-ToF in APCI positive mode, the presence of the desired compound could be verified.

TLC indicated that the reaction is not anomerically selective, as in addition to the desired β-anomer also the α-anomer is formed. Kale et al. reported, that using TMSOTf at temperatures between -20°C and RT gives preferably the α-anomer [86], according to Habermehl however, the reaction proceeds under an inversion at the anomeric carbon atom, giving the β-anomer [1]. This discrepancy explains the presence of both anomers of the protected steryl glucoside.

Stigmasteryl 2,3,4,6- tetra-O-benzyl-D-glucopyranoside (5a)

The discussed reaction was performed with different sterol moieties, using stigmasterol as an example for phytosterols. The presence of the desired compound with a molecular weight of 926 g/mole could be verified using LC/MS-ToF immediately after the addition of the promotor. According to the mass spectra, only marginal impurities can be observed when monitoring the reaction, but TLC with n-hexane/EtOAc 2/1 indicated the presence of side residues and an incomplete glycosylation. Performing the reaction in small scale, also TLC indicated no formation of side products; nevertheless, upscaling of the reaction gave rise to the problem that due to bad solubility of stigmasterol, complete solubility of the compound was not given. Therefore, a remarkable amount of the steryl moiety could not take part in the reaction. Only when applying the trichloroacetimidate in higher molar ratios and a higher solvent amount, no stigmasterol was detected. Stirring in MeOH/dioxane 10/1 and repeatedly performed centrifugation enabled the obtention of the desired compound as fine colourless solid as well as the separation of the side residues.

R_f value: product: 0.84 (n-hexane/ethyl acetate 7/3)

MP: 118°C

Yield: 2.02 g (2.2 mmol, 50 %)

LC/MS-ToF:

APCI positive mode: calculated for $[C_{63}H_{82}O_6+NH_4]^+$: 952.64497 $^m/_z$, detected: 952.64482 $^m/_z$, Δm: 0.47 ppm

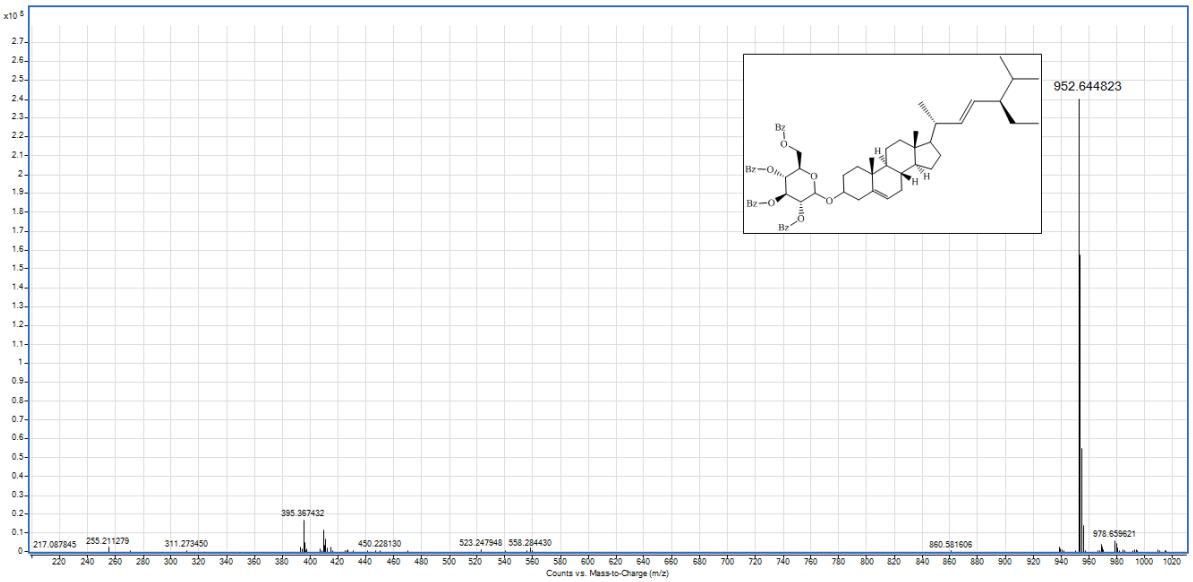

Figure 27: LC/MS-ToF APCI positive mode, step 4a

Cholesteryl 2,3,4,6- tetra-O-benzyl-D-glucopyranoside (5b) [8,9]

Cholesterol is not synthesised by plants and therefore, cholesteryl glucosides are often used as internal standard material for the analysis of steryl glucosides in biodiesel. The glycosylation using cholesterol as steryl moiety has been described in the working group before by Ludwig [8] and Weiss [9]. The presence of the desired compound was verified using LC/MS-ToF, where some minor impurities were detected, which couldn't be removed when carrying out a recrystallisation.

Yield: 1.71 g (1.9 mmol, 59 %)

R_f value: 0.80 (n-hexane/ethyl acetate 3/1)

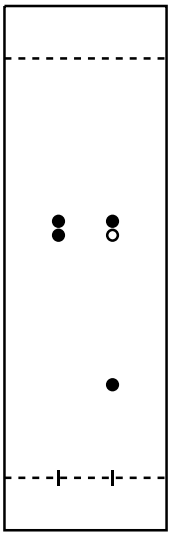

Figure 28: TLC of step 4 when using TMSOTf (left) and BF_3*Et_2O (right) as promotor;

According to Schmidt & Michel, using BF_3*Et_2O as promotor in DCM at a temperature of -20°C yields the desired anomerically pure compound [87] in contrast to the method described above, where the ratio of α to β-anomer is approximately 1:1. Therefore, the applicability on the given synthesis was tested. TLC with n-hexane/EtOAc 3/1 nevertheless indicated also the presence of a second anomer. Moreover, the glycosylation was not complete and a high amount of unreacted sterol was found due to the bad solubility at decreased temperatures, as can be seen in Figure 28.

LC/MS-ToF:

APCI positive mode: calculated for $[C_{61}H_{60}O_6+NH_4]^+$: 926.62932 $^m/_z$, detected: 926.62926 $^m/_z$, Δm: 0.07 ppm

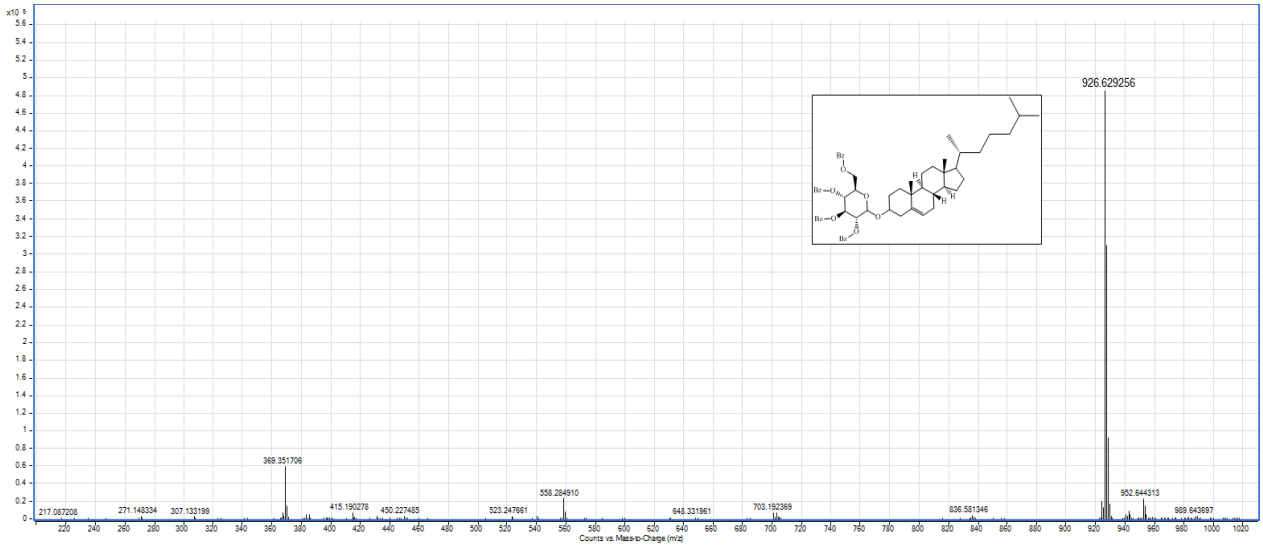

Figure 29: LC/MS-ToF APCI positive mode, step 4b

β-sitosteryl 2,3,4,6- tetra-O-benzyl-D-glucopyranoside (5c)

According to Fluka, the used natural sterol mixture contains > 60 % β-sitosterol; stigmasterol and campesterol make up the remainder. In a first attempt, it was not possible to synthesise the protected steryl glycoside when using β-sitosterol as sterol moiety. LC/MS-ToF, TLC and ^{1}H-NMR indicated an unsuccessful outcome of the reaction. Nevertheless, when using a new stock solution of the promotor, lower molar ratio of the sterol moiety and an increased solvent amount, the desired compound was obtained after stirring for prolonged reaction times. In order for the reaction to be successful, the TMSOTf solution should be colourless and smoke when getting in contact with air. The higher R_f value of the protected β-sitosteryl glycoside compared to **5a** and **5b** is due to a bulkier side chain without double bonds.

Yield: 0.89 g (0.9 mmol, 60 %)

R_f value: 0.87 (n-hexane/ethyl acetate 7/3)

MP: 119°C

5.1.5 Steryl-D-glucopyranoside (6)

In the last step of the synthesis route, the benzyl ether protection groups are removed in a hydrogenation reaction, where cyclohexene serves as hydrogen donor and $Pd(OH)_2$ as mild catalyst.

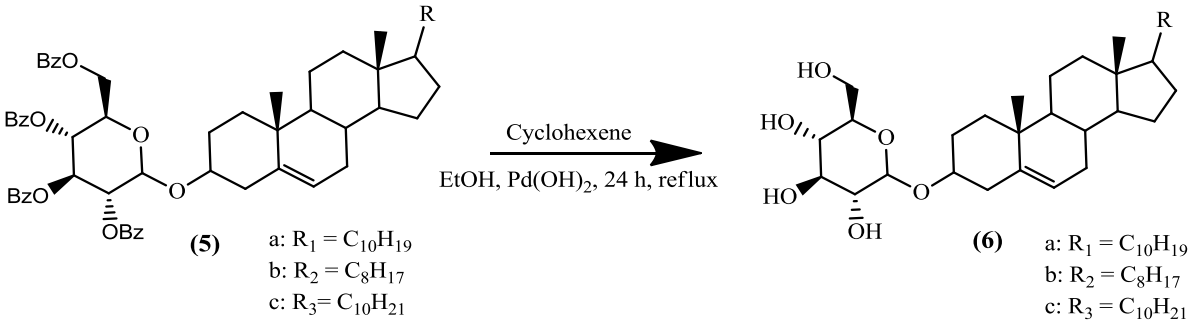

Figure 30: General reaction scheme step 5, deprotection

During the deprotection, inert atmosphere had to be supplied using a nitrogen filled balloon. To achieve a complete deprotection to the desired final compound, adding the catalyst and cyclohexene in several portions was crucial.

The protected steryl glucoside was not completely soluble in the given solvent; only after applying reflux conditions and removal of the first protection groups, complete solubility of the reactants was observed. This can be explained by the increase of polarity when removing the unpolar protection groups; the unprotected steryl glucoside is better soluble in EtOH as a result of the very polar free OH groups.

In contrast to the previous steps, analysis in APCI positive mode was not possible due to the mentioned free hydroxy groups and was performed in APCI negative mode instead.

Stigmasteryl-D- glucopyranoside (6a)

The reaction was monitored using LC/MS-ToF, where the stepwise deprotection of the benzyl ethers could be tracked, as the respective peaks feature a mass difference of 90 $^{m}/_{z}$ according to the loss of each protection group. The mass spectra in negative mode after 4 h and after 13 h are given in Figure 31 and Figure 32. As described for the forth step of the sequence, the reaction could be performed without problems in small scale, in bigger scale, however, high temperature GC indicated that the end product was not the desired steryl glucoside, but the unreacted stigmasterol. Using LC/MS-ToF, no side residues could be detected, as stigmasterol cannot be ionised applying the used parameters. Applying the improved conditions mentioned in 4.3.4 it was possible to obtain the desired end product. Figure 33 shows the gas chromatogram of stigmasteryl-D-glucopyranoside with a retention time of 27 minutes. Due to the high similarity in structure and boling point, complete resolution of the two anomers is not given.

Yield: 1.24 g (2.2 mmol, ≥ 99 %)

MP: 210°C

LC/MS-ToF:

APCI negative mode: calculated for $[C_{35}H_{58}O_6+HCOO]^-$: 619.42154 $^m/_z$, detected: 619.42095 $^m/_z$, Δm: 0.95 ppm

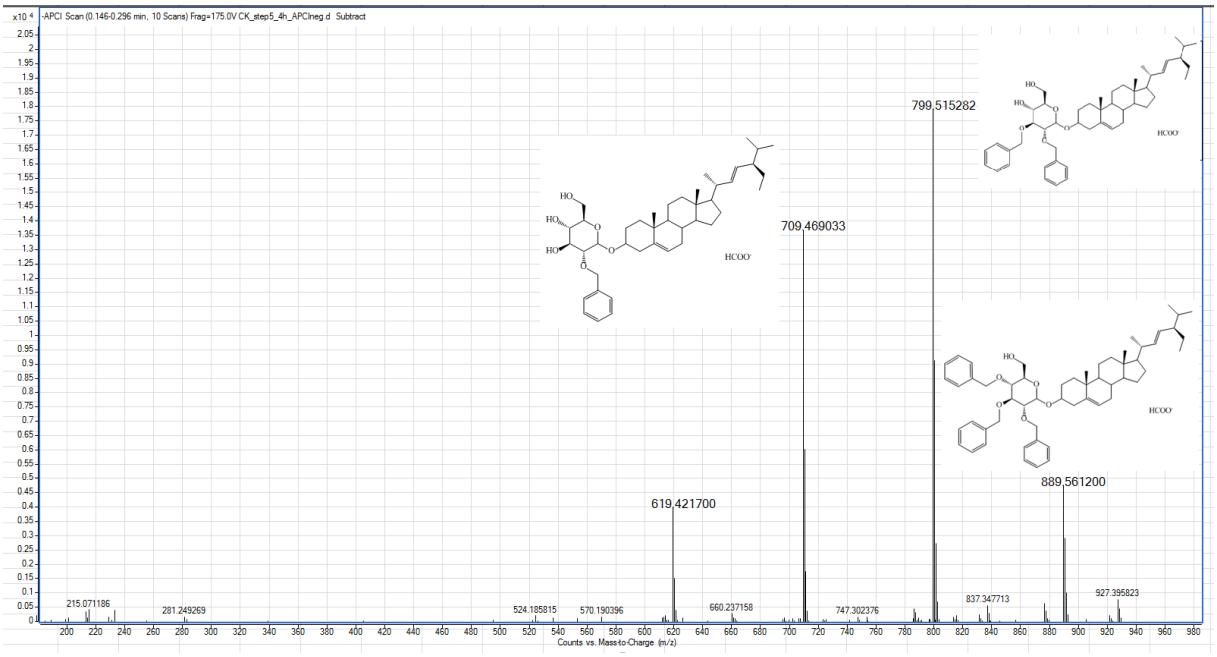

Figure 31: LC/MS-ToF APCI negative mode, deprotection step 5a after 4h

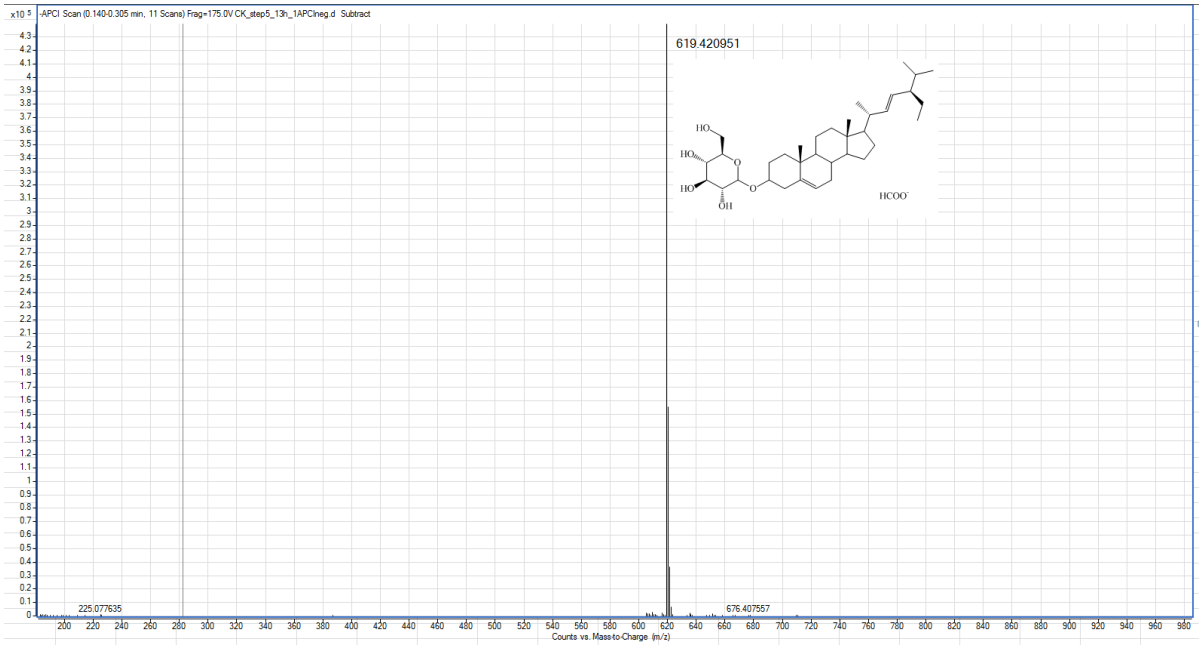

Figure 32: LC/MS-ToF APCI negative mode, deprotection step 5a after 13h

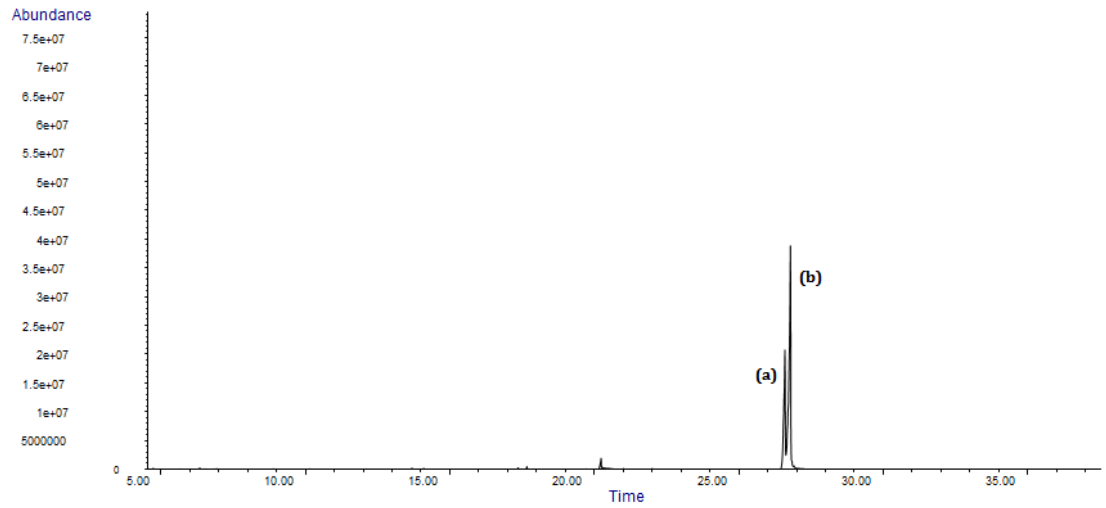

Figure 33: Gas chromatogram, step 5a silylated; RT (SG) = 27 min, (a) = α-anomer, (b) = β-anomer

NMR Spectroscopy

The obtained ^{1}H NMR is in good accordance with the theoretical expectations.

^{1}H NMR: δ 5.32 (1 H, m), 5.11 (1 H, m), 5.02 (1 H, m), 4.42 (2 H, m), 4.20 (1 H, d), 3.61 (1 H, m), 3.42 (2 H, m), 3.33 (4 H, m), 3.04 (3 H, m), 2.90 (1 H, m), 1.92-1.81 (6 H, m), 1.50-1.38 (10 H, m), 1.32-1.15 (5 H, m), 1.00-0.95 (8 H, m), 0.82-0.77 (8 H, m), 0.66 (3 H, s)

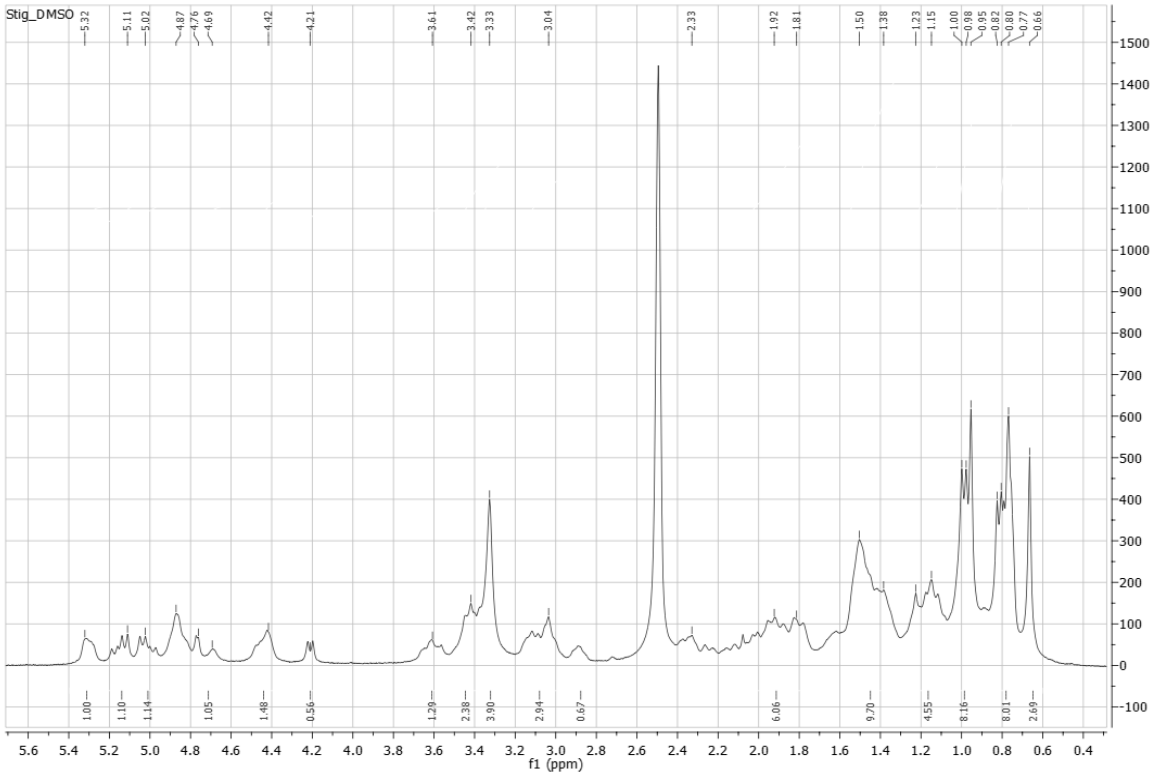

Figure 34: ^{1}H-NMR step 5a in d_6 DMSO at 300 MHz

Cholesteryl-D- glucopyranoside (6b) [8,9]

As for **5a**, the reaction occurred stepwise in the case of cholesteryl-D-glucopyranoside, as the presence of compounds with a varying number of benzyl ether protection groups was observable during the course of the reaction, when being monitored using LC/MS-ToF.

According to the gas chromatogram, the purity of the compound was 92 %. As for **6a**, the retention time of the SG is 27 minutes, the smaller peak at 20 minutes corresponds to cholesterol. GC/FID shows that the reaction was not anomerically selective, as two peaks can be observed at RT = 27 min. 52 % of the product are in α-configuration, 48 % in β; using BF_3*Et_2O as promotor, the natural more prevalent β-anomer was obtained with 90 %. The two gas chromatograms are given in Figure 35.

Considering the fact that a high amount of unreacted cholesterol was present in the end product due to incomplete conversion as well as lower yields and higher preparative effort, the choice of BF_3*Et_2O as promotor should only be taken, when anomerically pure compounds are crucial.

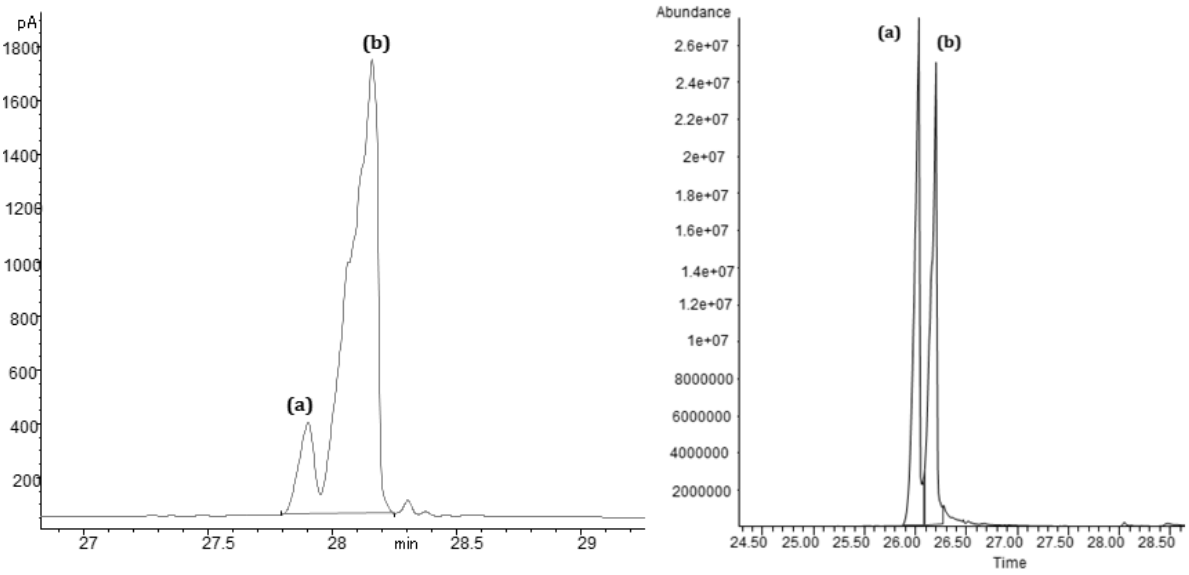

Figure 35: Gas chromatogram of sylilated 6b when using BF_3*Et_2O (left) and TMSOTf (right); (a) = α-anomer, (b) = β-anomer

LC/MS-ToF:

APCI negative mode: calculated for $[C_{33}H_{56}O_6+HCOO]^-$: 593.40589 $m/_z$, detected: 593.40885 $m/_z$, Δm: -0.69 ppm

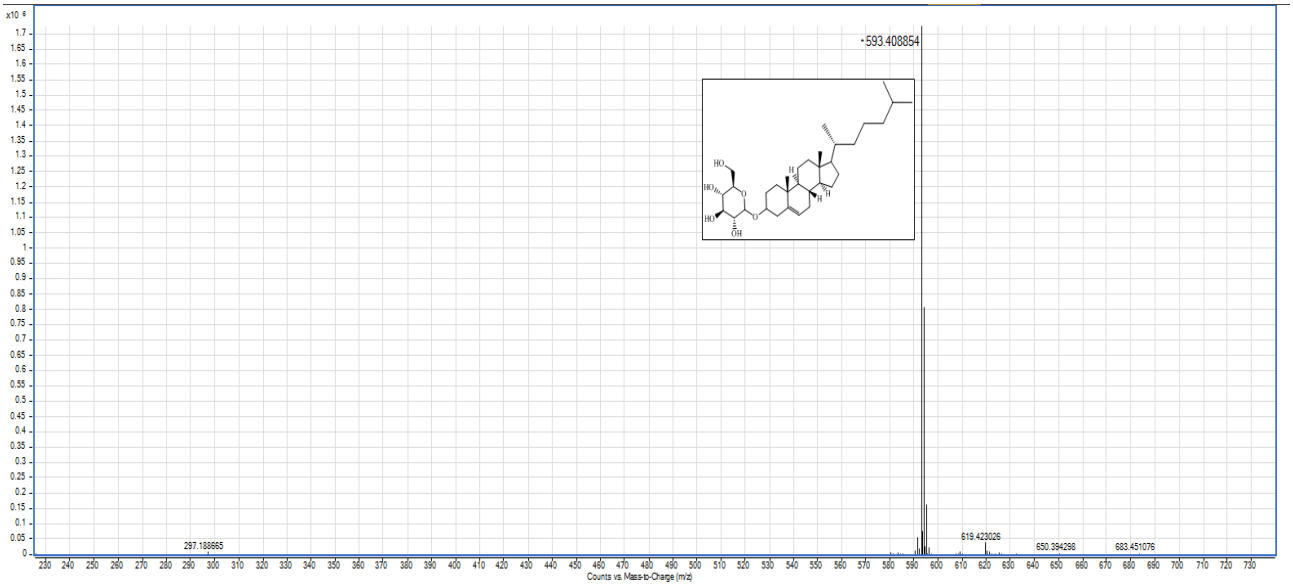

Figure 36: LC/MS-ToF APCI negative, step 5b

UPLC-MS was used to investigate the possibility of separating the two anomers upon the application of a liquid chromatography system. The separation efficiency was tested under the variation of the mobile phase, infusion volume and concentration of the compound. Due to the very similar chromatographic behaviour of the anomers, it was not possible to separate them under the tested conditions.

Wolucka et al. reported a difference of the fragmentation pattern of different anomeric compounds [70]. Therefore, tandem MS was applied to study the applicability on the given problem. Applying trap voltages of 12, 27 and 35 V in ESI MSMS positive mode, a possible difference in the fragmentation pattern was investigated. As can be seen in Figure 37, the mixture and the β-anomer show a very similar fragmentation pattern with differences only in the lower abundant peaks. The most predominant peak with $^{m}/_{z}$ = 369.35 corresponds to the aglycon, the charge results from the cleavage of the sugar. Due to the fact that the sugar residue is cleaved off prior to the actual fragmentation, a difference between the two anomers cannot be analysed using tandem mass spectrometry. Using formic acid (0.1 v%) in positive mode or switching to negative mode did not yield to a feasible fragmentation pattern at all.

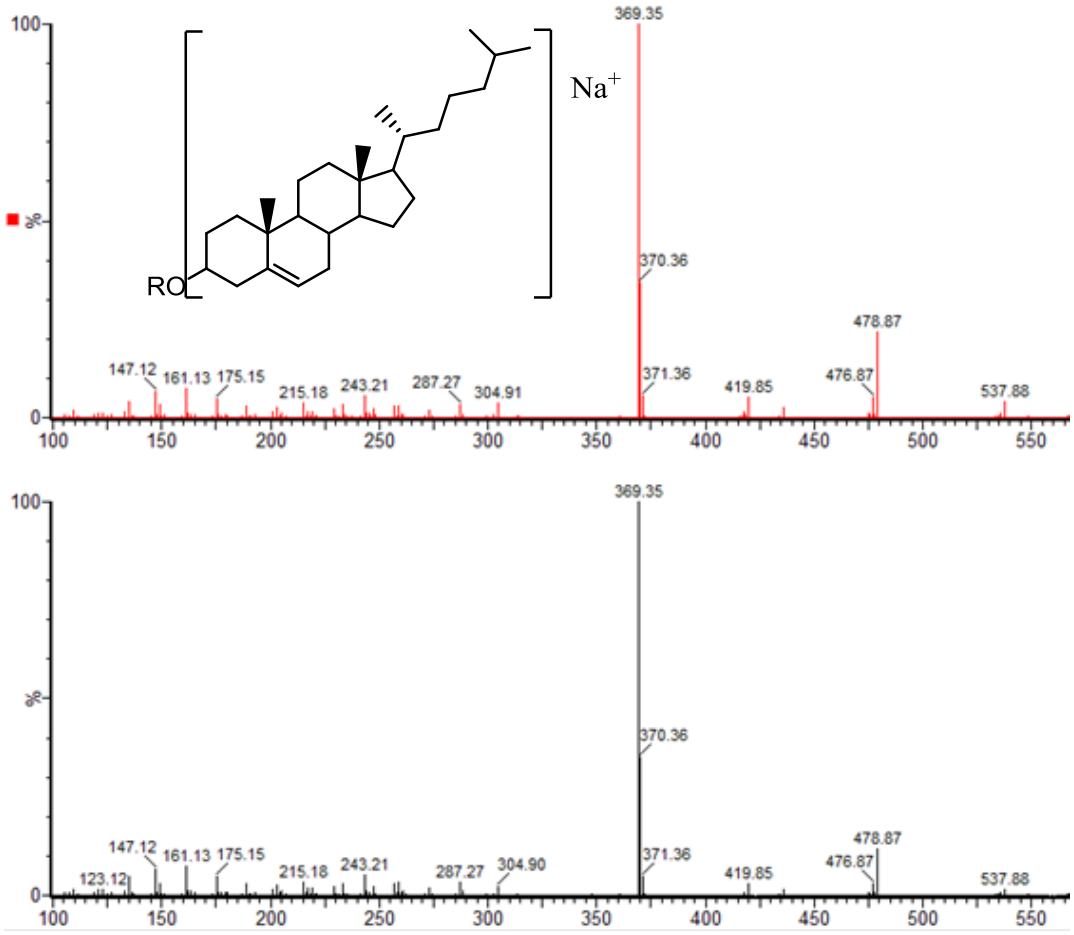

Figure 37: Fragmentation pattern of the anomeric mixture of cholesteryl-D-glucopyranoside (top) and cholesteryl-β-D-glucopyranoside (bottom) in ESI MSMS positive mode with 0.1 v% acetic acid and 1 µM NH_4Ac

Ion mobility mass spectrometry is a technique, which uses the different size and shape of the ions for separation [88] and can even be applied for the separation of anomers. Due to steric difference at the anomeric center, the respective α and β-anomer feauture slightly different mobilites and hence can be distinguished from each other. Applying this technique, it was possible to observe a difference between the mixed cholesteryl-D-glucopyranoside (2 spots) and the pure β-anomer (1 spot). The diagram of this meausurement is given in Figure 38; the $^{m}/_{z}$-ratio is plotted versus the drift time (bins). The upper spot in the right image corresponds to cholesteryl-β-D-glucopyranoside (drift time = 145 bins), the lower one to cholesteryl-α-D-glucopyranoside (drift time = 135 bins), which was determined on the drift time of the anomerical pure compound (drift time = 145 bins). The ratio of the two anomers can be estimated by the intensity of the respective spot. Therefore an approximate ratio of 50/50 of the respective alpha and beta anomer is expected in the present case, meeting the results obtained by GC/MS.

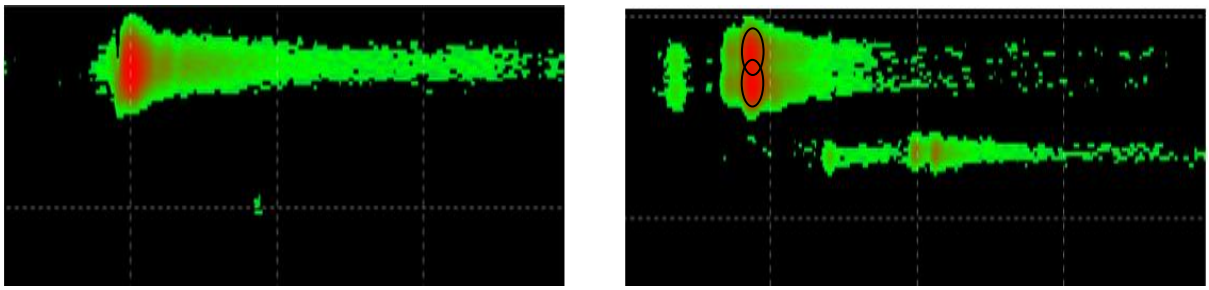

Figure 38: Ion mobility mass spectra of cholesteryl-β-D-glucopyranoside (left) and cholesteryl-D-glucopyranoside (right) in ESI positive mode with 0.1 v% formic acid

β-Sitosteryl-D-glucopyranoside (6c)

The deprotection was carried out until no more completely and partially protected SG was detected using LC/MS-ToF. The major peak at $^{m}/_{z} = 621$ corresponds to β-sitosterol-D-glucopyranoside and the smaller one at $^{m}/_{z} = 607$ to campesteryl-D-glucopyranoside. The detected peak at $^{m}/_{z}$ = 619 features only a very low abundance, but confirms the presence of stigmasterol in the natural sterol mixture.

The purity was determined using GC/FID and showed a satisfying value of 97 % with a retention time of the product at 29 minutes. The minor upstream peaks correspond to the two anomers of campesteryl-D-glucopyranoside and the compound with a retention time of 23 minutes to unreacted sterol.

Yield: 0.50 g, 0.9 mmol, 94 %

LC/MS-ToF, APCI negative mode:

Campesteryl-D-glucopyranoside: calculated for $[C_{35}H_{59}O_8+HCOO]^-$: 607.4215 $^{m}/_{z}$, detected: 607.4201 $^{m}/_{z}$, Δm: 2.31 ppm

β-Sitosteryl-D-glucopyranoside: calculated for $[C_{36}H_{61}O_8+HCOO]^-$: 621.4372 $^{m}/_{z}$, detected: 621.4357 $^{m}/_{z}$, Δm: 2.41 ppm

Stigmasteryl-D-glucopyranoside: calculated for $[C_{36}H_{59}O_8+HCOO]^-$: 619.4215 $^{m}/_{z}$, detected: 619.4216 $^{m}/_{z}$, Δm: -0.10 ppm

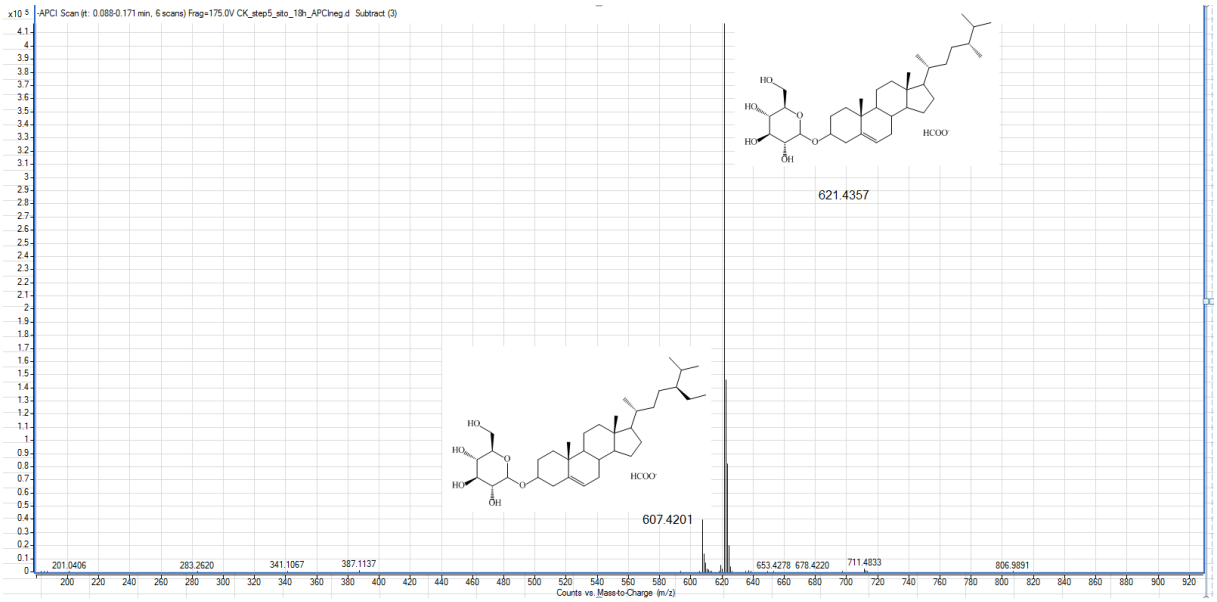

Figure 39: LC/MS-ToF APCI negative, step 5c, $^{m}/_{z}$ 607 = campesteryl glucoside, $^{m}/_{z}$ 621 = sitosteryl glucoside

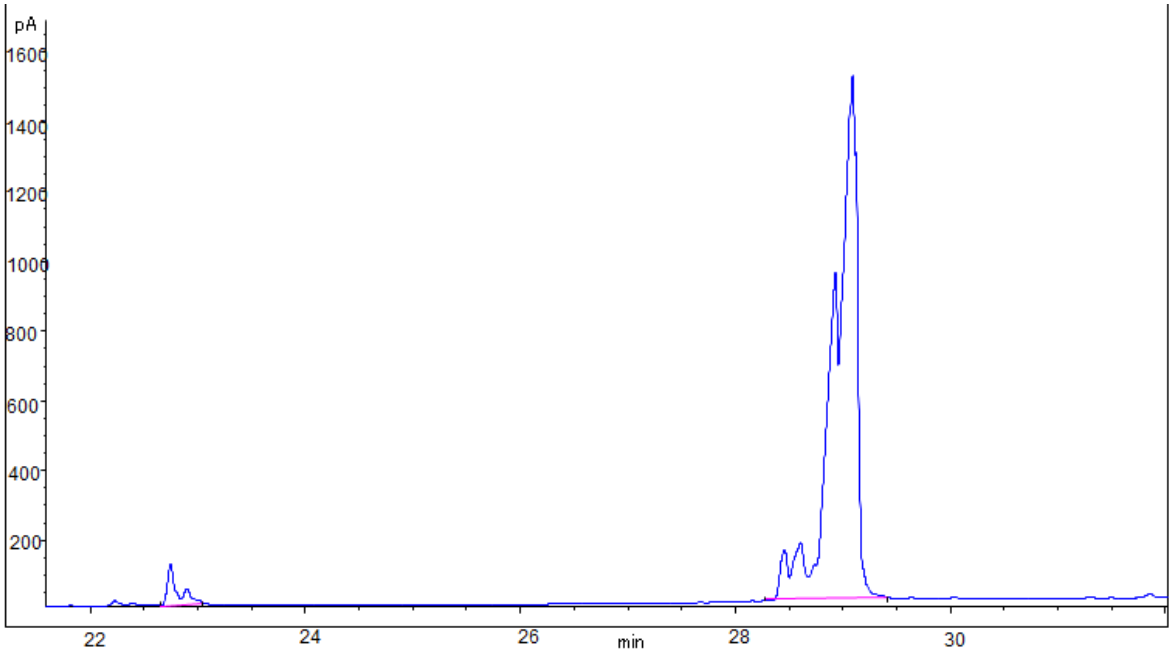

Figure 40: Gas chromatogram, step 5c silylated; retention time (campersteryl glucoside) = 28 min, retention time (sitosteryl glucoside) = 29 min

5.2 Synthesis of steryl-D-glucopyranoside using the Koenigs Knorr mechanism

The Koenigs Knorr method is a common and well-studied method for the introduction of glycosidic bonds and has been studied extensively for the synthesis of cholesteryl-D-glucopyranoside [8,80], but not for stigmasterol or β-sitosterol. In order to compare the outcome of the tested reaction pathway with the more expensive Koenigs Knorr mechanism, the reaction was performed using β-sitosterol as steryl moiety.

5.2.1 2,3,4,6-Tetra-O-acetyl-α-D-glucopyranosyl bromide [89]

In the first reaction of the synthetic pathway, the acetate group at the anomeric carbon atom is replaced by bromine during an S_N2 reaction. This results in an inversion of this group and therefore only the desired stereoisomer is formed due to the anomeric effect (see 2.2.1)

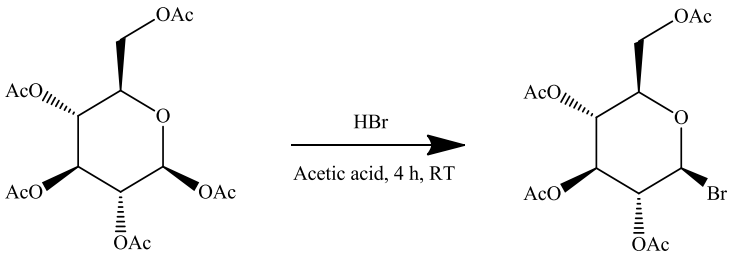

Figure 41: General reaction scheme for bromination of pentaacetyl glucose

In order to obtain the desired compound needed for the Koenigs Knorr reaction, acetobromo glucose was synthesized according to Ravindranathan-Kartha et al. [89]. The success of the reaction was confirmed by TLC and also the melting point of 90°C verified the formation of the desired compound.

Yield: 7.52 g (18.3 mmol, 89 %)

R_f value: 0.70 (PE/acetone 5/4)

MP: 90°C (88°C in lit)

5.2.2 β-Sitosteryl-2,3,4,6-tetra-O-acetyl-β-D-glucopyranoside

The second step of the reaction sequence represents the formation of the glycosidic bond following the Koenigs Knorr mechanism. Hereby, the brominated glycoside reacts with silver carbonate to yield first an oxocarbenium ion, which rearranges to the more stable dioxolanium ion; $AgBr_2$ is formed as side residue. In the following S_N2 reaction, the dioxolanium ion is attacked by MeOH. The resulting inversion and subsequent cleavage of one hydrogen atom yield the desired glucoside [90].

The reaction using cholesterol as steryl moiety has been described in literature as well as in the working group extensively [8,80]. In contrast, no literature for the synthesis of the protected steryl glucoside with phytosterols was found. The progress of the reaction was controlled using TLC and LC/MS-ToF, but also when applying a prolonged reaction time, a remarkable amount of the starting material could not be converted to the desired compound. Due to the fact that TLC indicated a very low conversion of the desired compound and purification using flash chromatography yielded only a few miligrams of the protected β-sitosteryl glycoside, the deprotection was not performed.

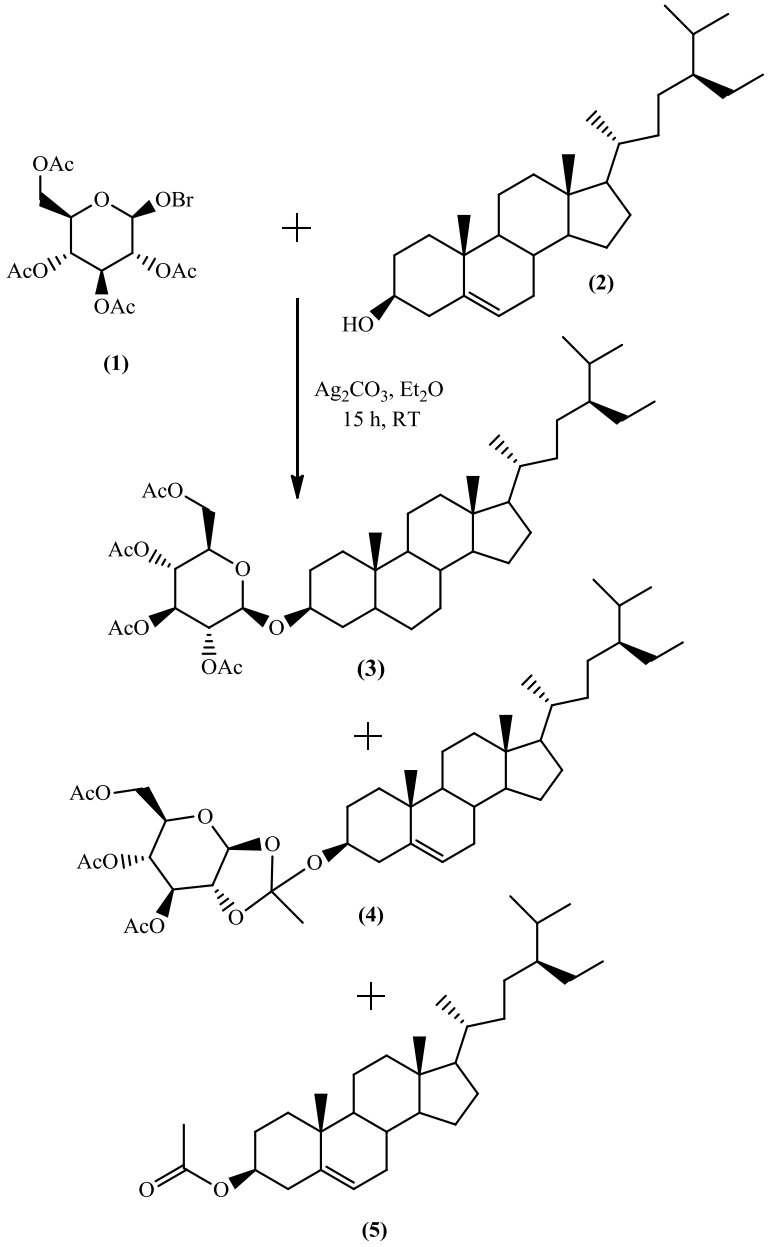

Figure 42: General reaction scheme of glycosylation applying the Koenigs Knorr method; 1: tetraacetyl glucose, 2: β-sitosterol, 3: protected β-sitosteryl glycoside 4: orthoester, 5: β-sitosteryl acetate

5.3 Enzymatic acylation of SG to ASG

In the present reaction, the acylation of SG into ASG is carried out using a biocatalytic reaction to enable a S_N2 reaction, where the primary OH group at the -6´-C- atom is nucleophilic attacked and acylated.

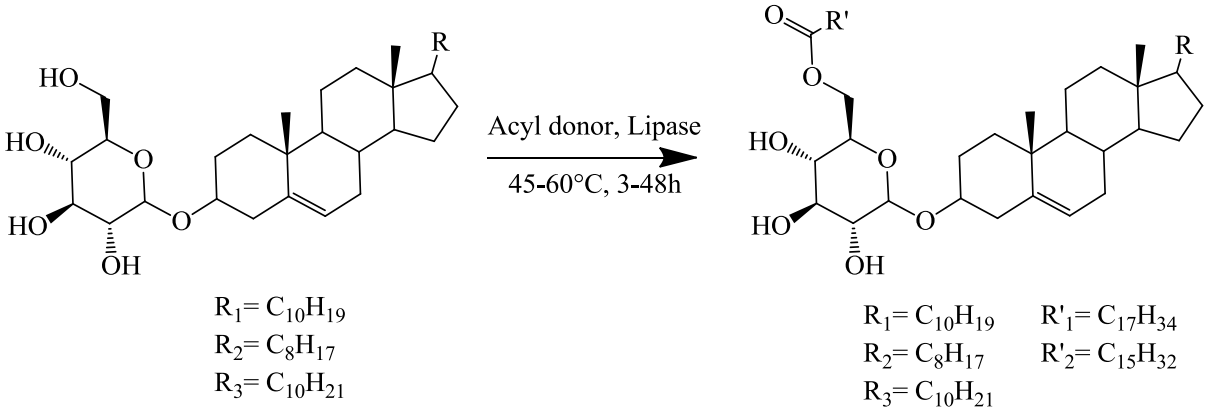

Figure 43: General reaction scheme of the enzyme catalysed acylation of SG

The reaction was modified from Paczkowski et al. who tested the possibility to obtain ASG in a biocatalytic acylation of fatty acids and fatty acid methyl esters [64]. They describe the reaction only in scales of nanomole without subsequent purification; conversion was determined using radioactivity measurements. An acyl donor to SG ratio of 80:1 and a mass excess of the enzyme of 100 times over the SG are not suitable for upscaling this reaction due to cost and time investments. Therefore, the reaction was modified in order to be able to synthesise the product in a scale suitable for the production of analytical standards.

5.3.1 Optimisation of the parameters

The influence of the variation of numerous different parameters on the conversion was studied for cholesteryl-D-glucopyranoside as well as for plant based SG. Table 19 gives the results of the screening for the acylation of cholesteryl-D-glucopyranoside. The conversion was estimated based on the ratio between SG and ASG observed with LC/MS-ToF in negative mode with APCI or ESI.

Table 19: Conversion of SG to ASG after 48 h when using cholesteryl-D-glucopyranoside

	T [°C]	Enzyme	Acyl donor	Acyl donor:SG	Solvent	Conversion [%]
1	40	Novozyme 435	OAME	60:1	n-hexane	67
2	50	Novozyme 435	OAME	60:1	n-hexane	85
3	60	Novozyme 435	OAME	60:1	n-hexane	87
4	50	Lipozyme	OAME	60:1	n-hexane	66
5	50	Lipolase	OAME	60:1	n-hexane	70
6	50	Novozyme 435	FAEE	60:1	n-hexane	---
7	50	Novozyme 435	FABE	60:1	n-hexane	---
8	50	Novozyme 435	OAME	60:1	tert-butanol	76

The dependence of the conversion on the temperature can be explained by a concurrence between the temperature optimum of the enzyme and the thermodynamic hindrance of the acylation. At low temperatures the energy barrier of the reaction cannot be passed, at high temperatures, the enzyme is inactivated. According to Sigma Aldrich, Novozyme 435 has a temperature optimum between 40 and 60°C [91], Yadav & Thorat describe a temperature optimum of the esterification at 60°C [92].

The highest conversion among the three tested lipases was achieved with Novozyme 435 under the given conditions and was therefore used for further experiments.

Pirozzi et al. describe a potential inactivation of the enzyme in the presence of MeOH [93], which is released during the acylation, when methyl esters are used as acyl donors. Therefore, the reaction was tested with ethyl and butyl esters too. However, hereby no conversion of the SG to the desired ASG could be observed.

Table 20 gives the results obtained when using stigmasteryl-D-glucopyranoside and a natural SG mixture with Novozyme 435, n-hexane, an acyl donor- SG ratio of 60:1 at 50°C.

Table 20: Conversion of SG to ASG after 48 h when using stigmasteryl-D-glucopyranoside and a natural SG mixture

	Stigmasteryl-D-glucopyranoside	Natural SG mixture
Conversion [%]	73	69

The high conversion achieved when using cholesteryl-D-glucopyranoside could not be observed when using plant based SG as starting material, which is probably due to a worse solubility of these compounds in the chosen solvent.

The most crucial parameter in the outcome of the reaction was found to be the ratio between the acyl donor and the SG, which was studied in a higher scale with conventional stirring. Both an equimolar and a ratio of 10:1 did not yield in a considerable conversion; only when applying the acyl donor in excess of 30 to 60 times, a complete acylation was observed after 48 h.
The chosen method was also tested on its applicability for palmitic acid methyl ester. The achieved conversions are comparable with the ones when using OAME; nevertheless the lack of a double bond of this compound asked for a different visualization method for the TLC.

5.3.2 Reactions under microwave heating conditions

Yadav & Thorat describe a lipase catalysed acylation of isoamyl alcohol with myristic acid using the microwave [92]. Based on this method, the acylation of SG under microwave heating conditions was tested. Table 21 gives the achieved conversions at an agitation speed of 400 rpm, with a temperature of 60°C, Novozyme 435 and a reaction time of 3 h. The reactions were tested with cholesteryl-D-glucopyranoside, stigmasteryl-D-glucopyranoside and a natural SG mixture.

Table 21: Conditions and achieved conversion of ASG when using microwave heating conditions

	SG moiety	Acyl donor	Molar ratio SG/ acyl donor	Solvent	Conversion [%]
1	Phytosteryl-SG	OAME	1:1	n-hexane	8
2	Phytosteryl-SG	OAME	1:10	n-hexane	25
3	Phytosteryl-SG	Oleic acid	1:10	n-hexane	40
4	Phytosteryl-SG	Palmitic acid	1:30	n-hexane	--------
5	Phytosteryl-SG	Oleic acid	1:30	none	62
6	Stigmasteryl-SG	Oleic acid	1:30	none	--------
7	Cholesteryl-SG	Oleic acid	1:30	none	75
8	Cholesteryl-SG	PAME	1:30	none	60

Comparing the conversion rates obtained when applying microwave heating conditions with the ones with conventional heating, a high increase can be observed. Nevertheless, a quantitative reaction of SG to ASG asks for further optimisation of the parameters. Especially the applicability of solvent free systems is a positive aspect of the method as the use of harmful solvents can be avoided to some extent.

5.3.3 Synthesis and purification of the desired ASG

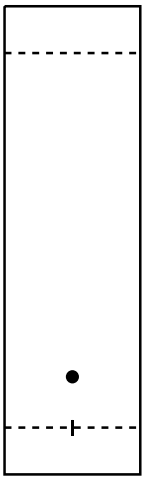

Figure 44: TLC of 7a

Cholesteryl-(6'-O-oleoyl)-D-glucopyranoside (7a)

The presence of the desired acylated steryl glucoside could be verified using LC/MS-ToF in APCI negative mode, TLC, ^{1}H-NMR spectroscopy as well as GC/FID; the latter one indicated a purity of > 99 %. The reaction was also tested with oleic acid and subsequent saponification of the fatty acid. Basic saponification of the acid as described by Ludwig et al. [8] resulted in a back reaction of the product to the non-acylated starting material.

As $NaHCO_3$ features a pH value of 7.5-8 in water, extraction and simultaneous saponification of the acyl donor was envisioned. Also when using a high excess of $NaHCO_3$, a quantitative removal of the excess acyl donor was not possible. In order to derive the pure product, column chromatography could not be circumvented.

Also when using methyl esters as acyl donors, the formation of fatty acids could not be prevented, as complete water free conditions could not be applied. The formed free fatty acids provoke a problem in the subsequent column chromatography, as they do not feature a well resolved peak. The additional peak in the mass spectrum in Figure 45 corresponds to the molecular weight of the substance in addition with Cl^-, whose formation seems to be in concurrence with the formation of the desired formiate ion.

Yield: 0.35 g (47 %)

R_f value: 0.14 ($CHCl_3$/MeOH 95/5)

LC/MS-ToF:

APCI negative mode: calculated for $[C_{51}H_{88}O_7+HCOO]^-$: 857.65121 $^m/_z$, detected: 857.65138 $^m/_z$, Δm: -0.198 ppm; calculated for $[C_{51}H_{88}O_7+Cl]^-$: 847.62241 $^m/_z$, detected: 847.62275 $^m/_z$, Δm: -0.401 ppm

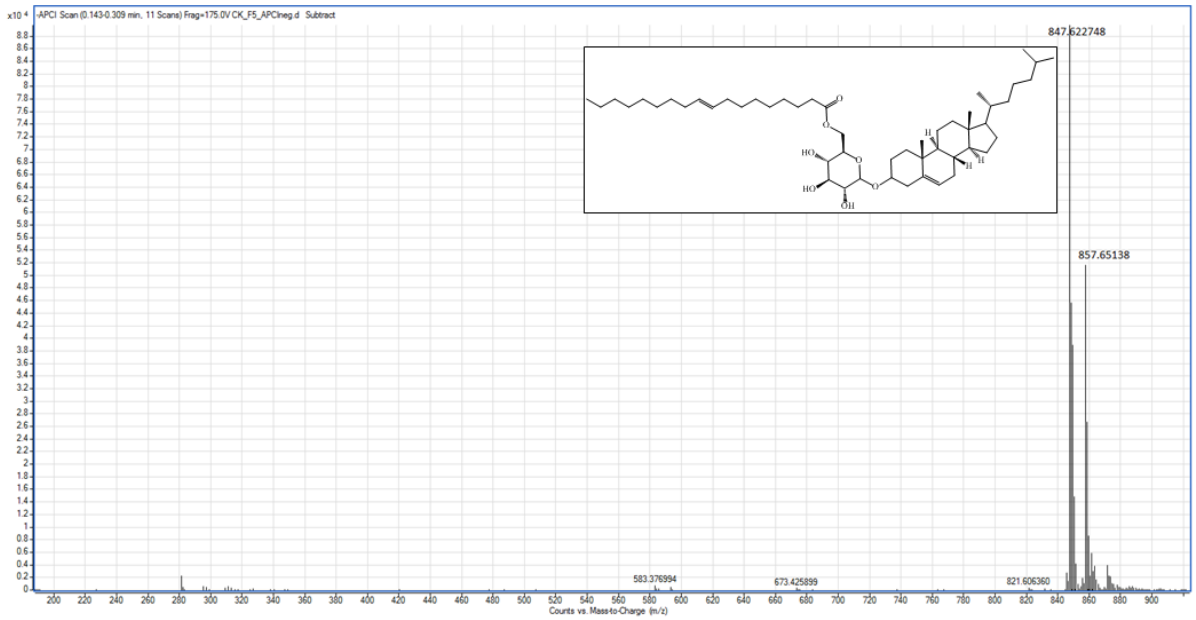

Figure 45: LC/MS-ToF APCI negative, cholesteryl-(6'-O-oleoyl)-D-glucopyranoside

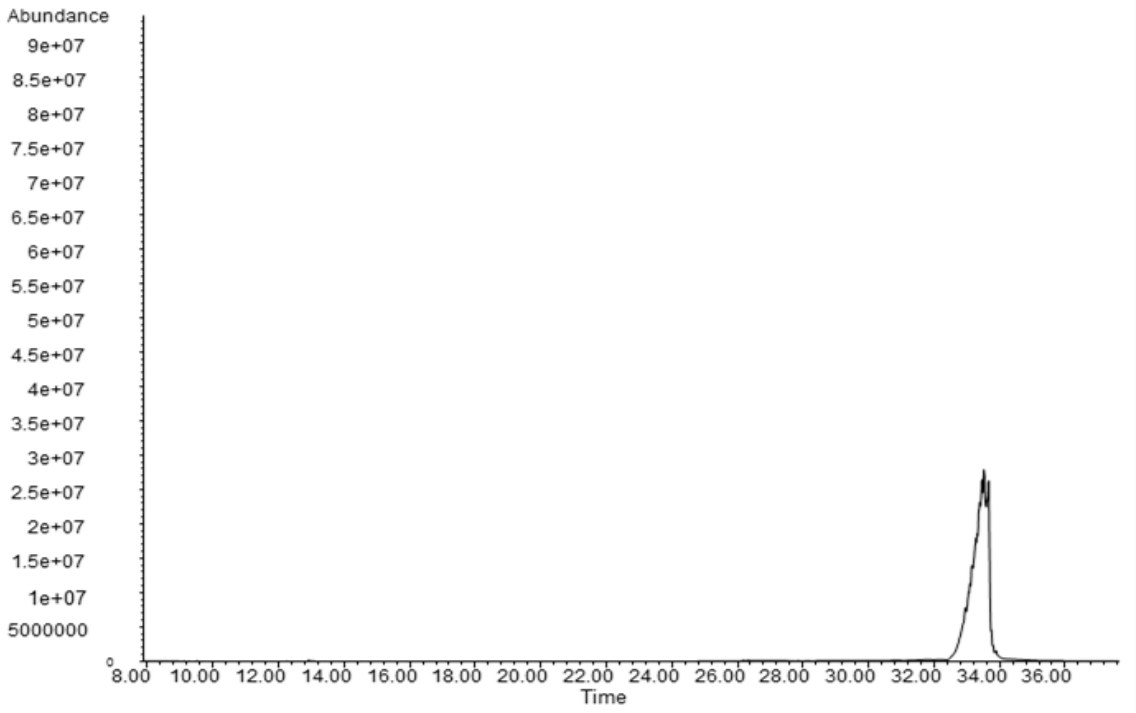

Figure 46: Gas chromatogram of silylated cholesteryl-(6'-O-oleoyl)-D-glucopyranoside, RT (ASG) = 33 min

Cholesteryl-(6'-O-palmitoyl)-D-glucopyranoside (7b)

The lack of a double bond in palmitic acid compared to oleic acid asked for the use of a different visualisation reagent during the column chromatography. The use of bromocresol green enabled the detection of the formed side residue and the desired compound was obtained with a purity of 83 % according to high temperature GC/MS. Due to the bad resolution of the palmitic acid and the similarity in the chromatographic behaviour of product and side residue, obtention of the desired compound in higher purity was not possible.

5.4 Analysis of steryl polyglucosides[1]

5.4.1 MS-ToF

Applying MS-ToF in positive mode, three different stigmasteryl polyglucosides were analysed; their mass spectra are given in Figure 48. All of them featured a 1-4 glycosidic bond and were either only α or β linked. Figure 47 gives the structure of stigmasteryl-β-D-glucopyranosyl-(1→4)-β-D-glucopyranoside. The most predominant peak in each spectrum corresponds to the molecular weight of the compound in addition with a sodium ion.

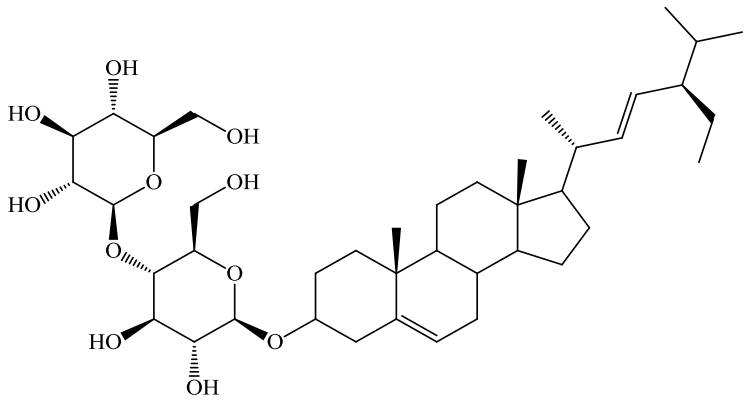

Figure 47: Structure of stigmasteryl diglucoside

[1] Performed at the Laboratory of Food Biochemistry at the ETH Zurich

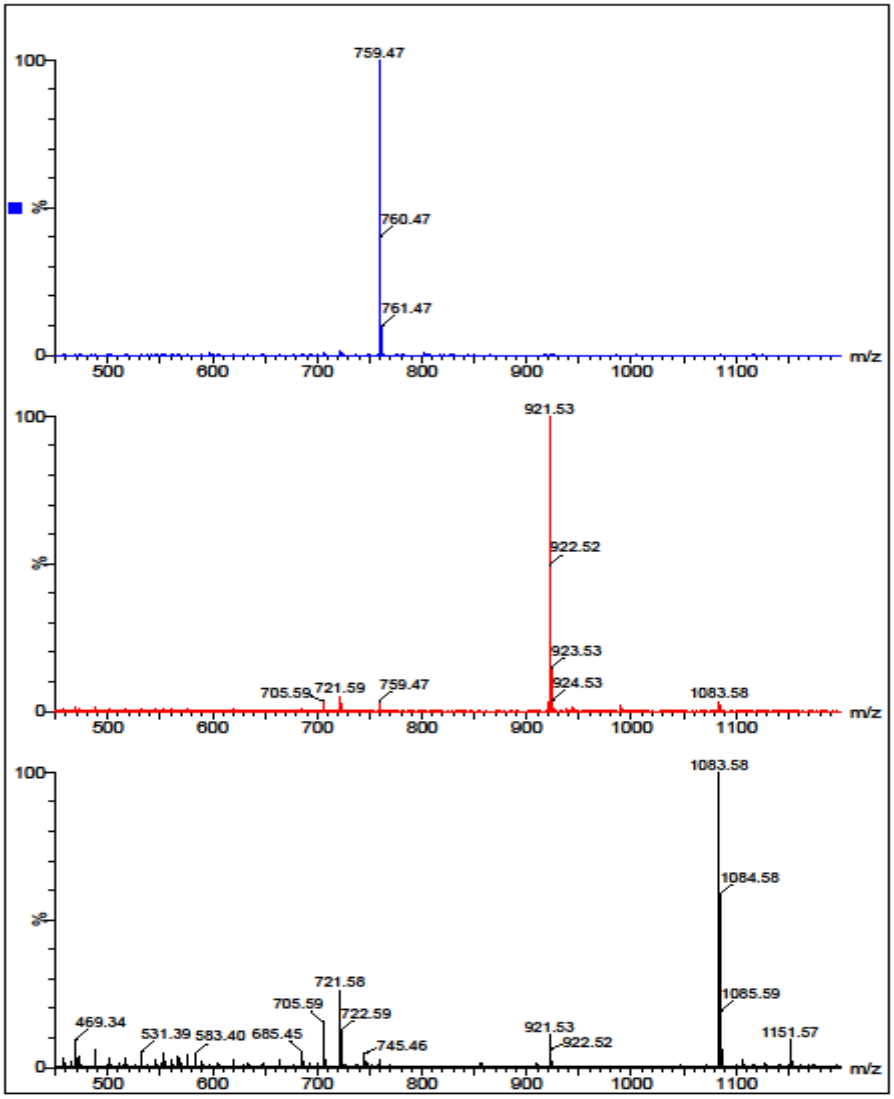

Figure 48: UPLC/MS-ToF ESI of stigmasteryl di- (top), tri- (middle) and tetrasaccharide (bottom) in ESI positive mode

5.4.2 UPLC/MS-ToF

After analysing the respective stigmasteryl mono-, di-, tri- and tetrasaccharide separately from each other, a mixture of the following concentrations was prepared:

Table 22: Concentration of the respective compound in the mixture prepared in MeOH

Compound	Concentration (µM)
Monosaccharide (α&β)	9.8
β-Disaccharide	12.3
α-Trisaccharide	13.2
α-Tetrasaccharide	10.3

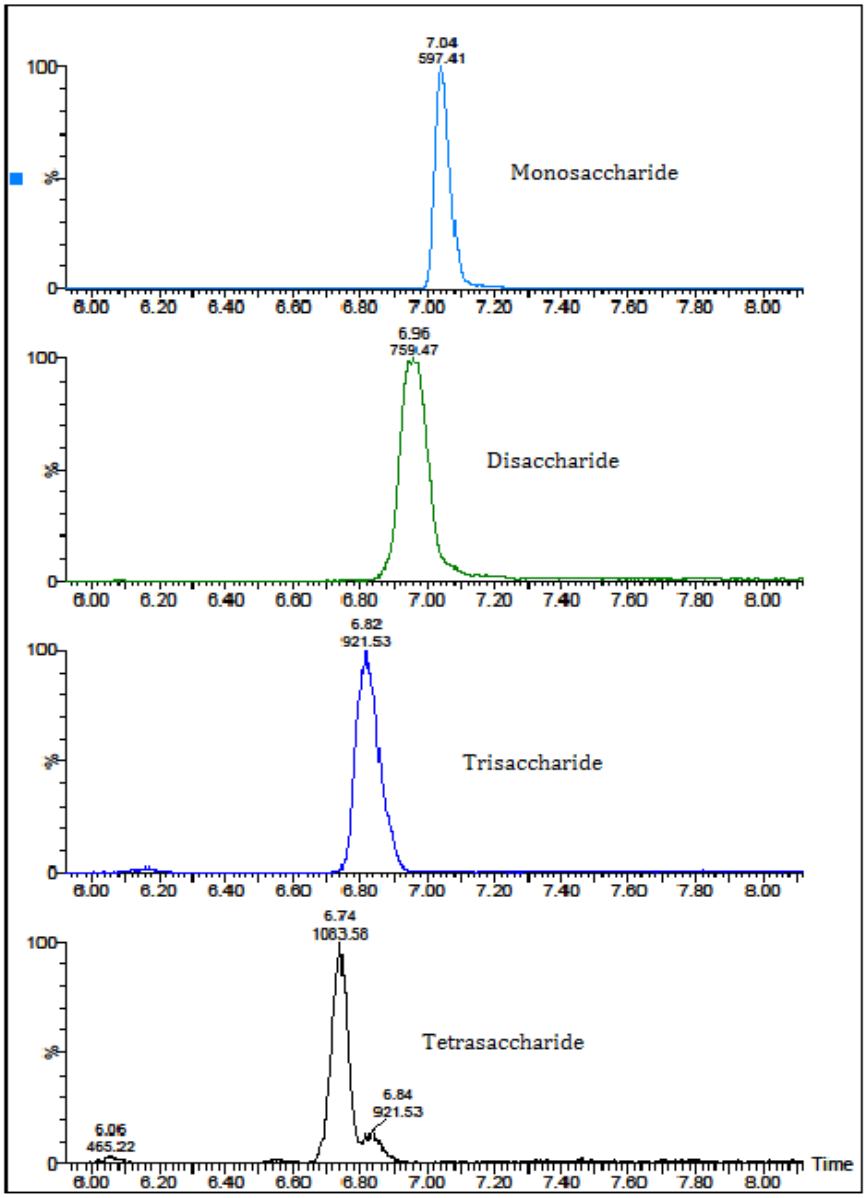

Figure 49: EIC obtained after the UPLC separation of the respective stigmasteryl saccharide in ESI positive mode, MeOH with 0.1 v% formic acid

Figure 49 gives the extracted ion current of the four analysed compounds. Stigmasteryl mono-, di- and trisaccharide could be separated from each other in time, only for the tetrasaccharide a complete separation from the trisaccharide could not be achieved with the tested conditions. Lowering the concentration and the application of a different gradient did not yield a better separation, switching to negative mode even decreased the intensity of the signal.

5.4.3 Ion mobility MS

Similarly as the steryl monoglucoside, separating the α and β-anomer of the respective steryl polyglucoside was tested using ion mobility MS. Figure 50 gives the IMS-MS of the pure β-anomer and the anomeric mixture of the disaccharide.

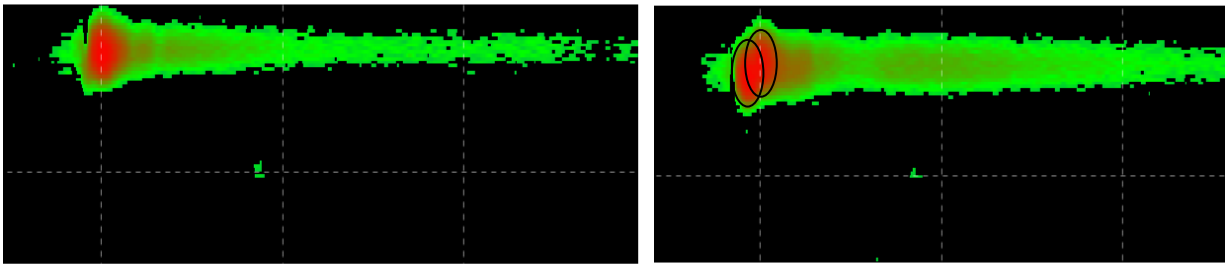

Figure 50: Ion mobility mass spectra of the β-disaccharide (left) and the anomeric mixture (right) in ESI positive mode with 0.1 v% formic acid

Although the separation is not as good as for the steryl monoglucoside, the presence of a second peak in the anomeric mixture can be observed. The reason for that may be an incomplete separation in both the UPLC and the IMS separation. A similar situation can be observed for the steryl tri- and tetrasaccharide; the diagrams are given in Figure 51 and Figure 52. The presence of a second less intense spot in the IMS-MS of the tetrasaccharide could either result from the presence of the other anomer or by an insufficient high concentration of the substance.

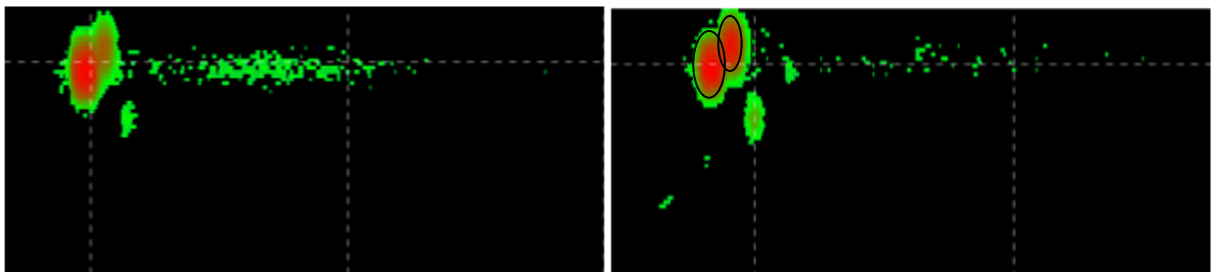

Figure 51: Ion mobility mass spectra of the α-trisaccharide (left) and the anomeric mixture (right) in ESI positive mode with 0.1 v% formic acid

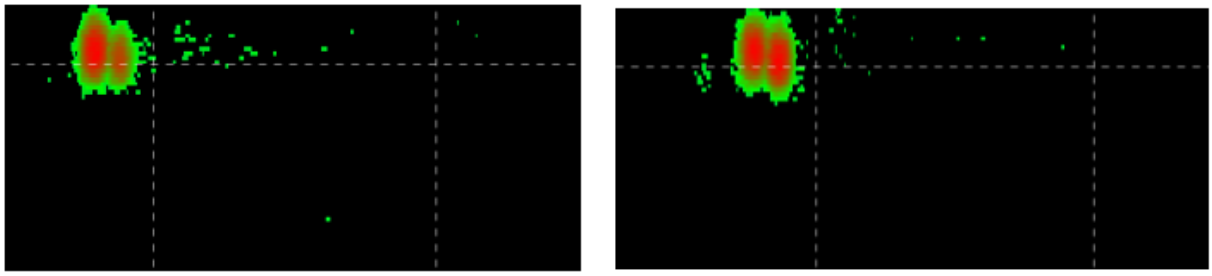

Figure 52: Ion mobility mass spectra of the α-tetrasaccharide (left) and the anomeric mixture (right) in ESI positive mode with 0.1 v% formic acid

5.4.4 Q-ToF-MS

As already mentioned, choosing formic acid as additive for the mobile phase did not lead to the desired fragmentation pattern. Therefore, a buffered solution of 0.1 v% acetic acid and 1 mM NH_4Ac was applied for the mobile phase in the MSMS measurements.

The fragmentation pattern of the respective α and β-anomer of the steryl polysaccharides did not feature remarkable differences. Nevertheless, differences could be observed between the di-, tri- and tetrasaccharide; the MSMS spectra are given in Figure 53.

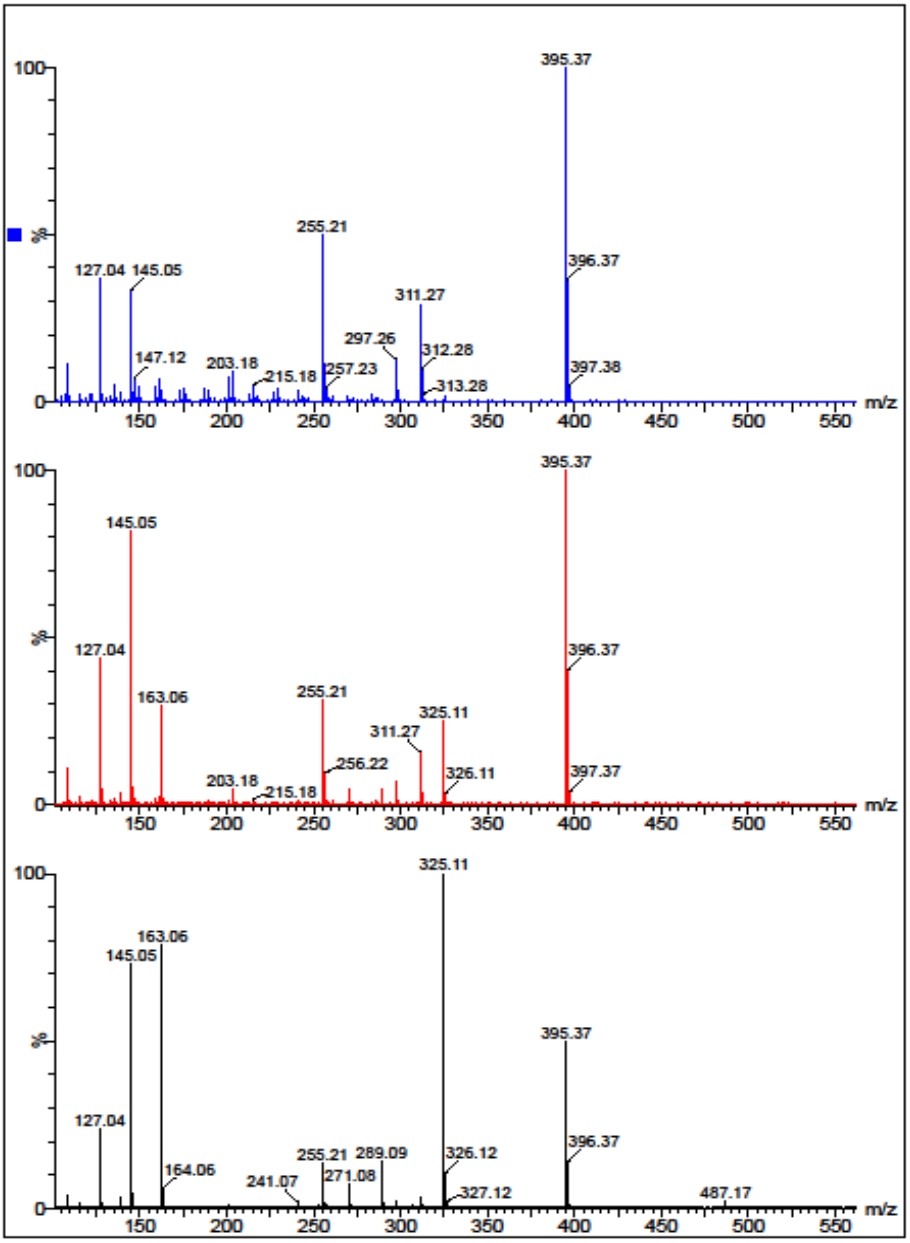

Figure 53: Fragmentation pattern of stigmasteryl di- (top), tri- (middle) and tetrasaccharide (bottom) in ESI MSMS positive mode with 0.1 v% acetic acid and 1 mM NH_4Ac

The observed $^{m}/_{z}$ = 163 corresponds to glucose after the loss of one hydroxy group, 325 to the respective di- and 487 to the trisaccharide. The higher the number of glucose monomers, the higher is the abundance of these signals, which meets the theoretical considerations that with a higher number of sugar monomers, more of the respective glycosyl fragments can be observed. A scheme of the processes involved in the fragementation is given in Figure 54.

The aglycone with $^{m}/_{z}$ = 397 and the aglycone under cleavage of the side chain at the C-17 atom ($^{m}/_{z}$ = 255) can be found in the mass spectra of all three different polyglucosides.

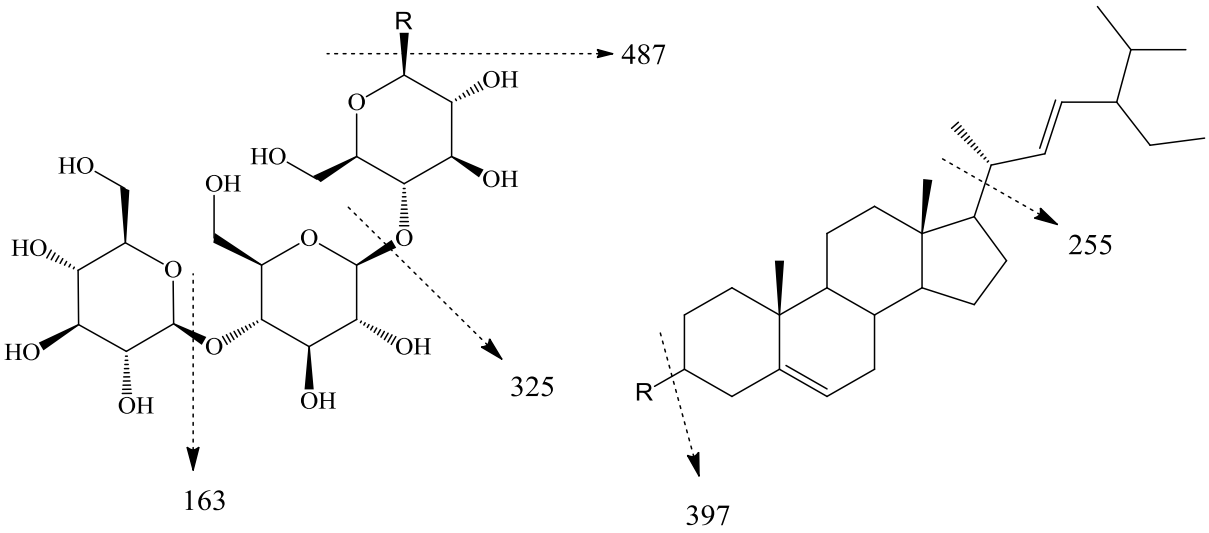

Figure 54: Schematic representation of the occurence of the detected fragements in steryl polyglucosides; the fragments corresponding to the sugar are shown at the left side, the ones corresponding to the aglycone on the right side

5.4.5 Steryl polyglucosides in food samples

Although different eluents were tested for the obtention of the steryl oligosaccharides from the food samples, the desired compounds could not be detected in neither of the investigated fractions. Also an increase of the sample concentration did not yield in the detection of the oligosaccharides. Due to the higher amount of free hydroxy groups, a remarkably high degree of polarity is given in this kind of compounds, which asks for a different extraction method than ASG and SG. ASE with MeOH or a different stationary phase in the SPE could be tested in order to derive the oligosaccharides.

6 Conclusion and outlook

Here we described a novel synthesis pathway for the obtention of high purity steryl glucosides. It has been shown that the five step reaction cascade is also applicable for plant based sterols, as β-sitosteryl- and stigmasteryl-D-glucopyranoside were synthesised with high purities and satisfying yields. In order to compare the outcome of the reaction with the well studied Koenigs-Knorr reaction, this synthesis pathway was studied by the use of β-sitosterol in the glycosylation step. Beside the need of costly Ag_2CO_3 and time consuming column chromatography, the desired compound was only obtained in unsatisfying yields. The novel synthesis pathway provides the possibility of synthesise standard materials needed for food chemistry or biodiesel industry without time consuming purification steps and costly reagents. The overall yield starting from sucrose for the respective steryl glucoside is given in Table 23. Applying BF_3*Et_2O in the glycosylation step enables the obtention of the natural compounds in a defined anomeric ratio.

Table 23: Yields of the five step synthesis pathway for the respective steryl glycoside; 6a = stigmasteryl, 6b = cholesteryl, 6c = β-sitosteryl moiety

Yields of the respective steps			
1st step	98 %		
2nd step	58 %		
3rd step	96 %		
	a	**b**	**c**
4th step	50 %	59 %	60 %
5th step	> 99 %	> 99 %	94 %
Overall	27 %	32 %	31 %

The acylation of the free steryl glucosides was envisioned using fatty acid methyl esters with environmental friendly lipases as catalysts. Cholesteryl-(6'-O-oleoyl)-D-glucopyranoside could be obtained with > 99 % purity and satisfying yields. Nevertheless, the need of time consuming column chromatography and the long reaction times are a drawback of this method. The conversions when using stigmasteryl- or steryl-D-glucopyranoside were lower compared to the one for cholesteryl-D-glucopyranoside and the use of palmitic acid methyl ester provoked problems. However, the achieved yields are comparable with other methods in the literature and feature the advantages of mild conditions and no formation of polyacylated SG. Microwave heating conditions could reduce both the required reaction times and enzyme amount and especially the solvent free system showed a satisfying reaction outcome.

6 Conclusion

LC/MS-ToF was heavily used during the research and proved to be the most suitable device for a fast and accurate measurement of SG. However, when information on the exact overall and anomerical purity of the compounds is needed, GC-MS and NMR spectroscopy have to be consulted as well.

Steryl polyglucosides could be detected with UPLC/MS-ToF and the respective mono-, di-, tri- and tetrasaccharide could be separated from each other in time. Stigmasteryl di-, tri- and tetrasaccharides feature a distinct fragmentation pattern, which could not be observed for the respective α- and β-anomer of each oligosaccharides.

In order to obtain anomerically pure standard materials, one should focus on the improvement of the yield achieved when using BF_3*Et_2O in the glycosylation step. Continuing research on the microwave heating conditions for the enzymatic acylation could enable a further decrease on reaction time, as well as the amount of acyl donor and enzyme needed. Beside the cost reduction this would also be beneficial in regard to the subsequent purification.

Concerning the steryl oligosaccharides, further improvement on the parameters applied in the ASE, the SPE or the UPLC-MS measurement would be necessary in order to analyse the desired compounds in a complex matrix.

7 List of figures and tables

Figure 1: Structure of androstan 3
Figure 2: Biosynthesis of sterols; 1: squalene, 2: cyclic squalene, 3: squalene epoxide, 4: protosterol cation, 5a: lanosterin, 5b: cycloartenol based on 1 4
Figure 3: Structure of β-sitosterol (1), stigmasterol (2) and campesterol (3) 5
Figure 4: Structure of β-D-glucose (1) and β-D-fructose (2) in Mills depiction 7
Figure 5: General reaction scheme of Fischer glycosylation; 1 = cyclic hemiacetal, 2 = oxocarbenium ion, 3 = glycoside based on 23 8
Figure 6: Representation of the orbital induced favorisation of the compound in axial, respective α, (a) to the one in equatorial, respective β, (b) position 8
Figure 7: Structure of stigmasteryl-β-D-glucopyranoside (left) and stigmasteryl-(1→4)polysaccharide (right) 10
Figure 8: Biosynthetic pathway for the synthesis of SG and ASG; enzymes are highlighted in red, steryl derivatives in blue from 3 11
Figure 9: General reaction scheme of the base induced transformation of ASG to SG during the transesterification of triglycerides 13
Figure 10: Reaction schemes of the possibilities for enzymatic biodiesel treatment; a = glucosidase, b = lipase or acyltransferase; 1 = SG, 2 = D-glucose, 3 = free sterol, 4 = ASG 16
Figure 11: Schematic setup of a ToF MS; from 68 20
Figure 12: Schematic representation of the processes involved in MS/MS 20
Figure 13: Schematic representation of an IMS system; the blue, green and yellow species correspond to molecules of different sizes from 72 21
Figure 14: Gas chromatogram of silylated steryl glucosides when using BSA+TCMS (left) and MSTFA (right); 4 = campesteryl-, 5 = stigmasteryl, 6 = β-sitosteryl glucoside from 78 23
Figure 15: Gas chromatogram of sylilated cholesteryl glucoside, (a) = α-anomer, (b) = β-anomer 24
Figure 16: Reaction scheme of the synthesis pathway starting from sucrose 39
Figure 17: General reaction scheme step 1, insertion of the protection groups 40
Figure 18: TLC, step 1, 4 h 40
Figure 19: LC/MS-ToF, APCI positive mode, step 1 41
Figure 20: General reaction scheme step 2, hydrolysis of octabenzyl sucrose 42
Figure 21: TLC, step 2, 2 h 42
Figure 22: LC/MS-ToF APCI positive mode, step 2 43
Figure 23: General reaction scheme step 3, synthesis of the trichloroacetimidate 44
Figure 24: TLC of step 3; left: t=0 min, center: t= 15 min, right: t= 4 h 44
Figure 25: ^{1}H NMR step 3 in $CDCl_3$ at 300 MHz 45

Figure 26: General reaction scheme step 4, glycosylation of steryl moiety 45
Figure 27: LC/MS-ToF APCI positive mode, step 4a 47
Figure 28: TLC of step 4 when using TMSOTf (left) and BF_3*Et_2O (right) as promotor; 47
Figure 29: LC/MS-ToF APCI positive mode, step 4b 48
Figure 30: General reaction scheme step 5, deprotection 49
Figure 31: LC/MS-ToF APCI negative mode, deprotection step 5a after 4h 50
Figure 32: LC/MS-ToF APCI negative mode, deprotection step 5a after 13h 50
Figure 33: Gas chromatogram, step 5a silylated; RT (SG) = 27 min, (a) = α-anomer, (b) = β-anomer 51
Figure 34: ^{1}H-NMR step 5a in d_6 DMSO at 300 MHz 51
Figure 35: Gas chromatogram of sylilated 6b when using BF_3*Et_2O (left) and TMSOTf (right); (a) = α-anomer, (b) = β-anomer 52
Figure 36: LC/MS-ToF APCI negative, step 5b 53
Figure 37: Fragmentation pattern of the anomeric mixture of cholesteryl-D-glucopyranoside (top) and cholesteryl-β-D-glucopyranoside (bottom) in ESI MSMS positive mode with 0.1 v% acetic acid and 1 µM NH_4Ac 54
Figure 38: Ion mobility mass spectra of cholesteryl-β-D-glucopyranoside (left) and cholesteryl-D-glucopyranoside (right) in ESI positive mode with 0.1 v% formic acid 55
Figure 39: LC/MS-ToF APCI negative, step 5c, $^m/_z$ 607 = campesteryl glucoside, $^m/_z$ 621 = sitosteryl glucoside 56
Figure 40: Gas chromatogram, step 5c silylated; retention time (campersteryl glucoside) = 28 min, retention time (sitosteryl glucoside) = 29 min 56
Figure 41: General reaction scheme for bromination of pentaacetyl glucose 57
Figure 42: General reaction scheme of glycosylation applying the Koenigs Knorr method; 1: tetraacetyl glucose, 2: β-sitosterol, 3: protected β-sitosteryl glycoside 4: orthoester, 5: β-sitosteryl acetate 58
Figure 43: General reaction scheme of the enzyme catalysed acylation of SG 59
Figure 44: TLC of 7a 62
Figure 45: LC/MS-ToF APCI negative, cholesteryl-(6'-O-oleoyl)-D-glucopyranoside 63
Figure 46: Gas chromatogram of silylated cholesteryl-(6'-O-oleoyl)-D-glucopyranoside, RT (ASG) = 33 min 63
Figure 47: Structure of stigmasteryl diglucoside 64
Figure 48: UPLC/MS-ToF ESI of stigmasteryl di- (top), tri- (middle) and tetrasaccharide (bottom) in ESI positive mode 65
Figure 49: EIC obtained after the UPLC separation of the respective stigmasteryl saccharide in ESI positive mode, MeOH with 0.1 v% formic acid 66

Figure 50: Ion mobility mass spectra of the β-disaccharide (left) and the anomeric mixture (right) in ESI positive mode with 0.1 v% formic acid 67
Figure 51: Ion mobility mass spectra of the α-trisaccharide (left) and the anomeric mixture (right) in ESI positive mode with 0.1 v% formic acid 67
Figure 52: Ion mobility mass spectra of the α-tetrasaccharide (left) and the anomeric mixture (right) in ESI positive mode with 0.1 v% formic acid 67
Figure 53: Fragmentation pattern of stigmasteryl di- (top), tri- (middle) and tetrasaccharide (bottom) in ESI MSMS positive mode with 0.1 v% acetic acid and 1 mM NH_4Ac 68
Figure 54: Schematic representation of the occurence of the detected fragements in steryl polyglucosides; the fragments corresponding to the sugar are shown at the left side, the ones corresponding to the aglycone on the right side 69

Table 1: Phytosterol content of selected plant oils from 22 6
Table 2: SG and ASG content in selected foods from 5 12
Table 3: Content of SG and ASG in selected plant oils and FAME from 44 13
Table 4: Overview of different ionisation methods 18
Table 5: Overview of different mass analysers and their respective advantages and disadvantages 19
Table 6: Quantities, yields, conditions and characteristics of the respective steryl glucoside a = stigmasteryl, b = cholesteryl, c = β-sitosteryl moiety 30
Table 7: Quantities, conditions, yields and characteristics of the respective sterylglucosides; 6a = stigmasteryl, 6b = cholesteryl, 6c = β-sitosteryl moiety 31
Table 8: Test series for acylation of SG using the shaker 32
Table 9: Test series for acylation of SG using the epi shaker 33
Table 10: Test series for acylation of SG using the microwave 34
Table 11: Tested strategies for the obtention of steryl oligosaccharides when applying SPE 35
Table 12: Parameters for LC/MS-ToF analyses 36
Table 13: UPLC gradient for steryl polyglucoside measurements based on 83 36
Table 14: Parameters for MS-ToF analyses performed at the ETH Zurich based on 83 37
Table 15: Additional parameters for IMS-MS 37
Table 16: Parameters for MSMS analyses 37
Table 17: Selected mass to charge ratios for the ionisation in the MSMS measurements 38
Table 18: Parameters for GC/MS analyses based on 80 38
Table 19: Conversion of SG to ASG after 48 h when using cholesteryl-D-glucopyranoside 60
Table 20: Conversion of SG to ASG after 48 h when using stigmasteryl-D-glucopyranoside and a natural SG mixture 60

Table 21: Conditions and achieved conversion of ASG when using microwave heating conditions 61
Table 22: Concentration of the respective compound in the mixture prepared in MeOH 65
Table 23: Yields of the five step synthesis pathway for the respective steryl glycoside; 6a = stigmasteryl, 6b = cholesteryl, 6c = β-sitosteryl moiety 70

8 References

1. Habermehl, G., Hammann, P. E., Krebs, H. C. & Ternes, W. *Naturstoffchemie. Eine Einführung.* 3rd ed. (Springer, Berlin Heidelberg, 2008).
2. Berg, J., Tymoczko, J. & Styrer, L. *Biochemistry.* 5th ed. (W H Freeman, New York, United States of America, 2002).
3. Grille, S., Zaslawski, A., Thiele, S., Plat, J. & Warnecke, D. The functions of steryl glycosides come to those who wait. Recent advances in plants, fungi, bacteria and animals. *Progress in Lipid Research* **49,** 262–288 (2010).
4. Wojciechowsk, Z. A. & Zimowski, J. Occurrence of UDPG: sterol glucosyltransferase activity in some lower plants. *Phytochemistry* **18,** 39–42 (1979).
5. Nyström, L., Schär, A. & Lampi, A.-M. Steryl glycosides and acylated steryl glycosides in plant foods reflect unique sterol patterns. *Eur. J. Lipid Sci. Technol.* **114,** 656–669 (2012).
6. Ostlund, R. Phytosterols in human nutrition. *Annu. Rev. Nutr.* **22,** 533–549 (2002).
7. Lee, I., Pfalzgraf, L. M., Poppe, G. B. & Powers, E. & Haines, T. The Role of Sterol Glucosides on Filter Plugging. *Biodiesel Magazine* **4,** 105–112 (2007).
8. Ludwig, C. Diploma thesis. Karl Franzens Universität, 2015.
9. Weiss, S. Master thesis. Karl Franzens Universität, 2016.
10. Jäger, S. N., Mittelbach, M., Cabrera, R. & Labadie, G. R. Simple method for high purity acylated steryl glucosides synthesis. *Eur. J. Lipid Sci. Technol.* **118,** 827–833 (2016).
11. Davis, R. A., Lin, C. & Gervay-Hague, J. Chemoenzymatic synthesis of cholesteryl-6-O-tetradecanoyl-α-D-glucopyranoside: a product of host cholesterol efflux promoted by Helicobacter pylori. *Chem. Commun.* **48,** 9083 (2012).
12. Kojima, M., Ohnishi, M., Ito, S. & Fujino, Y. Characterization of acylmono-, mono-, di-, tri- and tetraglycosylsterol and saponin in Adzuki bean (Vigna angularis) seeds. *Lipids* **24,** 849–853 (1989).
13. Fujino, Y., Ohnishi, M. & Ito, S. *Proceedings of the 7th world cereal and bread congress* (Prague, 1982).
14. Vollhardt, K. & Schnore, N. *Organische Chemie* (WILEY-VCH, 2000).
15. Onken, D. *Steroide. Zur Chemie und Anwendung* (Akademie-Verlag, Berlin, 1971).
16. Abidi, S. Chromatographic analysis of plant sterols in foods and vegetable oils. *Journal of Chromatography A* **935,** 173–201 (2001).

17. Rillinga, H. C. & Chayet, L. T. Chapter 1 Biosynthesis of cholesterol. Sterols and Bile Acids. *New Comprehensive Biochemistry* **12,** 1–39 (1985).

18. United States Department of Agriculture. *USDA Branded Food Products Database , ,* https://ndb.nal.usda.gov/ndb/search/list?fgcd=Branded+Food+Products+Database&ds=Branded+Food+Products.

19. Piironen, V., Lindsay, D. G., Miettinen, T. A., Toivo, J. & Lampi, A. Plant sterols. Biosynthesis, biological function and their importance to human nutrition. *Journal of the Science of Food and Agriculture,* 939–966 (2000).

20. Laraki, L., Andriamiarina, R., Pelletier, X. & Debry, G. Effects of stigmasterol-supplemented diets on fecal neutral sterols and bile acid excretion in rats. *Ann Nutr Metab* **33,** 297–303 (1989).

21. Ling, W. H. & Jones, W. Dietary Phytosterols. A review of metabolism, benefits and side effects. *Life Sciences* **57,** 195–206 (1995).

22. Mittelbach, M. & Stütz, A. *Renewable resources* (2014).

23. Lindhorst, T. K. *Essentials of Carbohydrate Chemistry and Biochemistry.* 3rd ed. (WILEY-VCH, 2007).

24. Rosak, C. & Mertes, G. Critical evaluation of the role of acarbose in the treatment of diabetes. Patient considerations. *Diabetes, Metabolic Syndrome and Obesity* **5,** 357–367 (2012).

25. Cates, J. E., Christie, R. V. & Garrodd, L. P. Penicillin-resistant Bacterial Endocarditis Treated by Penicillin and Streptomycin. *British Medical Journal* **1,** 653–656 (1991).

26. Helferich, B., Klein, W. & Schäfer, W. Synthese eines Disaccharidglucosids. II. *Justus Liebigs Annalen der Chemie,* 19–26 (1925).

27. Koenigs, W. & Knorr, E. Über einige Derivate des Traubezuckers und der Galactose. *Berichte der Deutschen Chemischen Gesellschaft zu Berlin* **34,** 957–981 (1901).

28. Kunz, H. & Harreus, A. Glycosidsynthese mit 2,3,4,6-Tetra-O-pivaloyl-α-D-glucopyranosylbromid. *Liebigs. Ann. Chem.* **1982,** 41–48 (1982).

29. Schmidt, R. R. & Stumpp, M. Synthese von 1-Thioglycosiden. *Liebigs. Ann. Chem.,* 1249–1256 (1983).

30. Pischetsriede, M. Chemistry of glucose and biochemical pathways of biological interest. *Perit Dial Int.* **20,** 26–30 (2000).

31. Boss R. & Scheffold, R. Cleavage of Allyl Ethers with Pd/C. *Angew. Chem. Int. Ed.* **15,** 558–559 (1976).

32. Lindhorst, T. K., Braun, C. & Withers, Stephen, G. Syntheses of 4'-deoxy-α-maltosyl fluoride and 4''-deoxy-α-maltotriosyl fluoride as probes of α-glucanotransferase mechanisms. *Carbohydrate Research* **268,** 93–106 (1995).

33. Lindhorst, T. K. & Thiem, J. En Route to Thromboxane Compounds from Carbohydrates, I. Synthesis of the Unsaturated Sugar Precursors. *Liebigs. Ann. Chem.* **1990,** 761–769 (1990).

34. Zemplén, G. & Pascu, E. Über die Verseifung acetylierter Zucker und verwandter Substanzen. *EurJIC* **62,** 1613–1614 (1929).

35. Hirai, Y. *et al.* Unique Cholesteryl Glucosides in Helicobacter pylori composition and structural analysis. *Journal of Bacteriology* **177,** 5327–5333 (1995).

36. Duperon, R., Thiersault, M. & Duperon, P. Occurrence of steryl glycosides and acylated steryl glycosides in some marine algae. *Phytochemistry* **22,** 535–538 (1983).

37. Muhideen, I. A. & et al. Characterization of human liver 3-O-β-D-glucopyranuronosyl-cholesterol by mass spectrometry and nuclear magnetic resonance spectroscopy. *Journal of Lipid Research* **25,** 1117–1123 (1984).

38. Dufourc, E. J. Sterols and membrane dynamics. *J Chem Biol* **1,** 63–77 (2008).

39. Lingwood, D. & Simons, K. Lipid Rafts As a Membrane- Organizing Principle. *SCIENCE* **327,** 46–50 (2010).

40. Flis, V. V. & Daum, G. Lipid Transport between the Endoplasmic Reticulum and Mitochondria. *Cold Spring Harbor Perspectives in Biology* **5,** 5:a013235 (2013).

41. Simons, K. & Vaz, W. Model system, lipid rafts and cell membranes. *Annu. Rev. Biophys. Biomol. Struct* **33,** 269–295 (2004).

42. Kunimoto, S., Kobayashi, T., Kobayashi, S. & Murakami-Murofushi, K. Expression of cholesteryl glucoside by heat shock in human fibroblasts. *Cell stress Chaperones* **5,** 3–7 (2000).

43. Sakaki, T. *et al.* Sterol glycosides and cerebrosides accumulate in Pichia pastoris , Rhynchosporium secalis and other fungi under normal conditions or under heat shock and ethanol stress. *Yeast* **18,** 679–695 (2001).

44. Lacoste, F., Dejean, F., Griffon, H. & Rouquette, C. Quantification of free and esterified steryl glucosides in vegetable oils and biodiesel. *Eur. J. Lipid Sci. Technol.* **111,** 822–828 (2009).

45. Moreau, R. A., Scott, K. M. & Haas, M. J. The Identification and Quantification of Steryl Glucosides in Precipitates from Commercial Biodiesel. *J Am Oil Chem Soc* **85,** 761–770 (2008).

46. van Hoed, V. *et al.* Identification and Occurrence of Steryl Glucosides in Palm and Soy Biodiesel. *J Am Oil Chem Soc* **85,** 701–709 (2008).

47. Dunn, R. O. Effects of minor constituents on cold flow properties and performance of biodiesel. *Progress in Energy and Combustion Science* **35,** 481–489 (2009).

48. Peiru, S. *et al.* An industrial scale process for the enzymatic removal of steryl glucosides from biodiesel. *Biotechnol Biofuels* **8,** 337 (2015).

49. Knothe, G., Krahl, J. & van Gerpen, J. *The Biodiesel Handbook.* 2nd ed. (AOCS Press, Urbana, Illinois, United States of America, 2010).

50. European Committee For Standardization. *Flüssige Mineralölerzeugnisse – Fettsäure-Methylester (FAME) zur Verwendung in Dieselmotoren und als Heizöl – Anforderungen und Prüfverfahren* (2014).

51. Westbrook, S. R. & LeCren, R. T. *Fuels for Land and Marine Diesel Engines and for Non-Aviation Gasturbines, Significance of Tests for Petroleum Products* (2003), 63–81.

52. European Standard EN116. *Diesel and domestic heating fuels. Determination of cold filter plugging point copy* (1997).

53. ASTM International. *Standard specification for biodiesel fuel blend stock (B100) for middle distillate fuels.* Annex A.1 (Annual book of ASTM standards, ASTM Press, 2008).

54. Tang, H., Guzman, R. de, Salley, S. & Ng, K. Y. Simon. Comparing Process Efficiency in Reducing Steryl Glucosides in Biodiesel. *J Am Oil Chem Soc* **87,** 337–345 (2010).

55. Bostyn, S., Duvalonen, F., Porte, C., Coic, J. & Fauduet, H. Kinetic modelling of the degradation of the α-tocopherol in biodiesel-rape methyl ester. *Bioresource Technology* **99,** 6439–6445 (2008).

56. Sohling, U., Ruf, F., Ortiz, N., Condemarin, V. R. & Bello, J. *Process for removing steryl glycosides from biodiesel. Patent: EP2285940 A1* (2008).

57. Menzella, H. G., Peiru, S. & Vetcher, L. *Enzymatic Removal of Steryl Glycosides. Patent: EP2825662 A4* (2013).

58. Aguirre, A. *et al.* Enzymatic hydrolysis of steryl glucosides, major contaminants of vegetable oil-derived biodiesel. *Appl Microbiol Biotechnol* **98,** 4033–4040 (2014).

59. Brask, J. & Nielsen, P. M. *Enzymatic removal of steryl glycosides in fatty acid alkyl esters. Patent: US9340752 B2* (2010).

60. Davis, R. A., Fettinger, J. C. & Gervay-Hague, J. Tandem Glycosyl Iodide Glycosylation and Regioselective Enzymatic Acylation Affords 6-O-Tetradecanoyl-α-D-cholesterylglycosides. *J. Org. Chem.* **79,** 8447–8452 (2014).

61. Münger, L. Dissertation. ETH, 2015.

62. Svendsen, A. Lipase protein engineering. *Biochim Biophys Acta* **1543,** 223–228 (2000).

63. Faber, K. *Biocatalysis* (2015).

64. Paczkowski, C., Musial, A., Wlodkowski, L., Kalinowska, M. & Wojciechowski, Z. A. Lipase-catalyzed regioselective synthesis of steryl (6′-O-acyl)glucosides. *Biotechnol Lett* **29,** 1403–1408 (2007).

65. Sölter, S. *Einsatzgebiete der LC/MS(MS) , ,* https://www.agilent.com/cs/library/slidepresentation/Public/MSDetektion.pdf.

66. de Hoffmann, E. & Stroobant, V. *Mass Spectrometry. Principles and Applications.* 2nd ed. (Wiley, Chichester, England, 2002).

67. Saf, R. *Material Science 2* (2015).

68. Agilent Technologies. *Agilent TOF LC/MS Techniques and Operation. Course Number R1874A, Volume 1, Student Manual* (2010).

69. McNaught, A. D. & Wilkinson, A. *Compendium of Chemical Terminology.* 2nd ed. (Blackwell Scientific Publications, 1997), http://goldbook.iupac.org.

70. Wolucka, B. A. & de Hoffmann, E. Determination of the Anomeric Configuration of Glycosyl Esters of Nucleoside Pyrophosphates by Fast-Atom Bombardment Tandem Mass Spectrometry. *J Am Sot Mass Spectrom* **1995,** 516–520.

71. Baumbach, J. I. & Eiceman, G. A. Ion Mobility Spectrometry: Arriving On Site and Moving Beyond a Low Profile. *Applied Spectroscopy* **53,** 338–355 (1999).

72. Cumeras, R., Figueras, E., Davis, C. E., Baumbach, J. I. & Gràcia, I. Review on Ion Mobility Spectrometry. Part 1: current instrumentation. *Analyst* **140,** 1376–1390 (2015).

73. Zangger, K. *Molekulare Analytik und Spektroskopie* (2013).

74. Clayden, J., Greeves, N. & Warren, S. *Organic chemistry.* 2nd ed. (Oxford University Press, 2012).

75. Friebolin, H. *Ein- und Zweidimensionale NMR-Spektroskopie. Eine Einführung.* 5th ed. (Weinheim: Wiley-VCH-Verlag, 2013).

76. Zhu, Y., Zajicek, J. & Serianni, A. S. Acyclic Forms of [1- 13 C]Aldohexoses in Aqueous Solution: Quantitation by 13 C NMR and Deuterium Isotope Effects on Tautomeric Equilibria. *J. Org. Chem.* **66,** 6244–6251 (2001).

77. Bubb, W. A. NMR spectroscopy in the study of carbohydrates: Characterizing the structural complexity. *Concepts Magn. Reson.* **19A,** 1–19 (2003).

78. Otto, M. *Analytische Chemie.* 3rd ed. (WILEY-VCH, Weinheim, Germany, 2006).

79. Gössler, W. *Instrumentelle Analytik* (2013).

80. Pieber, B., Schober, S., Goebl, C. & Mittelbach, M. Novel sensitive determination of steryl glycosides in biodiesel by gas chromatography–mass spectroscopy. *Journal of Chromatography A* **1217,** 6555–6561 (2010).

81. EUROPEAN COMMITTEE FOR STANDARDIZATION. *Determination of individual and total sterols contents -- Gas chromatographic method -- Part 1: Animal and vegetable fats and oils* (2014), 67.200.10.

82. Nyström, L., Moreau, R. A., Lampi, A.-M., Hicks, K. B. & Piironen, V. Enzymatic hydrolysis of steryl ferulates and steryl glycosides. *Eur Food Res Technol* **227,** 727–733 (2008).

83. Oppliger, S. L., Münger, L. & Nyström, L. Rapid and Highly Accurate Detection of Steryl Glycosides by Ultraperformance Liquid Chromatography-Quadrupole Time-of-Flight Mass Spectrometry (UPLC-Q-TOF-MS). *Journal of Agricultural and Food Chemistry* **62,** 9410–9419 (2014).

84. Kettelhoit, K. & Werz, D. B. Synthesis of stigmasteryl (β1→4)-oligoglucosides. *Journal of Carbohydrate Chemistry* **35,** 24–39 (2016).

85. Kessler, H. & Käsbeck, L. *Verfahren zur Herstellung von 2,3,4,6-Tetra-O-benzyl-D-glucopyranose und 2,3,4,6-Tetra-O-allyl-D-glucopyranose. Patent: DE 195 34 366 C2* (1995).

86. Kale, R. R. *et al.* Differentiation between Structurally Homologous Shiga 1 and Shiga 2 Toxins by Using Synthetic Glycoconjugates. *Angew. Chem. Int. Ed.* **47,** 1265–1268 (2008).

87. Schmidt, R. R. & Michel, J. Facile Synthesis of α and β-O-Glycosyl Imidates; Preparation of Glycosides and Disaccharides. *Angew. Chem. Int. Ed. Engl.* **19,** 731–732 (1980).

88. Lanucara, F., Holman, S. W., Gray, C. & Eyers, C. E. The power of ion mobility-mass spectrometry for structural characterisation and the study of conformational dynamics. *Nature Chemistry* **6,** 281–294 (2014).

89. Kartha, K. & Jennings, H. A Simplified, One-Pot Preparation of Acetobromosugars from Reducing Sugars. *J. Carboydr. Chem.* **9,** 777–781 (1990).

90. Kürti, L. & Czakó, B. *Strategic Applications of Named Reactions in Organic Synthesis. Background and Detailed Mechanisms* (Elsevier Academic Press, 2005).

91. Sigma Aldrich Co. (2016), http://www.sigmaaldrich.com/catalog/product/aldrich/537322?lang=de&region=AT.

92. Yadav, G. D. & Thorat, P. A. Microwave assisted lipase catalyzed synthesis of isoamyl myristate in solvent-free system. *Journal of Molecular Catalysis B: Enzymatic* **83,** 16–22 (2012).

93. Pirozzi, D., Di Lorenzo, M., Zuccharo, L. & Greco, G. *Enzymatic synthesis of biodiesel* (2013), http://folk.ntnu.no/skoge/prost/proceedings/icheap8-pres07/icheap8webpapers/141%20Pirozzi.pdf., accessed: February 15th, 2015